Management of Saltwater Intrusion in Coastal Aquifers: An Experimental and Numerical Investigation

Thesis submitted in partial fulfillment of the requirements for the award of the degree of

DOCTOR OF PHILOSOPHY

in

Civil Engineering

by

Bhrigumani Sharma

(Roll No: 136104019)

Under the guidance of

Prof. (Dr.) Rajib Kumar Bhattacharjya

Department of Civil Engineering

Indian Institute of Technology, Guwahati

Guwahati-781039, Assam, India

August 2020

भारतीय प्रौद्योगिकी संस्थान गुवाहाटी
INDIAN INSTITUTE OF TECHNOLOGY GUWAHATI

Guwahati – 781 039
Assam, INDIA

Phones: 0361-2582428 (O)
0361-2584428 (R)
Fax: 0361-2582440
E-mail: rkbc@iitg.ac.in
rajibkbc@gmail.com

DEPARTMENT OF CIVIL ENGINEERING

Dr. Rajib Kumar Bhattacharjya
Professor

Date: 28/08/2020

CERTIFICATE

This is to certify that the work contained in the thesis entitled "**Management of Saltwater Intrusion in Coastal Aquifers: An Experimental and Numerical Investigation**" submitted by **Bhrigumani Sharma** to the Department of Civil Engineering, Indian Institute of Technology Guwahati, for the award of the degree of Doctor of Philosophy in Civil Engineering is a record of bonafide research work carried out by her under my supervision and guidance. This thesis work, in my opinion, has reached the requisite standard fulfilling the requirements for the degree of Doctor of Philosophy.

The research work contained in this thesis has not been submitted in part or full to any other University or Institute for the award of any degree or diploma.

Place: Guwahati

(**Rajib Kumar Bhattacharjya**)

STATEMENT

I do hereby declare that the thesis entitled **"Management of Saltwater Intrusion in Coastal Aquifers: An Experimental and Numerical Investigation"** has been performed by me for the degree of Doctor of Philosophy in civil engineering under the guidance of Prof. (Dr.) Rajib Kumar Bhattacharjya, Department of Civil engineering, Indian Institute of Technology, Guwahati, Assam, India.

This work has not been submitted for the award of any degree or any diploma at this Institute or other Institute. I have also acknowledged whenever the work describes the findings based on the literature review.

Date: (**Bhrigumani Sharma**)

Place: Guwahati

ACKNOWLEDGEMENTS

Writing an acknowledgment has never been easy for anyone. For the simple reason that a heartfelt feeling of gratitude cannot be expressed in mere words. Any Ph.D. work undoubtedly carries blessings, sincere participation, and suggestions of an entire Institute and is not the creation of a single man.

To begin with, I would like to express my deep sense of gratitude and sincere thanks to my supervisor Prof. (Dr.) Rajib Kumar Bhattacharjya, Department of Civil Engineering, Indian Institute of Technology Guwahati for his great support, invaluable guidance, and continuous encouragement towards the successful completion of this work. His advice throughout the time of research and writing of this thesis is highly appreciated. It makes me feel a great privilege and honor to work under his guidance.

Besides my advisor, I would like to thank all my committee members, Prof. (Dr.) Subashisa Dutta, Prof. (Dr.) Bimlesh Kumar, and also thank Dr. Suresh A. Kartha, Department of Civil Engineering, Indian Institute of Technology Guwahati, for their insightful comments and encouragement that helped me to widen my research work from various perspectives. I am indebted to them for their constant source of inspiration and support throughout my thesis work.

I also wish to express my sincere thanks to Mr. Om Prakash Vats, Mr. D. S. Rishi, and Mr. Brishti Kumar Mudai, M. Tech. Student, Department of Civil Engineering, IIT Guwahati for their help in conducting the laboratory experiments and making the work successful.

My heartfelt thanks to my seniors Dr. Subhadeep Chakrabarti and Dr. Debraj Biswas, for their constant support and advice to carry out my research work successfully.

My sincere thanks to Dr. Sophia Leichombam, Ms. Mamata Das, Mr. Apratim Das, Mr. Jagadish Talukdar, Mr. Rajeev Gandhi BG, and Mr. Dilip Kumar Jha of Civil Engineering Department, IIT Guwahati, who helped me in different ways during various stages of my research work.

I wish to express my sincere thanks to the non-teaching staff of the Civil Engineering Department of IIT Guwahati for their help and support.

I express my deep love for IIT Guwahati and record my gratefulness to all the faculties who imparted me every bit of their valuable knowledge. I warmly thank and appreciate to all my

friends for helping me to get out through the difficult times, and for all the emotional support, entertainment and all the care they provided in my stay in IIT Guwahati.

On a personal note, I am grateful to my elder brother and younger sister for their presence in my life. Last but not least, I owe a lot to my parents for their love, inspiration, and moral support during the entire period of my work. I dedicate this thesis to my parents.

Lastly, I would like to thank almighty for blessing me in completing the whole thesis work without any difficulties.

(**Bhrigumani Sharma**)

DEDICATED TO

MY PARENTS.....

ABSTRACT

Saltwater intrusion (SI) into coastal aquifers is the most widespread groundwater contamination problem that has become a considerable prominent concern faced by water resource planners worldwide as it not only leads to the depletion of available water resources but also adversely affects the social and economic developments of coastal communities. Coastal aquifers play a pivotal role all over the world due to the availability as well as the high quality of groundwater resources they provide. In the last few decades, with the growing global population and the tendency of people to live in the coastal areas, the demand for freshwater has been rising at an alarming rate and also has increased excessive groundwater pumping to satisfy their daily water requirements for coastal communities. The indiscriminate and overexploitation of coastal aquifers has led to severe SI problems and consequently deteriorates groundwater quality in coastal subsurface systems. The interest in better understanding the mechanism of saltwater intrusion processes in coastal aquifers is, therefore, garnering increased attention worldwide in the past few years. In this study, a series of physical experiments have been performed in a laboratory-scale aquifer model to develop a better scientific understanding of the dynamics of this phenomenon. The variable-density flow and transport model FEMWATER is used to simulate the flow and transport processes for the experimental setup on the same scale, and simulations have been carried out to verify the observed phenomena for all the physical experiments. It has been found that the numerical predictions are in good agreement with all the experimental results.

In general, the construction of subsurface flow barriers is one of the most extensively used engineering countermeasures to prevent SI problems in coastal aquifers. An investigation has successfully been conducted to assess the efficiency of bentonite clay slurry on controlling the problem in the present study. The results reveal that there is no further movement of the saltwater intrusion wedge towards the inland side after implementation of the barrier. The research also suggests that the physical barrier created by bentonite slurry can be employed for preventing the movement of saltwater intrusion in coastal aquifer systems. A considerable mixing of saltwater and freshwater flows during the initial intrude period has been observed. Further, the effect of pumping on the saltwater intrusion dynamics has been studied, and results show that the saltwater interface rapidly advances through the system towards the freshwater aquifer after the

application of pumping. Also, the influence of the injection of the freshwater on the dynamics of saltwater intrusion processes has been investigated in this study. The evaluation of the results suggests that the saltwater wedge gradually recede through the system towards the saltwater boundary upon injection of freshwater and could be concluded the injection of freshwater as a hydraulic barrier can be used in impeding saltwater intrusion in coastal aquifers.

However, the saltwater diffusion zone present within the coastal aquifer system plays a significant role in the transport and fate of contaminants. This study examines the behavior of contaminant transport patterns in saltwater intruded aquifer with and without pumping conditions. The results demonstrate that the contaminant travels upward towards the seaward boundary when it approaches the saltwater intrusion wedge and then exits around the coastline. It is a remarkable observation that the contaminant plume does not travel further seaward through the saltwater intrusion wedge. Upon installation of a pump, the wedge advances rapidly into the freshwater system, and the contaminant plume is also drawn along with the wedge towards the pump location. It has been observed that the contaminant plume did not follow the ideal circular flow path. Due to the effect of advection, the circular plume forms an elongated shape as it approaches the saltwater-freshwater interface. Moreover, the behavior of contaminant plume under the influence of a horizontal clay lens has also been examined and observed that there are two saltwater wedges develop, one at the base of the aquifer, and the other one is above the clay lens. The results also indicate that the contaminant plume travels vertically along with the saltwater wedge towards the seaward boundary.

Image analysis (IA) techniques have widely been employed to quantify the spatial and temporal concentration distribution profiles in laboratory-scale flow tank experiments. In this study, the IA technique is used to measure the saltwater concentration field in the laboratory-scale aquifer model domain. A statistics-based error analysis method is also undertaken to assess the reliability of the method and to quantify the error associated with the measurements. As the toe length (TL) and width of the mixing zone (WMZ) are the typical parameters used to define a saltwater intrusion wedge, therefore, these parameters have been calculated using the IA technique for all the laboratory-scale experimental cases, and results are compared with the numerical predictions. This study shows the IA technique could be effectively used for quantification of the solute concentration distributions profile in laboratory-scale flow tank experiments. The presented IA technique is non-invasive and of relatively lower cost as compared to the other methods.

Groundwater circulation well (GCW) is one of the most promising in-situ remedial techniques of groundwater. In this work, an effort has been made to investigate the behavior of

saltwater intrusion dynamics under a GCW with partial extraction of water using both experimental and numerical approaches. The main focus is not only to cease the further migration of saltwater wedge towards inland but also to extract some percentages of water partially for human needs. The results indicate that there is no further movement of saltwater intrusion wedge towards the inland side upon implementation of GCW, and act as a hydraulic barrier in controlling saltwater intrusion in coastal aquifers. Furthermore, different scenarios have numerically been developed, and the model was simulated for all the scenarios to obtain the optimal percentage of the partial extraction. For all the developed scenarios, it has been observed that the initial steady-state wedge position is pushed at least 15% towards the seaward boundary. Hence, no further saltwater intrusion is possible around the sphere of influence of the well. Moreover, the evaluation of the results suggests that almost 30% partial extraction is likely to be possible if the screen length of GCW is shorter and non-uniform. The present study reveals that the GCWs system with partial abstraction can effectively mitigate the saltwater intrusion problem in coastal regions and could be considered as one of the most efficient management strategies for controlling the problem.

Keywords: Groundwater, Saltwater intrusion, Unconfined coastal aquifer, Laboratory experiment, Numerical simulation, FEMWATER, Image analysis, Groundwater circulation well.

Contents

List of Figures

List of Tables

List of symbols

a_L	Longitudinal dispersivity
a_T	Lateral dispersivity
a_m	Molecular diffusion coefficient
B_d	Dirichlet boundary
C	Solute concentration in aqueous phase
C_i	Solute concentration in the source
c	Solute concentration
c_i	Prescribed solute concentration
c_d	Concentration on the Dirichlet boundary
$\boldsymbol{D}$	Dispersion coefficient tensor
F	Storage coefficient
g	Acceleration due to gravity
h	Pressure head
h_i	Prescribed pressure head
h_d	Head on the Dirichlet boundary
$\boldsymbol{K}$	Hydraulic conductivity tensor
$\boldsymbol{K_{S0}}$	Reference saturated hydraulic conductivity tensor
K_s	First-order biodegradation rate through adsorbed phase
K_w	First-order biodegradation rate constant through dissolved phase
$\boldsymbol{k}$	Permeability tensor
k_r	Relative permeability or relative hydraulic conductivity
$\boldsymbol{k_s}$	Saturated permeability tensor
m	Artificial mass rate
q	Source and/or sink
S	Degree of saturation
S^a	Solute concentration in adsorbed phase
t	Time
$\boldsymbol{V}$	Darcy's velocity vector
z	Potential head
Δh	Difference of reference pressure head between prescribed location
Δt	Time step
α'	Modified compressibility of the porous medium
β'	Modified compressibility of the water
δ	Kronecker delta tensor
θ	Moisture content
μ	Dynamic viscosity of water at solute concentration C
μ_0	Reference dynamic viscosity at zero solute concentration
ρ	Water density at solute concentration C
ρ_0	Reference water density corresponding to zero solute concentration
ρ^*	Density of either the injection fluid or the withdrawn water
ρ_b	Bulk density of the porous medium
τ	Tortuosity
n	Porosity of the porous medium
$\boldsymbol{\lambda}$	Decay constant

List of Abbreviations

2D	Two Dimensional
3D	Three Dimensional
2D-FED	Two Dimensional Finite Element model for Dispersion
3DFEMFAT	Three Dimensional Finite Element Model of Flow And Transport through Saturated-Unsaturated Media
CO_2	Carbon dioxide
CODESA-3D	Coupled variable Density and Saturation 3-Dimensional model
FEFLOW	Finite Element subsurface FLOW system
FEMWATER	Finite Element Model of Water Flow Through Saturated-Unsaturated Media
GA	Genetic Algorithm
GCW	Groundwater Circulation Well
IA	Image Analysis
3DLEWASTE	Three-Dimensional Lagrangian-Eulerian Finite Element Model of Waste Transport Through Saturated-Unsaturated Media
MATLAB	MATrix LABoratory
MOCDENSE	Two-Constituent Solute Transport Model for Ground Water Having Variable Density
MTBE	Methyl tert-butyl ether
NaCl	Sodium chloride
NAPL	Nonaqueous Phase Liquids
PCE	Perchloroethylene
RDX	Royal Demolition Explosive
SGD	Submarine Groundwater Discharge
SHEMAT	Simulator of HEat and MAss Transport
SI	Saltwater Intrusion
SIMLA	SIMulation of Linkage and Association
SUTRA	A Model for 2D or 3D Saturated-Unsaturated, Variable-Density Ground-Water Flow With Solute or Energy Transport
TL	Toe Length
WMZ	Width of the Mixing Zone

CHAPTER 1

Introduction

1.1 General

Water is the most indispensable natural resources found on earth. Approximately 99.4% of all the earth's water is surface water, and subsurface water occurs only as 0.6% of the total volume of water. Of all the surface water, about 97% is found in oceans and inland seas in the form of saline water, and only 2% of the total volume of water represents fresh surface water. As groundwater accounts for only 22% of all freshwater on the earth, and almost 77% of the total amount of freshwater is present as polar ice. The other freshwater resources that are available for human beings are particularly in lakes and streams, with 0.3% and 0.003%, respectively (Bear *et al*., 1999). However, groundwater resources play a pivotal role in the social and economic developments in many developing countries as groundwater already emerges the reliable resource for freshwater supply to satisfy domestic, industrial, and agricultural needs and supplies half of the world's drinking water (UNESCO-WWAP, 2009).

With the growing population density, rapid and unplanned urbanization, and agricultural requirements, the demand for freshwater has been accelerating at an alarming rate throughout the world. The extensive abstraction of groundwater resources, especially in coastal regions, has become inevitable to meet the ever-increasing demands for freshwater. The indiscriminate and overexploitation of coastal aquifers, therefore, has lowered the hydraulic potential significantly, and this has led to a global saltwater intrusion problems and consequently deteriorates groundwater quality within coastal subsurface systems (Bear *et al*., 1999; Barlow and Reichard, 2010). The high salinization of groundwater in coastal aquifers makes unfit and unusable for further human consumption and irrigation. It is a great challenge to preserve them from further contamination by saltwater intrusion and other anthropogenic contaminants for sustainable utilization of available groundwater resources.

1.2 Groundwater contamination

Water quality is a significant concern in the management and development of water resources. With the high intensive water demands, the quality of available water resources has become a key factor, along with the quantity (Bear, 1979). However, groundwater aquifers serve as significant sources for freshwater supply in many parts around the world. Nevertheless, most of these aquifers have become enormously vulnerable due to the contamination by anthropogenic

pollutants in the last few decades. In general, the contaminants from surface sources first infiltrate to the unsaturated zone and then further percolates into the saturated aquifer and eventually migrate along with groundwater flow. These anthropogenic contaminants are inadvertently discharged from various sources such as landfills of solid wastes, industrial wastes disposal, leakage from underground septic tanks, and widespread use of pesticides, fertilizers, and herbicides for agricultural activities, etc., (Bear and Cheng, 2010). As reported, the sources of groundwater pollution have been classified into four categories (Bear, 1979):

- Environmental: This type of pollution is owing to the result of the dissolution of dangerous chemicals and minerals during the flow of groundwater through the aquifer comprising them. For example, flow-through carbonate rocks, seawater intrusion, and incursion by brackish groundwater from a contiguous aquifer.
- Domestic: Domestic pollution refers to the leakage of sewer pipes, infiltration of rainwater through sanitary landfills, percolation of sewage from septic tanks, and biological contaminants (e.g., bacteria and viruses), etc.
- Industrial: This type of pollution could enter from sewage disposal that contains heavy metals, non-deteriorating toxic compounds, and radioactive materials.
- Agricultural: This pollution is due to the infiltration of irrigation water containing dissolved fertilizers, salts, herbicides, pesticides, etc. into the groundwater aquifer.

These anthropogenic sources not only contaminate the local aquifers but also threatens human health and the integrity of aquatic ecosystems of the region. Special attention has to be given to protect them from pollution because once it gets highly contaminated, its restoration is challenging and expensive to remediate contaminated groundwater aquifers.

Saltwater intrusion (SI) is one of the most extensive sources of groundwater contamination. With about 70% of the world's population resides in coastal regions (Bear *et al*., 1999; Cheng and Ouazar, 2003; Webb and Howard, 2011), it has become a prominent environmental concern faced by water resource planners worldwide. As it not only pollute the available groundwater supply but also adversely affects the social and economic developments of coastal communities. There is a need to prepare and implement proper remediation techniques for mitigating the problems and protecting groundwater resources from further contamination by saltwater intrusion.

1.3 Saltwater intrusion problem

Coastal regions represent among the most vulnerable areas in the world, as almost half of the world's population dwells within 100 km of the shoreline (Dose *et al*., 2014). This percentage is expected to increase in the future with the growing community and the tendency of people to live in the coastal zones. These areas commonly face severe hydrological problems, including scarcity of freshwater and groundwater contamination caused by saltwater intrusion. As such, protection and sustainable utilization of groundwater resources of these regions undertake great significance.

The rising demand for freshwater to satisfy the water requirements in different domestic, industrial, and agricultural sectors, is emplacing more emphasis on the development of groundwater resources. The overexploitation of groundwater resources along with reduced natural recharge, especially in arid and semi-arid coastal areas, leads to the large-scale depletion of groundwater levels and causing severe saltwater intrusion problems in coastal aquifers. Many researchers have reported the contamination of coastal aquifers as a result of saltwater intrusion in different parts of the world. Shi and Jiao (2014) reported saltwater intrusion problems have occurred in the area around the Bohai Sea, China, due to excessive groundwater pumping. Degradation of the coastal aquifer in California, the USA, was reported by Anders *et al*. (2014). Cary *et al*. (2015) also reported that deterioration of groundwater reservoir by saltwater intrusion in Recife coastal plain, Pernambuco, Brazil. Moreover, several coastal states of India have already been experienced groundwater contamination problems threatened by saltwater intrusion. Pramada *et al*. (2018) reported the freshwater aquifers of the Ernakulam coast of Kerala State, India, severely affected by saltwater intrusion. As stated, the leading causes of saltwater intrusion in coastal aquifers are the excessive unplanned withdrawal of groundwater resources and improper arrangement of pumping wells (Bhattacharjya *et al*., 2009).

Saltwater intrusion (SI) is a natural dynamic process that defines as the movement of saline water into an aquifer system that is in hydraulic continuity with the sea or ocean and mainly driven by the density contrast between ambient freshwater and seawater. In general, a hydraulic gradient exists towards the sea in coastal systems that aid the inflow of the excess freshwater to the sea. The presence of seawater in the aquifer beneath the sea involves a zone of contact between the lighter freshwater, which flows to the sea, and the denser saltwater tends to underlie freshwater due to hydrodynamic mechanism. A mixing zone with varying density also exists between them on account of hydrodynamic dispersion, and this zone is known as the transition zone or zone of dispersion or diffusion. The density of the mixed water gradually increases from

the freshwater side to the saltwater side across this zone. Figure 1.1 shows a schematic illustration of an unconfined coastal aquifer.

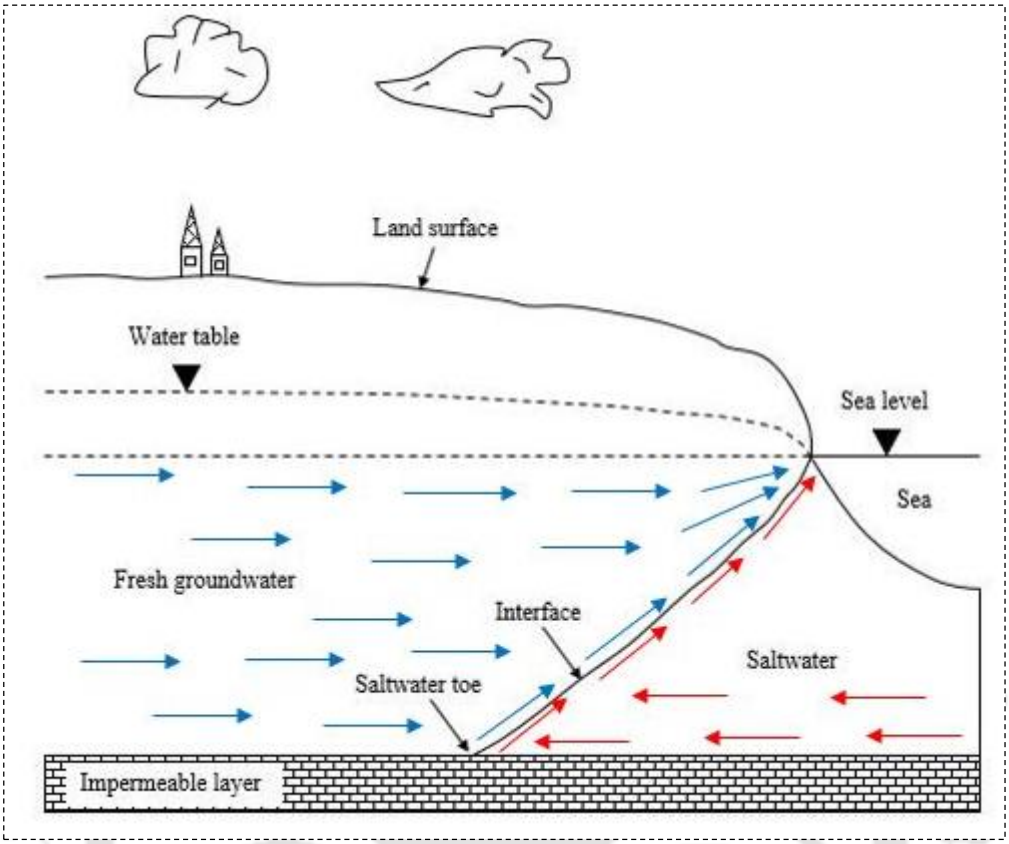

Figure 1.1: Schematic illustration of an unconfined coastal aquifer

Under certain situations, the thickness of the transition zone is relatively small, as compared to the width of the aquifer, so that freshwater and saltwater are assumed to be immiscible liquids, and the interface would be considered as a sharp interface that separates the freshwater and saltwater regions. But, if the transition zone is wide as compared to the thickness of the aquifer, then the interface approximation becomes invalid (Bear, 1979). A diffusion zone, therefore, needs to be considered for simulating real-world saltwater intrusion problems in coastal aquifers. Indeed, the extension of saltwater intrusion into the coastal aquifers depends on various factors such as groundwater recharge, aquifers lithology, hydraulic gradient, and coastal topography (Freeze and Cherry, 1979; Kouzana *et al*., 2010; Fadili *et al*., 2016), and the diffusion zone could vary from a few meters to several kilometers (Barlow and Reichard, 2010).

In undisturbed natural conditions, fresh groundwater flows to the sea or ocean in a coastal aquifer because of the existence of a hydraulic gradient towards the sea. On excessive pumping from a coastal aquifer, the water table gets declined significantly to the level that the hydraulic head in the freshwater body becomes less than the contiguous sea level. Then the interface starts to progress further inland until a new equilibrium is established. This phenomenon is called

saltwater intrusion or encroachment. As the saltwater wedge progresses, the transition zone widens, and once the advancing wedge enters inland pumping well, the well becomes polluted. While pumping occurs in a well-located above the wedge, the upconing of saline water near the pumping well could take place. If the pumping rate is prudently not controlled, saline water would eventually enter the pumped well, and the well could be abandoned. The saltwater intrusion into coastal aquifers is a serious hydrological issue for coastal inhabitants. It often results in depletion of fresh groundwater resources and also threatens human health and their economic development. The quantitative understanding of the mechanism of the saltwater intrusion process in coastal aquifers is, therefore, essential as regards water resources planning, development, and management in coastal marine and estuarine environments.

1.4 Control of saltwater intrusion

Groundwater is an indispensable freshwater resource for communities and ecosystems of the coastal regions that are continuously threatened by saltwater intrusion. Saltwater intrusion is considered a common groundwater contamination problem often exacerbated by overexploitation of coastal aquifers. Saltwater intrusion extensively leads to an increase in salinity levels in coastal aquifers, thus making it unsuitable for human utilization and further restricts future exploitation of coastal aquifers. Therefore, efficient planning and management strategies should be implemented in coastal aquifer systems to protect them and for continued utilization of groundwater resources on a sustainable basis under the threat of saltwater intrusion. However, several management strategies have been proposed to prevent or mitigate saltwater intrusion and to secure groundwater reserves in coastal aquifers (Todd, 1959; Dam, 1999; Oude Essink, 2001). These approaches in controlling the problem extensively depend on various factors such as the source of saline water, the extension of saltwater intrusion, local geological conditions, utilization of water, and economic factors (Todd, 1959). These could be generally recognized into the following methods:

- Modification of pumping pattern: This practice involves the reduction in pumping rates or adequate relocation of pumping wells within coastal zones. The coastal aquifer can be managed by changing the location of extraction wells by dispersing them in the inland regions, which eventually aid in raising the groundwater level and maintain groundwater storage. Furthermore, the reduction of withdrawal rates in existing wells could yield a similar beneficial effect.

- Artificial recharge: This method helps to increase the outflow of groundwater through the coastal aquifer and hence reduce the saltwater intrusion wedge in length. Recharge wells and surface spreading are used for confined and unconfined coastal aquifers, respectively. It involves the development of an additional water source.
- Extraction barrier: In this method, a line of extraction wells are constructed adjacent to the sea or ocean and pumped to forming a trough parallel to the coast. Seawater moves from the sea in the inland direction towards the trough when freshwater would flow seaward to the trough within the aquifer. The saline water or brackish groundwater is pumped and generally discharged into the sea.
- Injection barrier: This method maintains a freshwater ridge along the shore by a line of recharge wells. Injected freshwater flows in both the seaward and landward directions. High quality of water is necessary for injecting into recharge wells. It helps to increase the volume of groundwater storage in the aquifer that retards saltwater intrusion. Moreover, a combination of injection and extraction barriers is possible. The combination technique decreases both the recharge and abstraction rates, although it requires a large number of wells.
- Subsurface barrier: This method involves the creation of an impermeable subsurface barrier paralleling the coastline and through the vertical extent of the aquifer. It helps to prevent the movement of a saltwater wedge into the aquifer. This technique is only applicable to shallow aquifers, and also too costly. The establishment of this barrier could achieve through sheet piles, clay trenches, cement grout, or injection of chemicals.
- Land reclamation: In this process, a foreland created by the hydraulic fill above sea level, where a freshwater body could develop that may delay the inflow of saline groundwater.

Apart from these methods, a combination of some of the strategies as mentioned above have been employed by many researchers to better control of saltwater intrusion problems in coastal aquifers (e.g., Zhou *et al*., 2003; Narayan *et al*., 2007; Cherubini and Pastore, 2011; Javadi *et al*., 2015). Over the past decades, considerable attention has been received for examining the control of saltwater intrusion by using models. However, the model used in controlling the saltwater intrusion processes has some limitations (Abd-Elhamid and Javadi, 2008). As reported, most of these approaches are too expensive, and some of them are not applicable in some instances. The effective strategy to control saltwater intrusion is so far not developed that could efficiently manage this problem in coastal regions. As such, a reliable and cost-effective method is,

therefore, required to protect coastal groundwater resources under the threat of saltwater intrusion. This study focuses on an effort to investigate the effect of a groundwater circulation well (GCW) on controlling saltwater intrusion in coastal aquifers. This methodology is very cost-effective, has a less environmental impact, and could be employed for sustainable development of water resources in coastal zones. Furthermore, the method involves low energy requirements in terms of operation and monitoring and minimally invasive and non-disruptive to site conditions as compared to other conventional techniques.

1.5 Groundwater circulation well (GCW) system

Groundwater circulation well (GCW) is one of the most promising in-situ remedial techniques of groundwater. This technique was first suggested by Herrling and Buermann (1990) and Herrling *et al*. (1990) for remediating contaminated groundwater aquifer. In general, the typical GCW comprises two-screen segments that are separated by an impervious casing. One screen section used to extract the contaminated water from the subsurface system. The extracted contaminated water is treated in the well casing, and after the treatment, the water is injecting back into the aquifer through the other screen of that same well with equal flow rates. The extraction and injection of water create a vertical circulation flow between the extraction and injection screens (Herrling *et al*., 1991; Gonen and Gvirtzman, 1997; Stamm, 1998). As the circulation flow induced by GCW is force water in a circular pattern between abstraction and recharge screens, which flushes the contaminated water within the proximity of the well. As reported, single GCW should be used for remediation of only one aquifer and should not associate with different aquifer systems (Stamm *et al*., 1996).

The GCW technique that could operate in two flow mode, such as standard and reverse circulation mode. In a standard circulation mode, water abstracts upward inside the well that allows entering the lower screen and injects it to the upper screen, which exits the screen to form circulation cells [Figure 1.2(b)]. Under reverse flow condition, groundwater extracts through the top screen, which moves toward the well and injects to the lower screen, that move away from the well [Figure 1.2(c)]. In both the operation, groundwater circulates the center of GCW, but no groundwater is removed from the aquifer system. The vertical circulation flow of a GCW is illustrated in Figure 1.2.

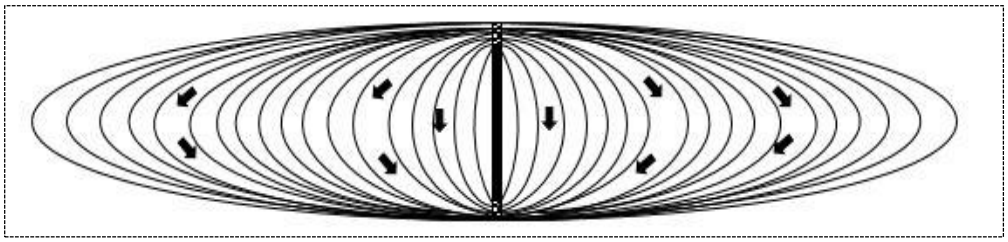

(a) GCW without gradient

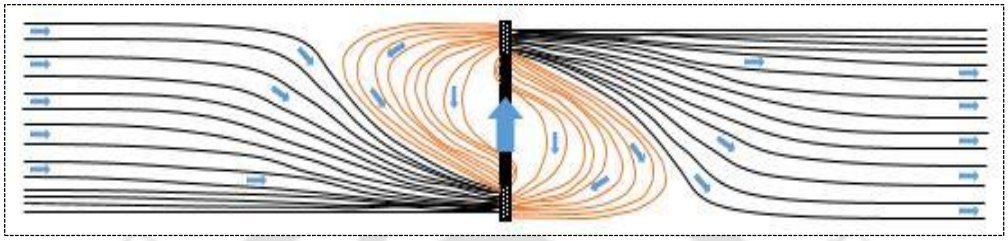

(b) GCW standard circulation flow

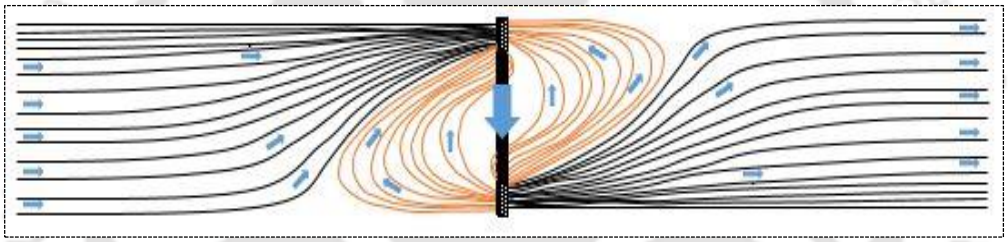

(c) GCW reverse circulation flow

Figure 1.2: GCW, (a) without gradient, (b) standard circulation flow with the gradient, and (c) reverse circulation flow with the gradient

Figure 1.2(b) and Figure 1.2(c) demonstrate the streamline of the vertical circulation flow pattern in a plane parallel to the natural groundwater flow. In the case of no gradient in groundwater or no groundwater flow [Figure 1.2(a)], the circulation cell extends such that a sphere of influence is infinite. From Figure 1.2, it can be seen that with increasing groundwater flow gradient, the circulation cell area decreases and vice-versa.

However, the GCWs have extensively been used for in-situ remediation of groundwater in porous media (e.g., Herrling *et al*., 1991; U.S. EPA, 1995, 1998; Knox *et al*., 1997; Miller and Roote, 1997; McCarty *et al*., 1998) in the last few decades. Many researchers have suggested that GCW is a very useful in-situ remediation technique for removing NAPL contaminants in groundwater (e.g., Scholz *et al*., 1997, 1998a; Mohrlok *et al*., 2000, 2003; Kirubaharan *et al*., 2008; Papini *et al*., 2016). Moreover, GCWs have already been applied to remove volatile organic contaminants (e.g., Gvirtzman and Gorelick, 1992; Stamm *et al*., 1998; Allmon *et al*.,

1999; Drizin *et al*., 2008; Zhao *et al*., 2016; Tawabini and Makkawi, 2018) and nonvolatile organic substances (Elmore and Graff, 2002) from the subsurface. With the proper placement of a GCW system, the water can be treated before it enters a domestic well (Miller and Elmore, 2005). To date, several researchers have also used the GCW technique to determine the aquifer properties such as the hydraulic conductivity, dispersivity and the specific storativity (e.g., Kabala, 1993; Zlotnik and Zurbuchen, 1998, 2003; Sutton *et al*., 2000; Zlotnik *et al*., 2001). The GCW technique has also been used for the estimation of aquifer hydrodynamic and sorption parameters.

In this study, an attempt has been made to investigate the effect of a groundwater circulation well (GCW) on controlling saltwater intrusion in coastal aquifers. The reverse circulation flow GCW has been used for the analysis that abstracts freshwater from the upper screen section and reinjects back into the system through the lower screen in a single well. The extraction and injection of freshwater generate a vertical circulation flow between the extraction and injection screens, which pushes the saltwater wedge towards the seaward boundary. Hence, GCW can act as a hydraulic barrier to prevent or mitigate saltwater intrusion problems and to secure groundwater reserves from saltwater intrusion in coastal aquifers. The method presented here could be considered as one of the most effective strategies for the management of coastal aquifers.

1.6 Objectives of the thesis

Saltwater intrusion (SI) into coastal aquifers has become a prominent environmental concern faced by water resource planners worldwide as it not only pollute the available groundwater supply but also adversely affects the social and economic developments of coastal communities. There is a need to prepare and implement proper remediation techniques for mitigating the problem and protecting groundwater resources from further contamination by saltwater intrusion. The main objective of this study is to develop a reliable and cost-effective remedial technique for controlling the saltwater intrusion in coastal groundwater aquifers. The present study is intended to meet the following specific objectives:

- To conduct laboratory-scale experiments to have a better understanding of the saltwater intrusion phenomena in an unconfined coastal aquifer.
- To develop the numerical model to simulate the saltwater intrusion process in a coastal unconfined aquifer.

- To quantify the spatial and temporal salt concentration distributions profile in laboratory-scale flow tank experiments using an image analysis technique.
- To develop a management strategy to mitigate the saltwater intrusion problem in a coastal aquifer system.
- To develop different management scenarios to study the dynamics of saltwater intrusion processes in an unconfined coastal aquifer.

1.7 Organization of the thesis

This thesis is organized in seven chapters, including the present chapter, which provides a brief introduction and the specific objectives of the thesis. This chapter closes by stating the organization of the thesis.

Chapter 2 outlines a comprehensive review of related literature. This chapter has been divided into five subheadings. These are including simulation model for saltwater intrusion processes, dynamics of saltwater and freshwater interaction, impacts of sea-level rise on saltwater intrusion processes, control of saltwater intrusion problem and applications of groundwater circulation well.

Chapter 3 describes the experimental setup of the physical model and peripheral equipment used during the study. This chapter presents a series of laboratory-scale experiments conducted in the physical model, and the details of this laboratory study are discussed in this chapter.

Chapter 4 covers a detailed description of the numerical model developed for the present study. In this chapter, the numerical model is used to simulate the laboratory-scale experiments presented in Chapter 3. This chapter also presents a comparison of simulation results with the experimental observations.

In chapter 5, the spatial and temporal salt concentration distributions profile have been quantified from digital photographs using an image analysis technique. The details of the work are summarized in this chapter.

Chapter 6 deals with the development of a management strategy to mitigate the saltwater intrusion problem for coastal aquifers. This chapter also presents the development of different management scenarios to study the dynamics of the saltwater intrusion processes in coastal unconfined aquifer systems.

Finally, chapter 7 includes the summary, conclusions, and recommendations for future work.

CHAPTER 2

Literature Review

2.1 Introduction

Saltwater intrusion (SI) into coastal aquifers is the most widespread groundwater contamination problem that has become a considerable prominent concern faced by water resource planners worldwide as it not only pollute the available groundwater supply but also adversely affects the social and economic development of coastal communities. Several natural and anthropogenic activities can intensify the impacts of saltwater intrusion. As the alarming growth in populations, substantial developments of coastal urbanization, and increasing agricultural activities, the excessive pumping of groundwater is thus unavoidable to satisfy the daily water requirements for coastal communities. These pumping activities can aggravate the saltwater intrusion processes in coastal systems (Bear *et al*., 1999). Shi and Jiao (2014) reported saltwater intrusion problems have occurred in the area around the Bohai Sea, China, due to excessive groundwater pumping. Furthermore, catastrophic events such as droughts induced by climate change would affect a decrease of freshwater recharge and, consequently, would enhance saltwater intrusion within coastal aquifer systems. Several modeling and field studies were revealed that climate change could reduce the net freshwater flux to groundwater reserves (e.g., Oude Essink, 2001; Ranjan *et al*., 2006; Feseker, 2007; Rozell and Wong, 2010; Yu *et al*., 2010) and this could exacerbate the effects of saltwater intrusion. As such, protection and sustainable utilization of groundwater resources of these regions undertake great significance. Therefore, it is imperative to study the dynamics of saltwater intrusion processes in coastal aquifers so as to investigate their transport patterns and work out appropriate remedial countermeasures for sustainable management of coastal aquifer systems.

In this chapter, the general review of literature specific to saltwater intrusion in coastal aquifers is presented. In the past decades, mathematical models have been developed to simulate the saltwater intrusion processes. These models are descriptive that could be solved analytically or numerically to simulate the natural aquifer system processes or the system response to some induced stress conditions as regards pumping and recharge. The literature on descriptive models for saltwater intrusion processes in coastal aquifers is presented in this chapter. Also, the studies related to the dynamics of saltwater and freshwater interactions and impacts of sea-level rise on

saltwater intrusion processes in coastal aquifers are reviewed. The main objective of this study is to develop a reliable and cost-effective remedial technique for controlling the saltwater intrusion in coastal groundwater aquifers. Therefore, more emphasis is given to the discussion on available management strategies used to reduce and manage the saltwater intrusion problem. Moreover, this study also makes an effort to investigate the effect of a groundwater circulation well (GCW) on controlling saltwater intrusion in coastal aquifers. As such, the general history of the applications of GCW is also discussed.

2.2 Simulation model for saltwater intrusion processes

Saltwater intrusion (SI) is a natural dynamic process where saline water moves into a groundwater aquifer system that is hydraulically connected with the sea or ocean and primarily driven by the density contrast between the denser seawater and the lighter freshwater. The presence of seawater in the aquifer beneath the sea involves a zone of contact between the lighter freshwater, which flows to the sea, and the denser saltwater tends to underlie freshwater due to hydrodynamic mechanism. A mixing zone with varying density also exists between them on account of hydrodynamic dispersion, and this zone is known as the transition zone or zone of dispersion. The transition zone could vary from a few meters to several kilometers in coastal aquifers (Barlow and Reichard, 2010). It is mainly controlled by transport process constituents such as density gradients, diffusion, dispersion, and kinetic mass transfer (Lu *et al*., 2009; Werner *et al*., 2013). The simulation of flow and transport processes in coastal systems can be done mathematically by two hydraulic approaches, *i.e.*, the sharp interface and the diffuse interface approaches.

In the sharp interface approach, the effects of mixing zone are not taken into account compared to the aquifer thickness, and the saltwater and freshwater are assumed to be two immiscible liquids, separated by a sharp interface. The sharp interface models are extensively used to simulate the saltwater intrusion process. They are based on the Ghyben-Herzberg approach that assumes a sharp interface between the saltwater and freshwater. This approach only gives satisfactory results while the mixing zone is very narrow, and it fails once freshwater flows into the sea or ocean. The sharp interface approach has widely been employed in analytical as well as numerical models in the past years because of its simplicity and lesser computational burden (Henry, 1959; Bear and Dagan, 1964; Dagan and Bear, 1968; Strack, 1976; Park and Aral, 2004; Mantoglou and Papantoniou, 2008). Numerical simulation of a sharp interface model was presented by Mercer *et al*. (1980) to simulate the motion of saline water and ambient freshwater in coastal aquifer systems. The areal equations were based on the Dupuit

approximation and are obtained from partial integration over the vertical directions. They used a finite difference technique to approximate the partial differential equations. Guvanasen *et al*. (2000) employed a sharp interface model to simulate regional groundwater flow and saltwater intrusion in Hernando County, Florida. The authors used the SIMLA code to simulate the saltwater intrusion process. Yet again, Cheng *et al*. (2000) developed solutions to estimate the wedge location in coastal aquifers under pumping conditions from one well, two wells, and multiple wells. However, the incapability of this approach in the investigation of the saline water flow through the transition zone and can simulate only solute transport through the advection process are the main limitations of this approach.

In the diffusive interface approach, the hydrodynamic dispersion controls the mixing process between saltwater and freshwater. The developed mixing zone between these two liquids takes the form of a transition zone that is more realistic and closer to the actual physical behavior of the flow and solute transport in coastal aquifer system than the sharp interface approach (Sherif *et al*., 1990; Bear and Zhou, 2007). This approach considers the flow and transport processes are density-dependent. Because of this, the flow and transport equations are required to be simultaneously solved. The simultaneous solution of these two coupled equations leads to high non-linearity in the simulation of density-driven flow and transport processes. Spatial and temporal simulation of this process needs the numerical methods to solve the nonlinear governing equations of flow and solute transport through porous media system. In recent years, several numerical models were developed and successfully used to solve the nonlinear flow and solute transport equations under steady-state and transient conditions and in both 2D and 3D. Most widely used models are including SUTRA (Voss, 1984; Voss and Provost, 2010), MOCDENSE (Sanford and Konikow, 1985), FEFLOW (Diersch, 1988), SWICHA (Lester, 1991 based on Huyakorn *et al*., 1987), CODESA-3D (Galeati *et al*., 1992; Gambolati *et al*., 1999), FEMWATER (Lin *et al*., 1997) and SEAWAT (Guo and Langevin, 2002). A general review of such codes for simulation of saltwater intrusion is given by Sorek and Pinder (1999), Bear and Cheng (2010), and Werner *et al*. (2013).

2.3 Dynamics of saltwater and freshwater interaction

Coastal regions are considered to be the most vulnerable areas around the world, as about half of the world's population dwells within 100 km of the shoreline (Dose *et al*., 2014) and rely on freshwater aquifers for their survival. In the last few decades, with the growing global population and the tendency of people to live in the coastal areas, the demand for freshwater has been rising at an alarming rate and also has increased excessive groundwater pumping to satisfy

their daily water requirements for coastal populations. The indiscriminate and overexploitation of coastal aquifers has resulted in the significant decline of groundwater levels, and this has led to severe saltwater intrusion problems within coastal aquifers around the world. Therefore, a better understanding of the dynamics of saltwater and freshwater interaction is the severe concern in protecting water resources and other environmental challenges such as nuclear waste storage and geologic sequestration of CO_2. Over recent years, the predicted sea-level rise because of climate change has made it even more critical. However, several studies have been reported as regards to seawater-freshwater interactions using analytic and numerical models in the past years (e.g., Voss and Sousa, 1987; Oldenburg and Pruess, 1995; Gotovac *et al*., 2003; Simpson and Clement, 2004; Held *et al*., 2005; Servan-Camas and Tsai, 2010). Cooper *et al*. (1964) performed a study to examine the likely saltwater intrusion in coastal aquifers. They concluded that saltwater moves in constant cyclic motion, whereas a significant amount of intruding saltwater is passed back to the sea by dispersive mixing as a result of the tidal action and seasonal rainfall. The study revealed that the dispersion causes the wedge to be blunt in shape and so a wide transition zone exists between saltwater and freshwater. Through the numerical investigation, Ataie-Ashtiani *et al*. (1999) demonstrated that tidal effects are more significant in unconfined coastal aquifers that create a broad transition zone between saltwater and freshwater. Cheng *et al*. (2004) also numerically examined the impacts of tidal loading in the coastal aquifer of China, and they showed that the length of the aquifer roof increasing under the sea corresponds to the specific aquifer parameters in the extrapolation zone. Brovelli *et al*. (2007) conducted a numerical study to investigate the transport pattern of a dense contaminant plume subject to tidal variation in coastal aquifers. Simulation results indicated that the contaminant plume was mostly discharged from the seashore surface. They also simulated Zhang *et al*. (2002) experimental datasets to further study the interactions between the dense contaminant plume and the saltwater interface in the coastal aquifer system. They observed that the two dense water phases were never completely mixed, and the plume front was continuously removed from the main contaminated volume by the freshwater flow. Lately, Lu *et al*. (2009) and Lu and Luo (2010) numerically suggested that kinematic mass transfer between mobile and immobile domains could significantly explain the broad mixing zones. Yet again, Abd-Elhamid and Javadi (2011a) developed a finite element model to study saltwater intrusion in unconfined coastal aquifers. They considered transient density-driven flow and different phenomena governing solute transport in the model. Their numerical results demonstrated the performance of the model for simulating variable-density flow, velocity-dependent dispersion, and the effect of various

phenomena governing solute transport in saturated and unsaturated soils. The study concluded that the developed model could be employed in simulating of saltwater intrusion problems into unconfined coastal aquifers. In contrast, the effects of rainfall and surface spread recharge on saltwater intrusion can be examined.

In recent years, a few laboratory and field study has been carried out to investigate the interactions between saltwater and freshwater in coastal aquifers (e.g., Boufadel, 2000; Barlow, 2003; Kim *et al*., 2006; Taniguchi *et al*., 2006; Maekawa *et al*., 2007). Thorenz *et al*. (2002) presented an investigation to study the movement and interaction of freshwater and saline water in unconfined coastal systems. The laboratory experiments revealed that a significant lateral flow and coupled density-dependent flow effects would take place in the partially saturated zone as well as in the transition zone between the fully saturated and partially saturated regions. The findings from the experiments were corroborated by the numerical simulations, and the results suggested that the developed numerical model would be useful to provide realistic predictions. Goswami and Clement (2007) performed both laboratory and numerical experiments to investigate the saltwater wedge profile occurring in unconfined coastal aquifers. The authors used the SEAWAT model to simulate their experimental data sets. Their experimental data sets, along with the model results, were presented as benchmark problems for testing density-dependent groundwater flow models. The study concluded that their laboratory experimental data could be employed to evaluate the performance of saltwater intrusion models in both the steady-state and transient conditions. Abarca and Clement (2009) proposed a colorimetric method in order to characterize the transition zone between freshwater and saltwater in coastal aquifers. The experimental datasets were simulated using the SUTRA model. They estimated dispersivity coefficients by fitting model simulation results in a steady-state system. Based on their experimental results, they postulate that the proposed technique could be used for quantifying the mixing zone between saltwater and freshwater. Chang and Clement (2012) completed an experiment and numerical modeling study to investigate the saltwater intrusion dynamics in flux-controlled coastal subsurface systems. Their laboratory results were simulated using the numerical code SEAWAT. They presented a remarkable counterintuitive hypothesis that implies that the time scales associated with a receding saltwater wedge are relatively smaller than an intruding wedge. The insights gained from this investigation would be useful to understand the seawater intrusion processes occurring in a coastal aquifer. More recently, Lu *et al*. (2013) examined the effects of aquifer stratification on the thickness of a freshwater-seawater mixing zone under steady-state conditions. The authors conducted experiments in a laboratory

flow tank for homogeneous, high hydraulic conductivity (K)-low K-high K and low K-high K-low K cases. They also developed the tank-scale and field-scale numerical models to simulate the laboratory experiments and further to study the aquifer stratification effects on the steady-state mixing zone profile with varying layer formations. The authors demonstrate that the thickness of the mixing zone is independent of the magnitude of K for homogeneous aquifers and is a function of K contrast between layers in heterogeneous aquifers. They reported that the mixing zone profile in heterogeneous aquifers could significantly be affected by several factors, including layer thickness, K contrast between layers, freshwater head gradient, and dispersivities. The authors concluded that aquifer stratification would have significant impacts on associated physical, chemical, and biological processes in coastal subsurface systems.

2.4 Impacts of sea-level rise on saltwater intrusion processes

Saltwater intrusion (SI) in coastal aquifers is one of the main major challenges faced by water resource planners worldwide. Natural events such as the sea-level rise due to climate change and excessive pumping from the coastal aquifers are the leading causes that aggravate the saltwater intrusion problem significantly. Nevertheless, only a few research have devoted to understanding the combined impacts of anthropogenic factors and climate change (Li and Jiao, 2003a, b). Feseker (2007) performed a numerical study to examine the influences of climate change and changes in land-use patterns on the salt distribution in a coastal groundwater system. The study concluded that a significant rise of sea-level could accelerate the movement of saltwater intrusion. Several researchers have been conducted scientific investigations related to the effects of sea-level rise on saltwater intrusion dynamics in the last few decades. Oude Essink (2001) employed a 3D transient density-dependent groundwater flow model to simulate saltwater intrusion processes in the coastal aquifer in the Netherlands. They considered three types of sea-level rise scenarios, including without sea-level rise, a sea-level rise of 0.5 m per century, and a sea-level fall of 0.5 m per century. Based on the study, he concluded that a sea-level increase of 0.5 m per century would raise the salinity level in all lowland areas adjacent to the sea. Dausman and Langevin (2005) conducted a numerical investigation in coastal groundwater aquifer in Broward County, Florida. They used the SEAWAT code as the numerical simulator. The authors presented that several wells would be abandoned to chloride contamination if sea-level rise becomes more than 48 cm over the later 100 years. Lately, Loaiciga *et al*. (2011) used both FEFLOW code and hydrogeological data to evaluate the effects of sea-level rise and groundwater abstraction on seawater intrusion in the Seaside Area aquifer of Monterrey County, California, USA. They concluded that groundwater abstraction would

have a more significant contribution to seawater intrusion as compared to the sea-level rise. These investigations were based on field-scale modeling studies associated with a particular filed site. Through a conceptual modeling study, Werner and Simmons (2009) investigated the impacts of sea-level rise on groundwater aquifer systems with different types of boundary conditions. The modeling results demonstrated that the level of saltwater intrusion would depend on the inland boundary condition. They did not consider saltwater mixing effects and transient effects. Later, transient effects were explored by Webb and Howard (2011) under constant head boundary conditions. They employed a numerical model to investigate the changes in intrusion rates for a range of hydrogeological parameters. Moreover, several investigators have also presented fluctuations of sea-level and associated with the intrusion movement could impact on submarine discharge patterns adjacent to the coast and even influence the nutrient loading levels across the interface (Li *et al*., 1999; Li and Jiao, 2003b; Michael *et al*., 2005; Robinson *et al*., 2007; Li *et al*., 2008).

A few published studies have conducted laboratory-scale experiments to examine the impacts of sea-level rise on saltwater intrusion mechanisms. Illangasekare *et al*. (2006) investigated the transport pattern of seawater plumes in the tsunami-affected coastal aquifer system. They performed physical experiments in a laboratory flow tank model. The experimental results showed that the dense tsunami waters contaminated the deeper aquifer within a short duration of time. They observed that the tsunami waters remained floating over the saltwater intrusion wedge and eventually advected by the freshwater flow moving through the aquifer system along with the saltwater interface. Morgan *et al*. (2013) undertook physical experiments to assess the seawater intrusion overshoot phenomenon in the flux-controlled unconfined aquifer systems. They performed the sea-level rise (SLR) and sea-level drop (SLD) physical experiments in controlled laboratory conditions. They also conducted numerical simulations of both the SLR and SLD experiments for providing confidence in the results of the laboratory experiments. They observed an overshoot occurred for both the experimental cases. They reported that the magnitude of the overshoot changed 24% from the steady-state wedge position in both the physical experiments. They also demonstrate that the overshoot phenomenon is physically plausible and could be generated under controlled laboratory experiments. However, it is concern that a significant rise in sea levels would affect the quality of both surface and subsurface water supplies and also reduce the available freshwater resources. Therefore, the effect of climate change on saltwater intrusion in coastal systems is a severe environmental concern since almost

70% of the world's population resides in coastal areas (Bear *et al*., 1999; Cheng and Ouazar, 2003; Webb and Howard, 2011).

2.5 Control of saltwater intrusion problem

Groundwater is regarded as an indispensable freshwater resource for communities and ecosystems of the coastal regions that are continuously threatened by saltwater intrusion around the world. The leading causes of saltwater intrusion in coastal aquifers are the excessive unplanned withdrawal of groundwater resources and improper arrangement of pumping wells (Bhattacharjya *et al*., 2009). It extensively leads to increase salinity levels in coastal aquifers that making it unsuitable for human utilization and further restricts future exploitation of coastal aquifers. However, effective management strategies have to be taken to avoid further degradation of coastal aquifer systems under the threat of saltwater intrusion. The key to controlling saltwater intrusion is to maintain a seaward hydraulic gradient, and subsequently, an amount of fresh groundwater should be allowed to flowing towards the ocean. This hydraulic gradient delivers a hydraulic barrier against saltwater intrusion. Over the past decades, considerable attention has been received for examining the control of saltwater intrusion in coastal aquifers. However, several management strategies were proposed to prevent or mitigate saltwater intrusion and to secure groundwater reserves in coastal aquifers (Todd, 1959; Bruington, 1972; Dam, 1999; Oude Essink, 2001; Pool and Carrera, 2010; Kallioras *et al*., 2013). These including reduction of pumping rates, relocation of pumping wells, usage of physical subsurface barriers, natural or artificial recharge (injection or positive barriers), pumping of saline water along the coastline (extraction or negative barriers), combination techniques (mixed barriers) and land reclamation. Most of these methods are too expensive, and some of them are not applicable in some instances.

2.5.1 Reduction of pumping rates

The alarming growth in populations, substantial development of coastal resorts and coastal urbanization, and increasing agricultural activities, the demand for freshwater have been rising at an alarming rate. The excessive pumping of groundwater resources is thus unavoidable in many coastal regions throughout the world. As a result of the indiscriminate and overexploitation of groundwater resources leads to the significant decline of groundwater levels and resulting in saltwater intrusion along the coast (Bear *et al*., 1999). The reduction of extraction from pumping wells could be the most cost-effective countermeasure to maintain a proper balance between saltwater-freshwater in a coastal aquifer and control the saltwater intrusion. However, several

models have been developed to manage the saltwater intrusion problem by reducing the pumping rates from the aquifer system or using optimization models to optimize the extraction rates in controlling the saltwater intrusion. Zhou *et al*. (2000) conducted a study on the redistribution of pumping rates in existing wells in a coastal aquifer in Beihai city in China. They concluded that the removal of wells adjacent to the coast or across the intruded zone concurrently with the reduction of pumping in wells far away from the shoreline could secure the aquifer. Through a numerical study, Scholze *et al*. (2002) investigated the saltwater intrusion process in the coastal aquifer of Metro Cebu, Philippines. They used the SHEMAT code as the simulation model. The authors applied different scenarios of extraction and reduction in water consumption to securing groundwater reserves and evade saltwater intrusion. Based on the sensitivity analysis of saltwater intrusion to the pumping rate, Narayan *et al*. (2003) presented a numerical study of the Burdekin Delta aquifer in Australia. The authors used the SUTRA code as the simulation model for their research. They demonstrated that decreasing the groundwater extraction could effectually manage the seawater intrusion problem. This approach was also recommended by Tsanis and Song (2001) and Don *et al*. (2006). Yet again, Zhou *et al*. (2003) developed a quasi-3D finite element model to simulate the spatial and temporal distribution of groundwater levels in the layered aquifer in the Leizhou Peninsula in Southern China. The main focus of the study was to maximize the total extracted water by rearrangement of wells in controlling saltwater intrusion along the coast. Bhattacharjya and Datta (2005) used an artificial neural network (ANN) for density-dependent flow and transport in coastal aquifers to estimate salt concentrations of the extracted water. They formulated a linked simulation-optimization model to link the trained ANN models with a genetic algorithm (GA) based optimization model on solving saltwater intrusion management problems. The study aimed to allow the optimal extraction of groundwater from the aquifer system while maintaining the salt concentration of the pumped water under specified acceptable limits. Rejani *et al*. (2008) suggested that increasing the pumping rates from upstream and decreasing the rates in downstream regions could aid in receding the seawater intrusion in the Balasore basin in India, particularly in dry years. Recently, Sherif *et al*. (2013) revealed a 50% reduction of pumping would allow significant retardation of the dispersion zone of the order of a few kilometers in Wadi Ham aquifer in UAE. However, this approach is not a permanent solution to prevent seawater intrusion (Abd-Elhamid and Javadi, 2008). It only efforts to reduce it.

2.5.2 Relocation of pumping wells

In this practice, the existing pumping wells are usually relocated by dispersing them in the inland regions, which eventually aid in raising the groundwater level and maintain groundwater storage. It is noteworthy that finding the optimal pumping patterns, such as the locations and rates of extraction from relocated wells in controlling saltwater intrusion, has been mostly studied in the published literature using the simulation-optimization model. However, Maimone and Fitzgerald (2001) used the three-dimensional groundwater flow model, dual-phase sharp interface intrusion model, radial upconing model, and single-phase contaminant transport model to develop a management plan of coastal aquifers. They used two techniques based on developing new well locations away from the coastal area and the other one on the use of reverse osmosis (RO) treatment for desalinating brackish water for domestic purposes. Sherif and Al-Rashed (2001) employed 2D-FED and SUTRA model to simulate the saltwater intrusion problem in the Nile Delta aquifer in Egypt. They used the 2D-FED model as a simulator to assess the effect of sea-level rise in the Mediterranean Sea under the situation of global warming. The authors also employed SUTRA code to describe the adequate location of additional pumping wells under various pumping scenarios from the Nile Delta aquifer. Hong *et al*. (2004) developed a steady-state simulation-optimization model to assess both the optimal extraction and the location of pumping wells while diminishing adverse effects. The study involved experimental verification of the model in developing sustainable water resources in coastal zones. Ofelia *et al*. (2004) used a mathematical model in managing saltwater intrusion to secure groundwater in Santa Fe, Argentina. Several pumping wells were removed from the region, and a new pumping field was designed and implemented in the area. Mantoglou and Papantoniou (2008) investigated the optimal design of a pumping network for sustainable management of a coastal aquifer using two different optimization schemes. The GA was used to optimize both the pumping rate and locations of wells, and simultaneously, the combination of GA and sequential quadratic programming (SQP) was applied in two stages. The GA was firstly applied to find the optimal well locations at any generation, and then SQP was used to estimate the optimal pumping rates for relocated wells. They highlighted the performance of GA was better to find the optimal solutions than SQP. Lately, Datta *et al*. (2009) examined the effects of spatial variations of pumping from a set of five wells and in three different locations in a real study area in India. The sites of this set of wells in two different pumping regions along the coast presented better results while controlling saltwater intrusion rather than their locations in the middle zone. However, this

method could be a temporary solution and does not prevent seawater intrusion into the coastal aquifer system. This practice helps in reducing the occurrence of saltwater upconing.

2.5.3 Physical subsurface barriers

This method involves the creation of an impermeable subsurface barrier paralleling the coastline and through the vertical extent of the aquifer. The establishment of this barrier could achieve through sheet piles, clay trenches, cement grout, or injection of chemicals. The effectiveness of the injecting of cement grout was investigated by Sugio *et al*. (1987) in Okinawa-Jima Island in Japan using experiments and numerical simulations. Moreover, the Komesu underground concrete dam (cut-off wall) in Japan successfully developed on a large scale to protect the aquifer under the threat of saltwater intrusion (Nawa and Miyazaki, 2009). However, Harne *et al*. (2006) developed a 2D subsurface transport model for saltwater with constant seepage velocity under the homogenous and isotropic conditions. The authors employed the finite difference technique to solve the transport equation. The model investigated the efficacy of the subsurface barriers in controlling saltwater intrusion. A numerical study was carried out by Nishikawa *et al*. (2009) to investigate the effects of physical barriers in controlling saltwater intrusion. They simulated a 2D vertical section of Dominguez Gap coastal area of Los Angeles, California, using SUTRA code. Luyun *et al*. (2011) presented both laboratory and numerical experiments to examine the effects of subsurface flow barriers on controlling seawater intrusion in coastal unconfined aquifer systems. They used a finite-difference SEAWAT model to simulate their experimental results and found that their numerical model results closely match the experimental results. They reported that the physical barriers should be located adjacent to the seashore and at the toe front to be more productive. Recently, Kaleris and Ziogas (2013) used numerical models and approximate analytical solutions to examine the impact of the cut-off wall on the advancement of saltwater intrusion with or without the abstraction of groundwater. They reported that the physical barriers with more significant depth and located much closer to the shoreline, shown a great potential to retard saltwater intrusion. Abdoulhalik *et al*. (2017) conducted an experimental and numerical study to investigate the impact of physical barriers on saltwater intrusion dynamics under transient conditions. The authors suggested the mixed physical barrier (MPB) as a new barrier system to control saltwater intrusion, which combined an impermeable cutoff wall and a semi-permeable subsurface dam. The results showed that the MPB induced upward lifting of dense saltwater towards the coastline and induced significant length reduction to the saltwater. More recently, Li *et al*. (2018) carried out a detailed laboratory

and numerical investigation to study the saltwater intrusion dynamics with and without subsurface flow barriers. The authors adopted the finite-element numerical model FEFLOW to simulate their experimental results. They also evaluated the efficiency of subsurface flow barriers with different permeability coefficient values to prevent saltwater intrusion.

However, this is the most effective management strategy for preventing saltwater intrusion into the coastal aquifer and does not need maintenance and restoration activities over a lifetime (Allow, 2012). The technique is only applicable to shallow aquifers, and also too costly.

2.5.4 Artificial recharge

In this approach, freshwater is injected artificially into the aquifer system through recharge wells to maintain a proper balance between saltwater-freshwater. The injected water may be the surface water, rainwater, extracted groundwater, treated wastewater, or desalinated water. This method helps to increase the outflow of groundwater through the coastal aquifer and hence reduce the saltwater intrusion wedge in length. Recharge wells and surface spreading are used for confined and unconfined coastal aquifers, respectively. It involves the development of an additional water source. This technique is among the most popular approaches that are commonly recommended in the published literature.

Mahesha (1996) presented the steady-state solutions for the movement of saltwater intrusion wedge with a series of injection wells in a confined aquifer system using a sharp interface finite element model. He performed parametric studies on the influence of the set of injection wells locations, the spacing of the wells, and the injection rate of freshwater on the saltwater intrusion dynamics. The reduction of saltwater intrusion wedge (of up to 60-90%) could be attained through the appropriate selection of injection rate and spacing between the wells. He also studied the impact of the double series of injection wells and compared them with the single set of wells. He demonstrated that a double series of injection wells performs slightly better than a single series, and the staggered system of the series of injection wells is marginally better than the straight well system for long spacing. Liles *et al*. (2001) developed a groundwater model to forecast of injection quantities and well locations in preventing saltwater intrusion. They used highly treated wastewater for injecting into Orange County aquifers to retard saltwater intrusion. Papadopoulou *et al*. (2005) developed a 3D finite element-finite difference groundwater flow simulation model. The extension of the saltwater interface along the coast was only hydraulically determined. They did not consider dispersion owing to different densities of ambient freshwater and saltwater. Artificial recharge was presented under various scenarios with different well

locations and different injection rates. Vandenbohede *et al*. (2008) presented a numerical study in investigating sustainable water resource management via artificial freshwater recharge in the dunes of the western Belgian coastal plain by two recharge ponds. They produced recharge water from secondary treated wastewater effluent by the combination of ultrafiltration and reverse osmosis. Lately, through laboratory experiments, numerical and analytical modeling, Luyun *et al*. (2011) examined the effects of recharge wells on controlling seawater intrusion in coastal unconfined aquifer systems. They concluded that more effective saltwater repulsion could be achieved while the recharge water is injected at the toe of the saltwater interface. Also, the efficiency of this technique was numerically evaluated by Allow (2012) for a range of real-world case studies. Extensive research was carried out by Acosta and Donado (2015) to investigate the performance of hydraulic barriers in controlling seawater intrusion. They also studied the effects of location and rate of injection on saltwater wedge under homogeneous and stratified soil conditions. The experimental results indicate that the highest reduction of saltwater intrusion wedges can be achieved if the injection is applied at the extreme point of a wedge with a higher rate. More recently, the decisive role of freshwater recharge was analytically affirmed by Lu *et al*. (2017), introducing the two different recharge schemes (well injection and pond infiltration) in an aquifer system to control saltwater intrusion. The study highlighted that the performance of the two recharge schemes in controlling saltwater intrusion is the same if the infiltration pond is circular and not located above the interface region. They concluded the shape of the elliptic infiltration pond controls the maximum net extraction rate of the pond infiltration-well extraction system. However, the implementation of artificial recharge is often expensive and could be unproductive under extensive pumping (Narayan *et al*., 2007). Also, the unavailability of water in local regions, especially in dry seasons or areas that face scarcity of water, could be another significant restriction in applying this barrier (Abd-Elhamid and Javadi, 2011b).

2.5.5 Extraction barrier

This method aims to reduce the saline water volume by continuously abstracting brackish water through deep extraction wells located adjacent to the coastline. The abstracted brackish water can be directly discharged into the sea, or it may be used to feed desalination plants. It could also be used in industrial activities (Dam, 1999; Sherif and Hamza, 2001).

Sherif and Hamza (2001) developed a finite element model to simulate the effect of the extraction of saline water from the diffusion zone in coastal aquifers. Their results revealed a significant reduction of the width of the dispersion zone as a result of the abstraction of brackish

water. The same methodology of extracting brackish water near the seashore was assessed by Sherif and Kacimov (2008) using the SUTRA code for a hypothetical confined aquifer. They examined different pumping scenarios to reduce the extension of saltwater intrusion. The study concluded that saltwater intrusion problems could be managed through the proper pumping of saline water from the coastal aquifer systems. Park *et al*. (2011) employed the 3DFEMFAT model to investigate the influence of different parameters on the quality of extracted water from another production well. They considered different parameters, including the rate of pumping from the barrier well, the horizontal distance of barrier well from the coastline and the production well, the depth of the barrier well in the aquifer system, and the number of these barrier wells in their study. They examined in different cases of sensitivity analysis on a hypothetical aquifer model.

Moreover, many researchers were previously studied in protecting inland wells using a series of extraction barriers within simulation-optimization frameworks (e.g., Das and Datta, 1999, 2001; Bhattacharjya and Datta, 2009; Sreekanth and Datta, 2010, 2011; Hussain et al., 2015; Javadi *et al*., 2015). In general, the extraction barriers cause the decline of water level near the coastline that increases the seaward hydraulic gradient of ambient freshwater and protects the aquifer. The critical problem in these barriers involves the disposal of the salty water. Many researchers have previously attempted to solve this problem. However, it is still a research subject for further study.

2.5.6 Land reclamation

This approach involves the artificial extension of the shoreline towards the sea or ocean. In this process, a foreland is created by hydraulic filling of the proper soil at the preferred geometry and slope above sea level, where a freshwater body could develop that may delay the inflow of saline groundwater (Oude Essink, 2001). Increasing the distance between the inland well and the seaside and as well providing more area to cope up with the natural rainfall are the other useful effects of this barrier to retard saltwater intrusion (Chen and Jiao, 2007; Guo and Jiao, 2007, 2009). However, Chen and Jiao (2007) investigated the hydro-geochemical properties of coastal groundwater in Shenzhen city in China throughout the rapid urbanization phase. The study showed, based on the hydro-geochemical properties of groundwater, the coastal subsurface system experiences significant retardation of saltwater intrusion due to land reclamation. Yet again, the observing results of the groundwater levels in the coastal aquifer of Shenzhen city in China revealed the groundwater level also uplifted during the land reclamation (Hu and Jiao,

2010). Also, the rising of the groundwater level and saltwater intrusion movement towards the seaward were analytically demonstrated by Guo and Jiao (2007, 2009) under the land reclamation condition. However, the total cost of constructing this barrier on a large scale is the key restriction to this practice. Also, the properties of the filling soil should be reasonably well defined.

2.5.7 Combined barrier

Apart from above these methods, a combination of some of the strategies mentioned earlier has been used by many researchers to better control of saltwater intrusion problems in coastal aquifers. For instance, Zhou *et al*. (2003) and Hong *et al*. (2004) used a combination of a reduction in pumping rates and relocation of pumping wells to retard further saltwater intrusion. Maimone and Fitzgerald (2001) used the three-dimensional groundwater flow model, dual-phase sharp interface intrusion model, radial upconing model, and single-phase contaminant transport model to develop a management plan of coastal aquifers. They used two techniques based on developing new well locations away from the coastal area and the other one on the use of reverse osmosis (RO) treatment for desalinating brackish water for domestic purposes. Paniconi *et al*. (2001), Barrocu *et al*. (2004), and Narayan *et al*. (2007) employed a reduction of pumping rates and recharge of freshwater to the aquifer to control saltwater intrusion. Recently, Cherubini and Pastore (2011) suggested a solution based on a reduction of well density coupled with artificial recharge to retard saltwater intrusion for a local aquifer in Italy. Another possible technique of this strategy is the combination of positive and negative barriers known as the mixed barrier. This approach mainly involves the specification of both extraction and recharge. Javadi *et al*. (2012) proposed a combined methodology based on the continuous abstraction of saline water adjacent to the coastline, desalination of the extracted saline water and the desalinated water as a source of artificial recharge through injection wells in mitigating saltwater intrusion. The authors suggested that the technique is beneficial and economical for controlling saltwater intrusion problems in coastal systems. Further, many researchers have been recommended that the mixed barrier is the most effective technique in controlling saltwater intrusion among the other barriers (e.g., Troisi *et al*., 1994; Tsanis and Song, 2001; Rastogi *et al*., 2004; Koussis *et al*., 2010a, b; Kourakos and Mantoglou, 2013, Hussain *et al*., 2015; Javadi *et al*., 2015).

2.6 Applications of groundwater circulation well (GCW)

The GCW is one of the most promising in-situ remedial techniques of groundwater. This technique was first suggested by Herrling and Buermann (1990) and Herrling *et al*. (1990) for remediating contaminated groundwater aquifer. In this system, a circulation flow is created between the inlet and outlet screen located in a single well with specified vertical distance by keeping the head difference between the inlet and outlet screen (Herrling *et al*., 1991; Gonen and Gvirtzman, 1997; Stamm, 1998). This circulation flow flushes the contaminated water within the proximity of the well. The abstracted contaminated groundwater from the aquifer system could be cleaned with activated carbon, and after treatment, the remediated water can be injected back into the aquifer. Extreme care should be taken into account in designing and implementing the GCW system to the contaminants are removed efficiently and cost-effectively. The design process and operation of the GCW system have widely been explored (e.g., Herrling *et al*., 1990, 1991; Gvirtzman and Gorelick, 1992). Comprehensive studies were performed numerically to estimate the various parameters that influence the GCW system, the sphere of influence, and the remediation process (Herrling and Stamm, 1993). The data collected from several pilots and field-scale studies facilitated to improve the design procedure, operation, and application of the GCW system (Herrling *et al*., 1991; U.S. EPA, 1995; Stallard *et al*., 1996; Stamm 1998). Stallard *et al*. (1996) reported a groundwater circulation well design whereby extraction is achieved at the well bottom, treated in the well casing, and after treatment reinjected into the aquifer at the well top. However, the GCWs have extensively used for in-situ remediation of groundwater in porous media (e.g., Herrling *et al*., 1991; U.S. EPA, 1995, 1998; Miller and Roote, 1997; McCarty *et al*., 1998). Scholz *et al*. (1997, 1998a) and Mohrlok *et al*. (2000, 2003) studied the operation and treatment efficiency of GCW system through large-scale 3D laboratory experiments in a heterogeneous aquifer system with dense nonaqueous phase liquids (DNAPL) and light nonaqueous phase liquids (LNAPL) as contaminants. Scholz and Stamm (1997) and Scholz *et al*. (1998b) presented the results from a complete field study in a heterogeneous porous media for remediation of chlorinated hydrocarbons (CHC) using a GCW. Knox *et al*. (1997) conducted a field-scale study with the GCW system to assess surfactant-enhanced remediation of PCE contamination in an unconfined aquifer. Some experimental investigations suggested that GCW is a very useful in-situ remediation technique for removing NAPL contaminants in groundwater (e.g., Scholz *et al*., 1997, 1998a; Mohrlok *et al*., 2000, 2003). Kirubaharan *et al*. (2008) presented laboratory and numerical experiments for DNAPL remediation in an artificial aquifer using the GCW. The study demonstrated various flow and transport characteristics in the

groundwater circulation flow field for in-situ remediation. Lately, Papini *et al*. (2016) conducted a pilot study in a heavily contaminated industrial site to remove chlorinated solvents using the GCW technique. The study demonstrated that the GCW enhanced the biological reductive dechlorination inside the less permeable layer and also reducing the remediation time.

Moreover, GCWs have already been applied to remove volatile organic contaminants (e.g., Gvirtzman and Gorelick, 1992; Pinto *et al*., 1997; Scholz *et al*., 1998c; Allmon *et al*., 1999; Montgomery *et al*., 2002; Drizin *et al*., 2008) and nonvolatile organic substances (Elmore and Graff, 2002) from the groundwater aquifers. Elmore and Graff (2002) employed the GCW system to remove trichloroethylene (TCE) contaminants and the explosive compound (RDX) in Nebraska. The study showed that the GCW technology is competitive with conventional pump-and-treat methods. However, Zhao *et al*. (2016) investigated the efficacy of the GCW system for in-situ remediation of aniline contaminated aquifer. They demonstrated that the aniline contaminants survived the GCW treatment process with high aniline degrading efficiency. The study presented a novel methodology for the in-situ bioremediation of low-volatile pollutants. More recently, Tawabini and Makkawi (2018) presented a study to assess the efficacy of a groundwater remediation system to treat a shallow aquifer contaminated with MTBE. The study revealed a novel method for the removal of MTBE from contaminated groundwater using GCW combined with UV-based advanced oxidation technology. The study also indicated that the concentration of MTBE was decreased from 1,400 μg/L to 34 μg/L with a treatment efficiency of about 98%.

To date, several researchers have also been used the GCW technique to determine the aquifer properties (e.g., Kabala, 1993; Zlotnik and Ledder, 1994, 1996; Indelmaan and Zlotnik, 1997; Zlotnik and Zurbuchen, 1998, 2003; Halihan and Zlotnik, 2000; Zlotnik *et al*., 2001). Kabala (1993) developed a new single-borehole measurement technique named the dipole flow test (DFT) for the characterization of confined aquifers. This test creates a dipole flow pattern between the extraction and injection chambers in the aquifer. He used transient measurements of drawdown in the chambers to estimate both the horizontal and vertical hydraulic conductivities and the specific storativity. Sutton *et al*. (2000) developed the dipole flow tracer test (DFTT) for the estimation of particular aquifer properties. This test separates the abstraction and injection chambers in the borehole and employs a small pump to form a dipole flow pattern in the aquifer. They measured drawdown of hydraulic head in the well chambers at steady state. They also used the stream tube method to semi-analytically simulate the tracer transport in DFTT and determine the required relationships to estimate the radial and vertical hydraulic

conductivities as well as the longitudinal dispersivity. This test also allows for the estimation of the aquifer hydrodynamic and sorption parameters. However, the GCW system has been established as a most promising in-situ remedial technique of groundwater contamination. The technique involves low energy requirements in terms of operation and monitoring and minimally invasive and non-disruptive to site conditions as compared to other conventional methods.

2.7 Conclusions

This chapter reviewed the general mechanism of saltwater intrusion processes, its consequences, and potential solutions to reduce and manage the saltwater intrusion problems within coastal groundwater aquifers. A detailed review was also presented on the general history of the application of groundwater circulation well (GCW) systems. As evident from the review of the existing strategies for coastal aquifer management, the implementation of hydraulic barriers has increased in controlling the saltwater intrusion problem than other management strategies. However, the systematic review of the literature shows that many researchers have used the GCW for remediation of groundwater contamination. Nevertheless, the GCW system has not been tried to control the saltwater intrusion processes in coastal aquifers by using it as a hydraulic barrier. In the case of conventional hydraulic barriers, the groundwater is withdrawn from the coastal aquifer to create a hydraulic gradient, so that saltwater cannot cross the pumping well. However, in this process, the aquifer water is taken out and generally thrown into the sea. On the other hand, in the case of GCW, there is no loss in aquifer water. Thus by circulating the same water, a barrier can be created, and the saltwater wedge can be pushed back to the seaside. As such, there is a scope to make an effort to investigate the behavior of saltwater intrusion dynamics under a GCW system. Through the evaluation of this management strategy, the limitations on both the economic and environmental costs should be taken into account that could help to establish the most cost-effective management strategy to control saltwater intrusion problems in coastal aquifers.

CHAPTER 3

Laboratory-scale Investigation of Saltwater Intrusion Dynamics

3.1 Introduction

Saltwater intrusion (SI) in coastal aquifers is one of the main major challenges faced by water resource planners worldwide. The alarming growth in populations, substantial development of coastal resorts and coastal urbanization, and increasing agricultural activities, the demand for freshwater have been rising rapidly. The excessive pumping of groundwater resources is thus unavoidable in many coastal regions of the world. As a result of the overexploitation of coastal aquifers, the hydraulic potential has lowered significantly, and this has led to saltwater intrusion problems in coastal aquifers (Bear *et al*., 1999). Moreover, catastrophic events such as tsunamis, hurricanes, and droughts could result in severe saltwater intrusion into coastal aquifers and consequently deteriorates groundwater quality within coastal aquifer systems. A quantitative understanding of the dynamics of saltwater intrusion processes in coastal groundwater aquifers is, therefore, a significant research problem for efficient planning and management of coastal marine and estuarine environments.

In particular, physical models are valuable and efficient research tools to understand as well as visualize the processes and also for verifying the analytical and numerical models. In this regard, physical aquifer models have been extensively used to characterize the mixing zone profiles and to study the behavior of saltwater intrusion wedges (e.g., Schincariol and Schwartz, 1990; Zhang *et al*., 2002; Goswami and Clement, 2007; Abarca and Clement, 2009; Konz *et al*., 2009a, b; Werner *et al*., 2009; Abdollahi-Nasab *et al*., 2010; Jakovovic *et al*., 2011; Luyun *et al*., 2011; Stoeckl and Houben, 2012; Chang and Clement, 2012; Lu *et al*., 2013; Morgan *et al*., 2013; Dose *et al*., 2014; Mehdizadeh *et al*., 2014; Li *et al*., 2018). The overarching aim of this research is to conduct experimental studies to develop a better scientific understanding of the dynamics of saltwater intrusion processes in a coastal unconfined aquifer. In this effort, a series of physical experiments have been carried out in a laboratory-scale aquifer model to have a better understanding of the dynamics of this phenomenon under different scenarios. The current chapter gives a brief description of the experimental setup and materials that are used in experiments in order to achieve the objective of the present study. Moreover, the details of all the laboratory-scale experiments and results have also been presented in this chapter.

3.2 Laboratory Approach

3.2.1 Experimental Setup

A series of laboratory-scale experiments were carried out in a glass-sided flow tank. The flow tank used was constructed of 6 mm thick glass sheets so that the dyed plume could be distinctly observed. The cross-section of the flow tank was rectangular, with internal dimensions of length 55.6 cm, width 6.8 cm, and a total height of 40 cm (Figure 3.1).

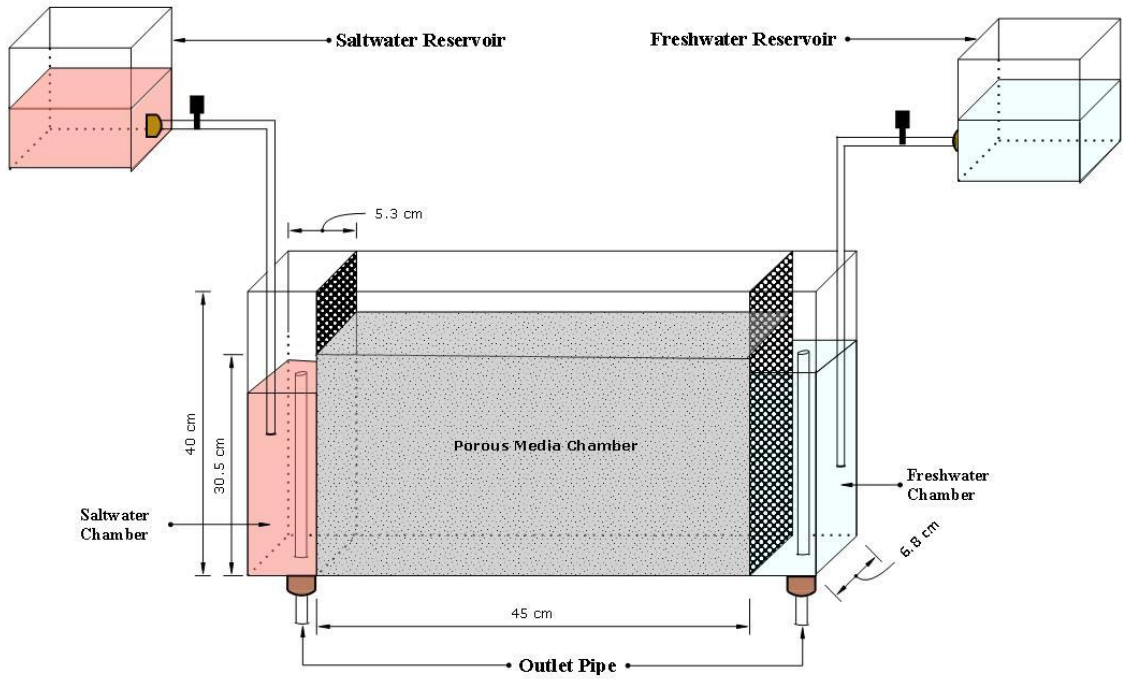

Figure 3.1: Schematic diagram of the experimental setup

As shown in Figure 3.1, the flow tank model is composed of three distinct flow chambers, and the central viewing flow chamber served as the porous media (the aquifer). To model a coastal unconfined aquifer system, the central flow chamber was packed with clear glass beads under fully saturated conditions. The tank used was flanked by two flow chambers at either side for maintaining constant hydrostatic pressure boundary conditions across the flow tank. The left and right side flow chambers were assigned to represent the coastal and inland boundary, respectively. The saltwater solution was supplied into the saltwater chamber from an overhead reservoir at a constant flow rate and discharged through an adjustable outlet pipe to hold a constant salinity and water head in the saltwater chamber throughout the experiments. In a similar way, the freshwater chamber was supplied with fresh water from the overhead reservoir

and maintained at the required level. The side flow chambers are each 5.3 cm long. Both the side flow chambers are each separated from the central chamber by perforated plexiglass sheet of thickness 7 mm and further wrapped by 500-micron fine stainless-steel mesh screens to prevent the passage of porous material from the central flow chamber to the side ones. Printable rulers were pasted on the sides and at the bottom of the flow tank for quick measurement of the saltwater wedge profile as well as the water heads at the side boundary.

3.2.2 Materials Used

Commercially available glass beads, commonly used for road marking, were used as the porous media in all the experimental runs (Figure 3.2). In particular, glass beads have been extensively used to represent the porous media as used by various researchers in their research work (Volker *et al*., 2002; Zhang *et al*., 2002; Goswami and Clement, 2007; Abarca and Clement, 2009; Luyun *et al*., 2009, 2011; Chang and Clement, 2012, 2013, etc.) and thereby the clear glass beads have been used to represent the aquifer material in this study.

Figure 3.2: Sample of glass beads used in the study

Sieve analysis was carried out to determine the particle size of the glass beads (Figure 3.3), and the median grain size (D_{50}) was found to be 0.57 mm. A uniformity coefficient (D_{60}/D_{10}) was also estimated as 1.78, indicating that the grain size distribution of the glass beads is relatively uniform (Simmons *et al*., 2002). The granulometric properties of porous media material were obtained as given in Table 3.1.

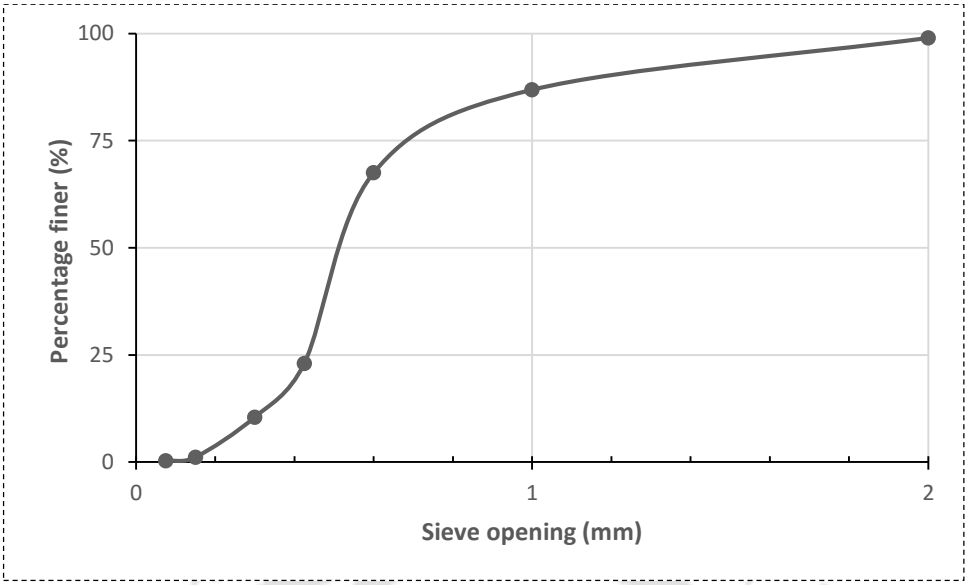

Figure 3.3: Grain size distributions of glass beads used in the study

Table 3.1: Granulometric properties of glass beads used in the present study

Parameter	Value
D_{10}, mm	0.359
D_{30}, mm	0.488
D_{50}, mm	0.575
D_{60}, mm	0.642
C_u (= D_{60}/D_{10})	1.788
C_c {= $(D_{30})^2/D_{10}\times D_{60}$}	1.033

Prior to the laboratory experiments, a saltwater solution was prepared by dissolving 35 g of commercial salt (NaCl) in 1 L of tap water, yielding an adequate concentration of 35 g/L. Food color has been effectively employed to act as a dye tracer in several variable-density flow experiments in the published literature (e.g., Zhang *et al*., 2002; Goswami and Clement, 2007; Luyun *et al*., 2009, 2011; Goswami *et al*., 2012; Kuan *et al*., 2012; Chang and Clement, 2013; Oz *et al*., 2014), and has the benefits of non-sorbing, very cheap and non-reactive. Therefore, 3.125 ml of red food color in a liter of the saltwater solution was added to discriminate it from ambient freshwater. The density of both dyed saltwater solution and freshwater was measured using a specific gravity hydrometer (G8030@JAPSINR). The density of dyed saltwater was estimated to be 1.025 g/cm^3 and that of freshwater to be 0.997 g/cm^3. The addition of red color dye did not produce any measurable change in the density of the saltwater solution (Chang and

Clement, 2013; Oz *et al.*, 2014). On the other hand, tap water used as freshwater in all the experiments. The laboratory-scale experiments were carried out at room temperature of 27^0C.

In the present study, a 12V micropump having a maximum discharge rate of 7 cm^3/s has been used to apply freshwater injection or extraction. To prevent the passage of porous material into the pump, a pump screen was made by rolling a fine stainless-steel mesh screen into a cylindrical shape (Figure 3.4). The pump screen was 4 cm long and a diameter of 1 cm. A tube of 4 mm diameter was inserted into it for connecting to the pump, and the bottom and top annular space between the tube and roll was sealed with M-Seal adhesive. A fitted mechanism is allowed to the pump withdrawal pipe for controlling the discharge.

Figure 3.4: Pump screen used in the present study

In addition, the slot for installing the flow barrier material was constructed by two Plexiglas strips wrapped by fine stainless-steel mesh screens that separate the barrier slot from the flow tank preventing the passage of glass beads inside the slot. The barrier slot is 32.5 cm height, 4.3 cm width, and a thickness of 1.3 cm (Figure 3.5).

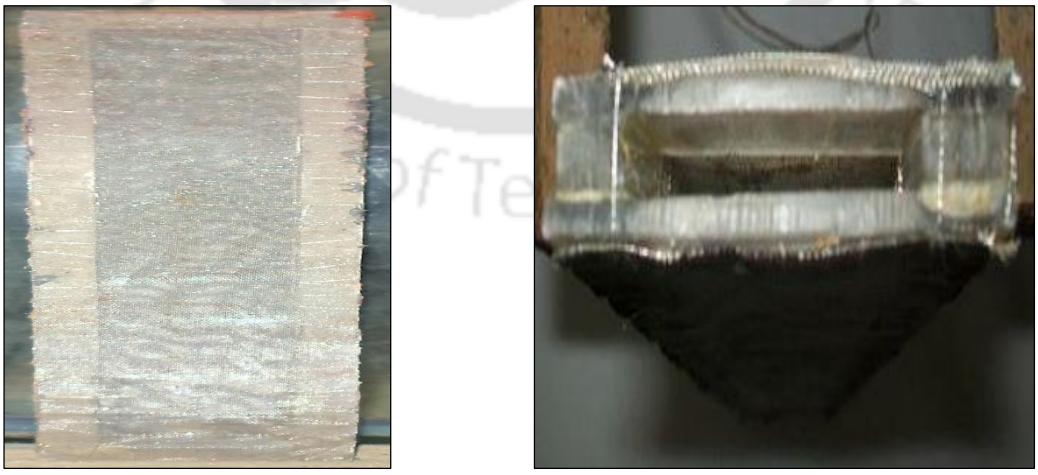

(a) Front view of barrier slot (b) Top view of barrier slot

Figure 3.5: Barrier slot used in the present study

3.2.3 Experimental Procedures

Prior to each laboratory experiment, the porous chamber of the flow tank was filled with clear glass beads to simulate a coastal unconfined aquifer. The glass beads were tamped under fully saturated conditions to avoid air entrapment within the aquifer. The glass beads were packed from the bottom up to a height of 30.5 cm in layers of about 5 cm. The glass beads were carefully compacted within the flow tank to achieve a homogenous packing condition after each layer was complete. After filling the aquifer, the entire system was initially flushed with tap water at a constant rate from the overhead freshwater reservoir through a fixed hydraulic head gradient. This hydraulic gradient was large enough to transmit fresh water through the system toward the saltwater chamber. The freshwater and saltwater heads in the respective chambers were measured from the bottom of the flow tank. The system was then allowed to continue until it reaches a steady-state flow. After the freshwater flow stabilized, the in situ method similar to that applied by Goswami and Clement (2007) was adopted to estimate the hydraulic conductivity of the porous media. The average value was determined to be 0.251 cm/s. The porosity of the porous media was calculated using the volumetric method, and its mean value was measured as 0.43. Table 3.2 presents the geometrical and hydraulic properties of porous media.

Table 3.1: Properties of the porous media

Parameter	Value
Average grain size, mm	0.57
Average bulk density, g/cm^3	1.443
Specific gravity	2.49
Average hydraulic conductivity, cm/s	0.251
Porosity	0.43

After a steady-state flow was established, the saltwater chamber was then fed quickly with the red-dyed saltwater solution from the overhead saltwater reservoir through the bottom to replace freshwater, and once the saltwater attained a constant level, the saltwater began to intrude the entirely freshwater aquifer. The saltwater intrusion process was then allowed to progress through the system until an equilibrium saltwater wedge position was obtained. As the saltwater intrusion process advanced, the location of the toe of the intruding wedge was determined and captured through digital images at different times. All the laboratory-scale experiments were performed after the establishment of the steady-state saltwater wedge.

The left bottom corner of the central chamber was considered as the origin to record experimental observations. All the laboratory-scale experiments were captured at various time

intervals with a Nikon digital camera. A digital timer is used to record the experimental timing. The captured color images were cropped and presented at a suitable scale to provide better visualization.

3.3 Laboratory-scale Experiments: Results and Discussions

A series of physical experiments have been carried out in a laboratory-scale flow tank model in the present study. They are presented in the following sections.

3.3.1 Pumping of freshwater

This first experiment has been carried out to investigate the effect of pumping on the saltwater intrusion dynamics in a coastal unconfined aquifer. The pump screen was initially emplaced within the aquifer at the desired location before packing the aquifer. That allows for starting the pump at any stage of the experiment without disruption of aquifer media. After filling the aquifer, the overflow outlet pipes were adjusted to maintain constant heads of 28.2 and 27.3 cm on the freshwater and saltwater boundary, respectively. This hydraulic gradient allowed to transmit freshwater towards the saltwater boundary. The steady-state saltwater intrusion wedge was achieved in about 30 min in the experiment. After attaining the steady-state saltwater wedge, the extraction pump was then started at a rate of 2.52 cm^3/sec. The time of starting the pump was noted as 30 min, and the location of the pump in the flow tank was: x = 33 cm, y = 4 cm, and z = 7 cm. The digital photographs were captured at different times to investigate the saltwater intrusion dynamics under the effect of pumping. This laboratory experiment was continued till at 58 min.

Figure 3.6 shows the transport patterns of saltwater intrusion wedge under the pumping condition. The color image taken from the flow tank experiment at the steady-state is shown in Figure 3.6(a). At the steady-state, the toe of the saltwater wedge was located at 11 cm from the saltwater chamber, and the height of the wedge at the saltwater boundary (at x = 0) was 15 cm. Figure 3.6(b) and Figure 3.6(c) shows the saltwater wedge profile at 48 min and 58 min respectively. The toe and elevation of the saltwater wedge were estimated respectively as 26 cm and 23 cm (at t = 58 min).

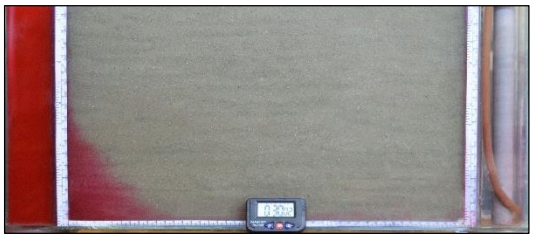

(a) 30 min (Steady State)

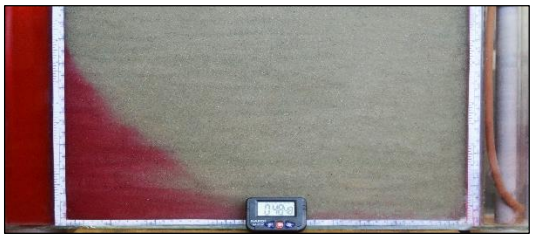

(b) 48 min

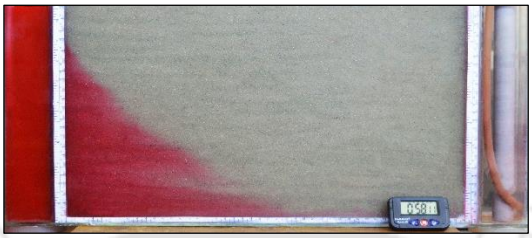

(c) 58 min

Figure 3.6: Pumping of freshwater experimental results at (a) 30, (b) 48, and (c) 58 min

The digital data depicts that after the initiation of pumping, the saltwater wedge rapidly advances through the system towards the freshwater boundary. As the initiation of pumping establishes a transient flow pattern that leads to a lowering in the water table within the system, and consequently, the wedge moves towards the landward direction. It might have eventually reached the pump if the pumping was continued. From the experimental data, it can be observed that a considerable mixing of saltwater and freshwater occurs during the intrusion period. The mixing takes place due to the advection occurs as a result of pumping. The laboratory data also indicate that the saltwater wedge forms a slight finger-like pattern near the bottom of the flow tank. It may be due to the non-uniformity of the packing of the porous media within the flow tank.

3.3.2 Injection of freshwater

This experiment was conducted to examine the effects of freshwater injection on the saltwater wedge in unconfined coastal aquifer systems. This laboratory-scale experiment was continued from the previous experiment. After completing the previous experiment, the freshwater head in the right flow chamber was instantly increased, and the saltwater supply was stopped into the left chamber for some time. That allowed the saltwater wedge to flush out from the system completely. After that, the head in the freshwater chamber was then readjusted to 28.2 cm as similar to the previous experiment. The head in the left flow chamber, as well as the position of the pump, was to remain unchanged from the previous experiment. The steady-state

saltwater intrusion wedge was reached in about 38 min. After steady-state saltwater wedge was attained, the injection pump was then initiated at a rate of 2.5 cm^3/sec. The injection pump was started at 55 min and continued till 89 min. Similar to the previous experiment, digital photographs were recorded at different time intervals to examine the dynamics of the saltwater wedge with injection.

Figure 3.7 indicates the transient datasets for the freshwater injection experiment. The transient datasets were recorded at various time intervals from starting of the experiment. The digital photograph taken at the steady-state is shown in Figure 3.7(a). At the steady-state, the toe of the saltwater wedge was located at 11 cm from the coastline, and the elevation of the wedge at the saltwater boundary (at x = 0) was 14 cm. Figure 3.7(b) and Figure 3.7(c) shows the transport patterns of the saltwater wedge from the steady-state. These photographs were taken at 75 min and 89 min, respectively. The toe and elevation of the saltwater wedge were measured respectively as 8 cm and 10 cm (at t = 89 min). A slight reduction of the saltwater wedge profile has been observed from the steady-state.

(a) 38 min (Steady State)

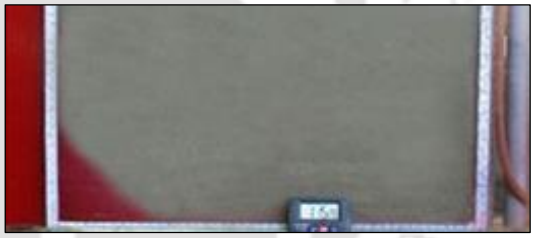

(b) 75 min

(c) 89 min

Figure 3.7: Freshwater injection experimental results at (a) 38, (b) 75, and (c) 89 min

It can be seen in Figure 3.7, upon application of the injection pump, the saltwater wedge gradually recedes through the system towards the saltwater boundary as the initiation of freshwater injection establishes a transient flow pattern that leads to an increase in the water table within the system, and that injected freshwater flow regime drives the wedge towards the coast. Hence, it could be concluded that the injection of freshwater as a hydraulic barrier can be used for preventing the saltwater intrusion towards the inland side.

3.3.3 Flow barrier experiment

In general, the construction of subsurface flow barriers is one of the most extensively used engineering countermeasures to prevent or mitigate the SI problems in coastal aquifers. A laboratory-scale experiment has successfully been conducted to assess the efficiency of bentonite clay slurry on controlling the problem.

In this experiment, the barrier slot and pump screen were initially emplaced at the desired location within the porous media before the packing of the glass beads. That allows for starting the pump or installation of barrier material at any stage of the experiment without disruption of aquifer media. The slot for installing the flow barrier is placed within the porous media at a distance of 10 cm from the coastal boundary, as flow barriers are usually located at distances less than or equal to twice the aquifer height from the seaside (Japan Green Resources Agency, 2004; Allow, 2012) and should be located within the saltwater wedge area for good effectiveness (Luyun *et al*., 2011). Bentonite clay slurry has been used as the barrier material in this study. The slurry was prepared by mixing 50 g of bentonite clay with tap water of 290 ml. Hydraulic conductivity of the used bentonite clay was determined by using the constant-head laboratory method, and the average value was estimated to be 1.39×10^{-10} cm/s. A thin layer of bentonite paste was also used on either side of the barrier slot to avoid any leakage of glass beads through sides. The height of water levels on the freshwater and saltwater boundary was set to 28.3 and 27.3 cm, respectively, yielding a head difference of 1 cm in this experiment. The steady-state saltwater intrusion wedge was obtained in about 28 min. After reaching the steady-state saltwater wedge, the extraction pump was then started at a rate of 1.52 cm^3/sec, and the subsequent migration pattern of the saltwater intrusion wedge was observed. The time of beginning the pump was noted as 29 min and stopped at 39 min. The location of the pump in the flow tank was: x = 33.5 cm, y = 3.6 cm, and z = 15 cm. The barrier material was inserted carefully into the slot at 35 min from starting the experiment. The experiment was continued until 85 min, and experimental observations were recorded at different time intervals.

Figure 3.8 represents the transport patterns of saltwater intrusion wedge in the flow tank. The photographs were taken at 28, 42, and 85 min after starting the experiment. The color image taken from the experiment at the steady-state is shown in Figure 3.8(a). At the steady-state condition, the toe of the saltwater wedge was located at 7.5 cm from the saltwater boundary, and the height of the wedge at the coastline (at x = 0) was 22 cm. Figure 3.8(b) and Figure 3.8(c) show the saltwater wedge profile at 42 min and 85 min, respectively. After 6 min of pumping, the toe and elevation of the wedge were shifted to 9 cm and 24 cm, respectively. As can be

observed in Figure 3.8(c), the toe and height of the saltwater intrusion wedge were estimated respectively as 9 cm and 27 cm (at t = 85 min).

(a) 28 min (Steady State)

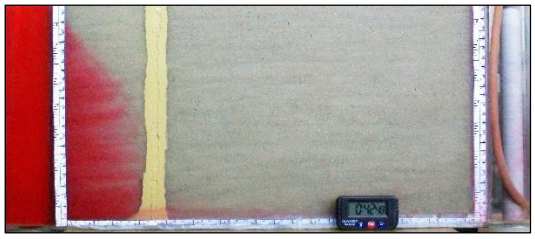

(b) 42 min

(c) 85 min

Figure 3.8: Flow barrier experimental results at (a) 28, (b) 42, and (c) 85 min

It has been observed from the experimental results (Figure 3.8) that after barrier implementation, the vertical extent of the saltwater wedge has increased while the horizontal extent remains the same as before. It reveals that there is no further movement of the saltwater wedge towards the freshwater aquifer. The study shows that physical barriers created by bentonite clay slurry can be employed for preventing the movement of the saltwater wedge towards the inland side.

3.3.4 Contaminant transport above a saltwater wedge

This experiment was performed to explore the contaminant transport processes occurring above the saltwater wedge in a coastal groundwater aquifer. In this experiment, the overflow outlet pipes were adjusted to maintain constant heads of 28.2 and 27.3 cm on the freshwater and saltwater boundary, respectively. This hydraulic gradient allowed to transmit freshwater towards the saltwater boundary. After achieving the steady-state saltwater wedge, about 12 ml of tracer slug was injected into the aquifer through a pipette to initiate the experiment. The pipette was initially buried within the aquifer while the aquifer media was wet packed. The tracer slug was poured at a constant rate with a fine-tipped syringe into the pipette. In this study, a food color (yellow) dye has been used as a tracer slug to visualize the contaminant transport patterns. The

location of the injection point was 22 cm from the coastal boundary and 16 cm above the bottom of the flow tank. The tracer plume was allowed to migrate with the freshwater flow, and the digital images were taken at various times after the injection. The time of injection of the tracer slug was recorded as 37 min from starting the experiment.

The experimental results for the contaminant transport patterns injected above the saltwater wedge are shown in Figure 3.9. The steady-state condition was achieved in about 37 min. At the steady-state, the toe of the saltwater wedge was located at 13 cm from the saltwater boundary, and the elevation of the wedge at the coastline (at x = 0) was 17 cm. As can be seen in Figure 3.9(a), the initial shape of the injected tracer slug is approximately circular. The laboratory result indicates that the tracer slug initially began to become sink, and this process was continued for about 30 min. As the tracer plume approaches the interface, the flow direction changes gradually, and the plume initiate to rise upwards under the influence of the wedge. It is a remarkable observation that the tracer slug traveled vertically along with the saltwater wedge, and the slug eventually discharged at the coastal boundary due to the strong advection-dominated flow condition that takes place near the wedge [Figure 3.9(c)]. Figure 3.9(b) and Figure 3.9(c) shows the migration pattern of the tracer plume in the flow tank. These photographs were captured at 23 min and 48 min, respectively, after injection of the tracer slug. This experimental investigation demonstrates that the existence of the saltwater diffusion zone in coastal aquifers plays a vital role in the transport patterns of the contaminant plume.

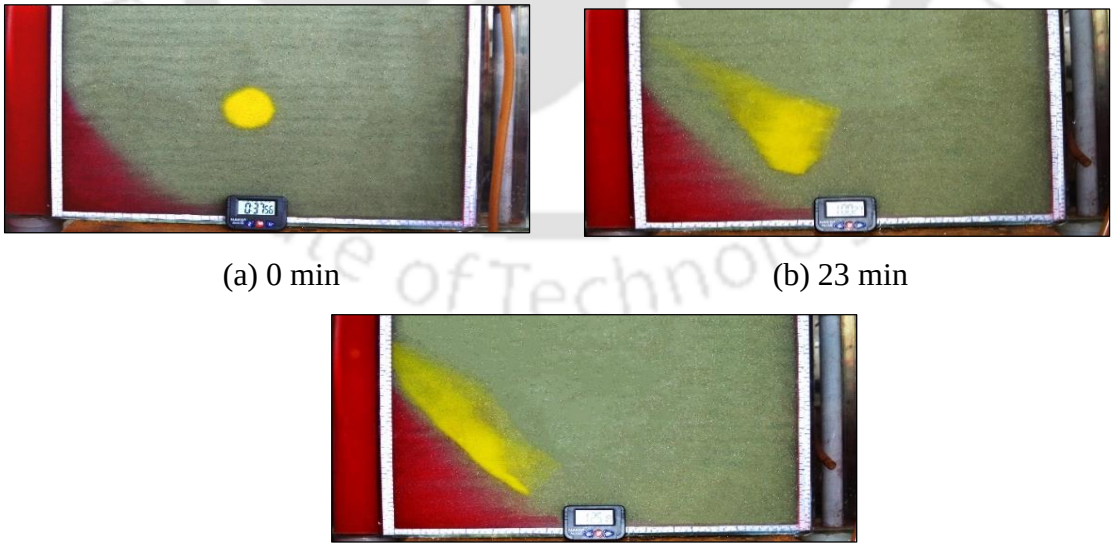

(a) 0 min (b) 23 min

(c) 48 min

Figure 3.9: Contaminant transport above saltwater wedge experimental results at (a) 0, (b) 23, and (c) 48 min

3.3.5 Contaminant transport above a saltwater wedge under pumping condition

This laboratory experiment was designed to study the effects of pumping on the contaminant migration patterns occurring above the saltwater interface. The height of water levels on freshwater and saltwater side were fixed to 28.2 cm and 27.3 cm, respectively as used in the previous experiment. The steady-state saltwater intrusion wedge was achieved in about 40 min. The injecting volume of the tracer slug was approximately 20 ml, and it was injected within 25 sec, yielding an effective injection rate of 0.8 ml/sec. The coordinates of the injection point were: x = 13 cm and z = 23 cm. The injection procedure was similar to the previous experiment. After a noticeable movement of the tracer plume, the pump was then started at a rate of 2.16 cm^3/sec. The location of pump in the flow tank was: x = 33 cm, y = 4 cm and z = 9 cm. The time of starting the pump was noted as 8 min after injecting the slug. Similar to the previous experiment, digital photographs were captured at different times to investigate the behavior of contaminant migration patterns.

Figure 3.10 shows the transient datasets of the contaminant migration processes occurring above the saltwater interface under pumping conditions. The images were recorded from the flow tank experiment at 0, 15, 30 min after injecting the slug. Analysis of the digital image shows that the height of the saltwater wedge at the saltwater boundary (at x = 0) is 14 cm, and the toe of the wedge was approximately located at 12 cm from the coastal boundary at the steady-state condition. It can be seen in Figure 3.10(a), the initial shape of the injected slug is nearly circular. The tracer slug initially began to become sink, and this process was continued for about 5 min. As time evolved, the tracer plume migrated slightly upward owing to the buoyancy forces induced by density contrast between the freshwater and saltwater present in the system. Furthermore, upon application of the pump, the saltwater intrusion wedge rapidly advanced through the system towards the freshwater boundary. The tracer plume was also drawn along with the saltwater wedge towards the pump location [Figure 3.10(c)] as the initiation of pumping establishes a transient flow pattern that leads to a lowering in the water table within the system. Consequently, the tracer plume, along with the wedge moves towards the inland direction. It is remarkable to note that the upconing characteristics of the plume along with the saltwater wedge, take place near the pump as a result of pumping.

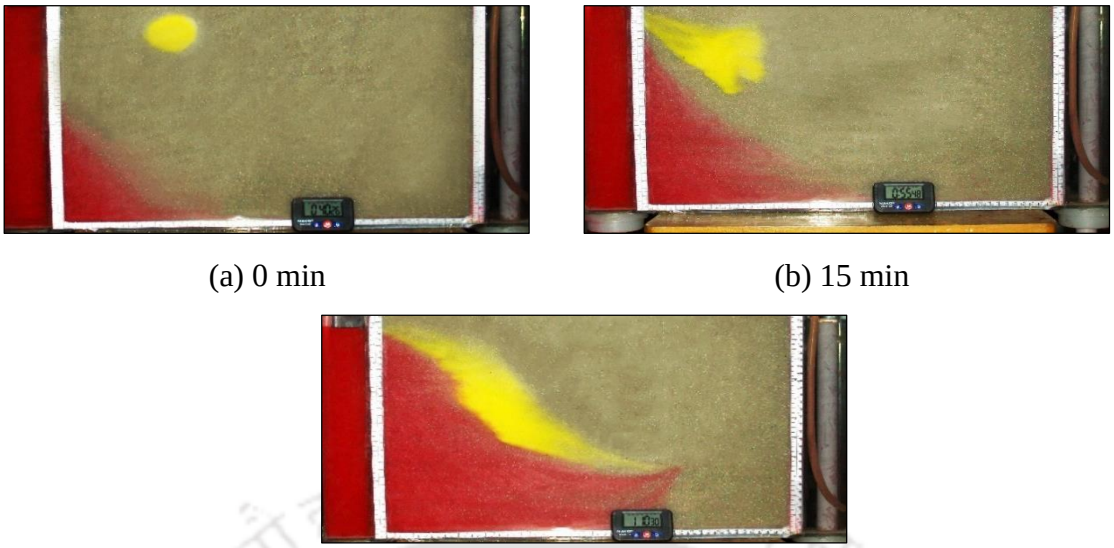

(a) 0 min (b) 15 min

(c) 30 min

Figure 3.10: Contaminant transport above the saltwater wedge under pumping condition experimental results at (a) 0, (b) 15, and (c) 30 min

3.3.6 Contaminant transport on a saltwater wedge

This laboratory-scale experiment was undertaken to simulate the contaminant transport patterns occurring on a saltwater wedge present in an unconfined coastal aquifer. In this experiment, the constant heads of 28.2 and 27.5 cm were set on the freshwater and saltwater boundary, respectively. The tracer slug almost 5 ml in volume was injected into the aquifer through a pipette, and the time of injection was noted as 34 min. The pipette was initially buried within the aquifer while the aquifer media was wet packed. The tracer slug was poured at a constant rate with a fine-tipped syringe into the pipette. A food color (yellow) dye has also been used as a tracer slug to visualize the behavior of contaminant transport patterns in this study. The total time taken for injection is 9 sec, yielding an effective injection rate of 0.55 ml/sec. The injection point was located at 9 cm from the saltwater chamber and 7 cm above the bottom boundary. This experiment was terminated at 40 min, after injecting the slug.

Figure 3.11 represents the experimental data for transport patterns of the injected tracer slug on the saltwater wedge. The picture shows color images of the tracer slug as it moved from the injection point towards the discharge boundary. The digital images were captured at 0, 29, and 40 min after injecting the tracer slug. The laboratory data implied that the tracer plume took almost 30 min to traverse the entire flow domain. In this laboratory experiment, the steady-state saltwater intrusion wedge was attained at about 34 min. At the steady-state condition, the toe of

the saltwater wedge was located at 14 cm from the shoreline, and the height of the wedge at the coastal boundary (at x = 0) was 17 cm.

Initially, the shape of the tracer plume was almost circular at the time of injection (t = 0 min) [Figure 3.11(a)]. The injected tracer slug did not follow the ideal circular flow path, usually demonstrated in texts (Fetter, 2001; Goswami *et al*., 2009). As time progressed, the circular plume attained an elongated shape due to dispersion effects. That is because higher velocities take place near the wedge, creates a rapid transport of tracer plume mass along the dispersion zone, forming this elongated shape. This pattern can be observed in Figure 3.11(b). It is interesting to note that the tracer slug does not move further seaward through the saltwater intrusion wedge. However, as observed from laboratory results, the tracer plume travels vertically by forming a thin layer over the saltwater wedge. It then exits around the coastline because of the strong advective flow field present near the wedge [Figure 3.11(c)].

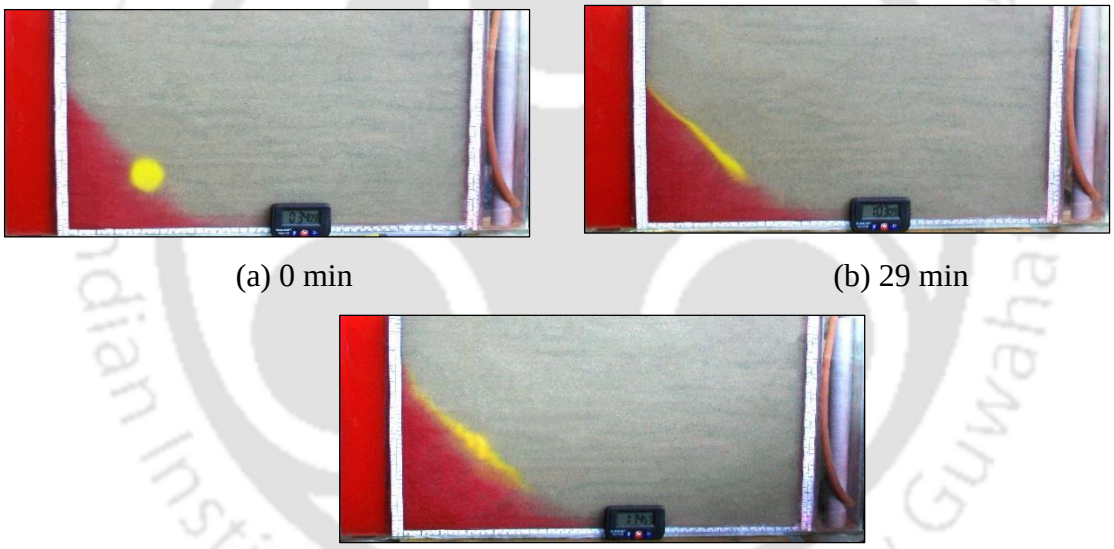

(a) 0 min (b) 29 min

(c) 40 min

Figure 3.11: Contaminant transport on saltwater wedge experimental results at (a) 0, (b) 29, and (c) 40 min

3.3.7 Contaminant transport on a saltwater wedge under pumping condition

This experiment aims to study the effects of pumping on the behavior of contaminant transport processes occurring on the saltwater interface. This laboratory experiment was performed immediately after the completion of the previous experiment. The pump was then initiated in the system at the rate of 1.45 cm^3/sec, and the subsequent migration patterns of contaminant plume were observed. The location of pump in the flow tank was: x = 29 cm, y =

3.2 cm and z = 7 cm. This experiment was continued until 16 min from the beginning of the experiment.

The laboratory results for the transport patterns of the injected tracer plume on the saltwater wedge with pumping conditions are shown in Figure 3.12. The experimental images were recorded at 0, 8, and 16 min after starting the experiment. As expected, upon application of the pump, the saltwater wedge was started to advance into the freshwater system rapidly. It can be seen in Figure 3.12(c), the tracer plume was also drawn along with the saltwater wedge towards the pump location. An upconing characteristics of the contaminant plume along with the saltwater wedge, also takes place near the pump because of pumping.

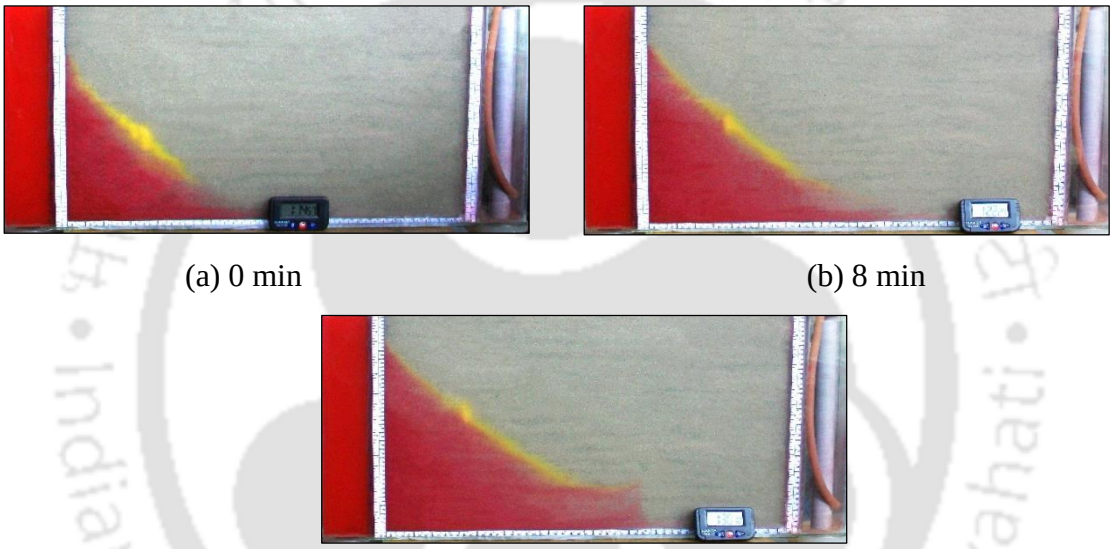

(a) 0 min (b) 8 min

(c) 16 min

Figure 3.12: Contaminant transport on saltwater wedge under pumping condition experimental results at (a) 0, (b) 8, and (c) 16 min

3.3.8 Horizontal clay lens experiment

This experiment focuses on studying the flow dynamics in the presence of a horizontal clay lens in an unconfined coastal aquifer system. To replicate a clay lens, an approximately 3 cm thick layer of bentonite clay was placed inside the flow tank. The clay lens was prolonged horizontally from the left side of the flow tank to a distance of about 28 cm and at the height of 20 cm from the bottom of the tank. It was covered the entire width of the flow tank. The pump screen was initially emplaced within the flow tank before packing the aquifer, and the location of the pump in the flow tank was: x = 32 cm, y = 2 cm, and z = 25 cm. In this experiment, the height of water levels on the freshwater and saltwater boundary was set to 28.5 and 27.5 cm,

respectively, yielding a head difference of 1 cm. The steady-state saltwater intrusion wedge was reached in about 37 min in the experiment. After achieving the steady-state saltwater wedge, the extraction pump was then started at a rate of 1.8 cm^3/sec, and the subsequent migration pattern of the saltwater intrusion wedge was observed. The time of starting the pump was noted as 45 min and continued till 89 min. This experiment was terminated at 89 min after beginning the experiment, and experimental observations were captured through digital images at different time intervals.

Figure 3.13 represents the transport patterns of saltwater intrusion wedge in the presence of a horizontal clay lens. The photographs were taken at 37, 62, and 89 min after starting the experiment. The color image taken from the experiment at the steady-state is shown in Figure 3.13(a). As can be seen in Figure 3.13(a), there are two saltwater intrusion wedge develops, one at the base of the aquifer, and the other one above the clay lens. Because of the presence of a horizontal stratified layer, it was observed that in addition to the formation of the usual saltwater wedge, there was an additional wedge formed on top of the clay lens. At the steady-state condition, the toe of the upper wedge was located at 3 cm from the saltwater boundary, and the elevation of the wedge at the coastline (at x = 0) was 2.5 cm. Also, the toe of the lower wedge was located at 13 cm from the coast, and the height of the wedge at the saltwater boundary (at x = 0) was 15 cm. Figure 3.13(b) and Figure 3.13(c) shows the transport patterns of the saltwater wedges at 62 min and 89 min, respectively. It can be seen in Figure 3.13(b), upon application of the pump, both the saltwater intrusion wedges advance rapidly through the system towards the freshwater boundary as the initiation of pumping establishes a transient flow pattern that leads to a depleting in the water table within the system. As a result of this, the wedges move towards the landward direction. At later times, the finger-like patterns have been observed in both the wedges [Figure 3.13(c)]. A slight upconing characteristic also occurs in the lower wedge because of pumping. It may be due to the extreme mixing of saltwater and freshwater flows near the interface as a result of pumping. The intruded wedge might have eventually reached the pump if the pumping was continued.

(a) 37 min (Steady State)

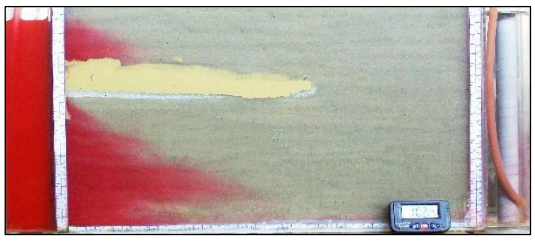

(b) 62 min

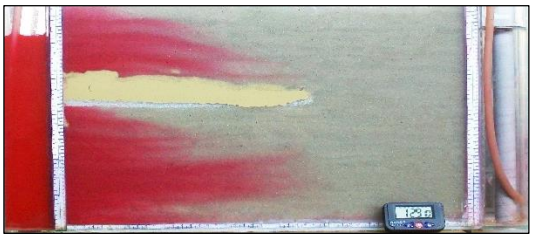

(c) 89 min

Figure 3.13: Horizontal clay lens experimental results at (a) 37, (b) 62, and (c) 89 min

3.3.9 Contaminant transport with horizontal clay lens

This experiment was performed to investigate the behavior of contaminant migration patterns under the influence of a horizontal clay lens in an unconfined coastal aquifer. This laboratory-scale experiment was continued from the previous experiment. After completing the previous experiment, the extraction pump was then stopped, and the tracer slug about 5 ml in volume was injected into the aquifer through a pipette. The pipette was initially buried inside the flow tank while the aquifer media was wet packed. The tracer slug was poured at a constant rate with a fine-tipped syringe into the pipette. In this study, a food color (yellow) dye has been used as a tracer slug to visualize the behavior of contaminant transport patterns. The location of the injection point was noted as x = 20 cm, y = 0.7 cm and z = 23.5 cm. The tracer slug was allowed to migrate with the ambient freshwater flow, and experimental observations were recorded at different times. The time of injection of the tracer slug was recorded as 35 min from starting the experiment.

The experimental data of the contaminant transport patterns under the influence of a clay lens are shown in Figure 3.14. The digital images were recorded to examine the behavior of the contaminant migration patterns, and photographs were taken at 0, 17, and 37 min after injecting the tracer slug. Figure 3.14 shows the tracer plume as it moves from the injection point towards the saltwater boundary. Figure 3.14(a) was captured instantly after the injection, and it indicates that the initial shape of the injected tracer slug was nearly circular. As time advanced, the tracer slug transported towards the saltwater wedge and eventually attained an elongated shape when it came closer to the saltwater wedge. The tracer slug did not follow the ideal circular flow path. Due to the higher level of mixing taking place near the interface, the plume formed an elongated shape as it approached the freshwater-saltwater interface. The shape of the migrating plume was elongated, as shown in Figures 3.14(b) and 3.14(c). It has also been observed that the tracer plume moved vertically along the top surface of the saltwater wedge because of the active

advective flow field present near the wedge. As can be seen in Figure 3.14(c), the plume eventually discharged at the saltwater boundary.

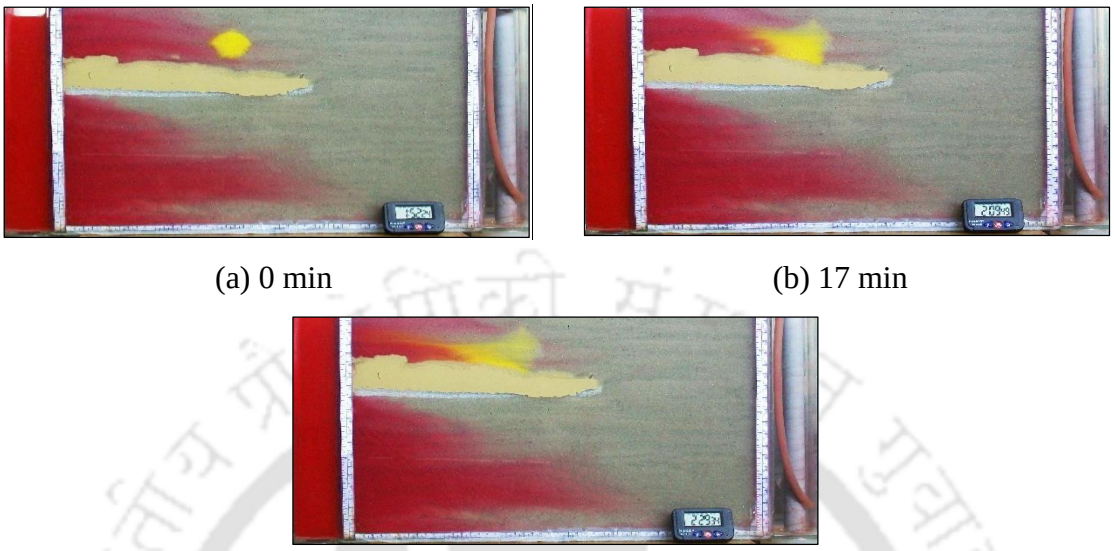

(a) 0 min (b) 17 min

(c) 37 min

Figure 3.14: Contaminant transport with horizontal clay lens experimental results at (a) 0, (b) 17, and (c) 37 min

3.4 Summary and Conclusions

Saltwater intrusion into coastal aquifers has become a prominent environmental problem worldwide since about 70% of the world's population lives in coastal regions. The interest in better understanding the mechanism of saltwater intrusion processes in coastal aquifers is, therefore, garnering increased attention in the last few decades. The overall goal of this work is to perform laboratory-scale experiments with regard to develop a better scientific understanding of the dynamics of saltwater intrusion processes in a coastal unconfined aquifer. In this effort, a series of physical experiments have been carried out in a laboratory-scale aquifer model to have a better understanding of the dynamics of this phenomenon under different scenarios.

The experimental setup designed in this study that could be used to simulate groundwater flow and contaminant transport processes in unconfined coastal aquifers. The mixing of freshwater and saltwater inside the saltwater chamber was nominal during the experiments, and therefore, the system was capable of simulating the constant-head saltwater boundary condition. The experimental results are used to develop a better understanding of the dynamics of saltwater intrusion processes in a coastal unconfined aquifer. The laboratory data presented in this study can be used for testing the performance of density-coupled flow and transport models. The

findings from this investigation would be useful to understand better the saltwater intrusion processes occurring in a coastal unconfined aquifer.

An investigation has successfully been conducted to assess the efficiency of bentonite clay slurry on controlling the SI problem in the present study. As experimental results reveal that there is no further movement of the saltwater intrusion wedge towards the inland side after the barrier implementation. The research suggests that the physical barrier created by bentonite slurry can be employed for preventing the movement of saltwater intrusion in coastal aquifer systems. The laboratory data indicate that a considerable mixing of saltwater and freshwater flows during the initial intrude period. Further, the effect of pumping on the saltwater intrusion dynamics has been studied, and results show that the saltwater interface rapidly advances through the system towards the freshwater aquifer after the application of pumping. Moreover, the influence of the injection of the freshwater on the dynamics of saltwater intrusion processes has also been investigated in this study. This study suggests that the saltwater wedge gradually recede through the system towards the saltwater boundary upon injection of freshwater and could be concluded that the injection of freshwater as a hydraulic barrier can be used in impeding saltwater intrusion in coastal aquifers.

However, contaminant transport in a coastal aquifer system is a significant concern owing to its impact on the coastal marine and estuarine environments. An exhaustive understanding of contaminant transport in coastal aquifers is, therefore, necessary to manage the contaminant problems effectively. In this effort, laboratory-scale experiments have been conducted to investigate the contaminant transport processes occurring above and on a saltwater wedge in coastal aquifers under pumping or without pumping conditions. The main purpose of these experiments is to examine the behavior of contaminant transport patterns in an unconfined coastal aquifer under pumping conditions. The experimental data indicate that the contaminant travels upward towards the seaward boundary when it approaches the saltwater wedge and then exits around the coastline. It is a remarkable observation that the contaminant plume does not travel further seaward through the saltwater intrusion wedge. As expected, upon installation of the pump, the saltwater intrusion wedge starts to advance into the freshwater system rapidly, and contaminant plume is also drawn along with the saltwater wedge towards the pump location. The experimental data also clearly show that the injected tracer slug did not follow the ideal circular flow path. The circular plume forms an elongated shape as it approaches the saltwater-freshwater interface due to a strong advection effect near the saltwater wedge. The experimental

investigations demonstrate that the saltwater diffusion zone present in the coastal aquifer system plays a pivotal role in the behavior of contaminant transport.

Furthermore, an experiment has also been undertaken to understand the behavior of contaminant plume in unconfined coastal aquifers under the influence of a horizontal clay lens. The laboratory results show that there are two saltwater intrusion wedges develop, one at the base of the aquifer, and the other one above the clay lens. Because of the presence of a horizontal stratified layer, it has been observed that in addition to the formation of the usual saltwater wedge, there is an additional wedge form on top of the clay lens. Experimental results also show that the contaminant travels vertically along the top surface of the saltwater wedge towards the seaward boundary.

CHAPTER 4

Numerical Investigation of Saltwater Intrusion Processes

4.1 Introduction

The rising demand for freshwater in different domestic, industrial, and agricultural sectors in coastal regions is emplacing more emphasis on the development of groundwater resources. The groundwater available in an unconfined and confined aquifer already constitutes the only reliable source of freshwater resources to satisfy the daily water requirements for coastal populations. As a result of the indiscriminate and overexploitation of groundwater resources along with reduced natural recharge, especially in arid and semi-arid coastal zones, leads to the significant decline of groundwater levels and resulting in saltwater intrusion problems within coastal aquifers. Moreover, natural events such as climate change and sea-level rise also accelerate seawater to intrude into fresh coastal groundwater aquifers. It causes severe consequences on the environment, ecology, and the economy of the coastal zones. As such, protection and sustainable utilization of groundwater resources of these regions undertake great significance. Therefore, it is imperative to study the dynamics of saltwater intrusion processes in coastal aquifers so as to investigate their transport patterns and work out appropriate remedial countermeasures for sustainable management of coastal aquifer systems.

In general, the simulation of saltwater intrusion process in a coastal aquifer is intrinsically complicated and highly nonlinear as the flow and transport processes are density-dependent. However, mathematical models, i.e., either analytical or numerical, can solve the real-world saltwater intrusion problems. The saltwater intrusion process could be mathematically modeled by partial differential equations characterizing the flow and transport processes. Hence, modeling of saltwater intrusion process in coastal aquifer systems involves a coupled groundwater flow equation with a solute transport equation. These density-dependent flow and transport equations represent the behavior of the saltwater intrusion process and are solved in order to simulate the saltwater intrusion process in coastal aquifers. The solution of the solute transport equation depends on the groundwater flow field, which is generally affected by salt and distribution of its density in the groundwater field. The simultaneous solution of these two coupled equations leads to high non-linearity in the simulation of density-driven flow and transport processes. Indeed, an exact solution of groundwater flow and transport equation can be obtained by using analytical models. Nevertheless, it is sometimes unable by analytically to simplify the 3D differential

equations easily. On the other hand, numerical models could also be used to solve three-dimensional groundwater flow and solute transport problems. It provides an efficient solution to a problem quickly. Thus, the interest is mainly on numerical modeling to simulate the saltwater intrusion processes in coastal aquifers in the present study. However, there are various density-driven groundwater simulation models such as the SUTRA (Voss, 1984; Voss and Provost, 2010), FEFLOW (Diersch, 1988), FEMWATER (Lin *et al*., 1997), and SEAWAT (Guo and Langevin, 2002), which can solve the complex density-dependent groundwater flow and transport phenomenon. Therefore, the variable-density flow and transport model FEMWATER (Lin *et al*., 1997) is adopted to simulate the flow and transport processes in the coastal aquifer system.

4.2 Density-dependent flow and transport simulation model

The density-dependent flow and transport simulation model FEMWATER (Lin *et al*., 1997) is used to simulate the coupled flow and transport processes in coastal aquifers. FEMWATER is a three-dimensional (3D) finite-element based model that can simulate the variable-density flow and mass transport through saturated-unsaturated porous media. It was developed as a collaborative effort of the U.S. Environmental Protection Agency (AERL) and the U.S. Army Engineer Waterways Experiment Station (WES) from two previous models, 3DFEMWATER (Yeh, 1987) and 3DLEWASTE (Yeh, 1990). The model is developed by combining the two codes, 3DFEMWATER (flow) and 3DLEWASTE (transport), into a single coupled flow and transport model. The FEMWATER model is integrated into the Department of Defense Groundwater Modeling System (GMS © Aquaveo). The relevant governing equations used in FEMWATER are as follows (Lin *et al*., 1997).

4.2.1 Flow Equation

The governing equation for flow is the modified Richards equation, which is as follows (Lin *et al*., 1997):

$$\frac{\rho}{\rho_0} F \frac{\partial h}{\partial t} = \nabla . \left[\boldsymbol{K} . \left(\nabla h + \frac{\rho}{\rho_0} \nabla z \right) \right] + \frac{\rho^*}{\rho_0} q \tag{4.1}$$

Where, F = storage coefficient, h = pressure head, t = time, $\boldsymbol{K}$ = hydraulic conductivity tensor, z = potential head, q = source and/or sink, ρ = water density at solute concentration C,

ρ_0 = reference water density corresponding to zero solute concentration, ρ^* = density of either the injection fluid or the withdrawn water.

The storage coefficient F is defined as,

$$F = \alpha' \frac{\theta}{n} + \beta' \theta + n \frac{dS}{dh} \tag{4.2}$$

Here, α' is the modified compressibility of the porous medium, β' is the modified compressibility of the water, n is the porosity of the porous medium, θ is the moisture content, h is the pressure head, and S is the degree of saturation.

The hydraulic conductivity $\boldsymbol{K}$ depends on fluid density (ρ), viscosity (μ), and acceleration due to gravity (g). The hydraulic conductivity $\boldsymbol{K}$ is defined as,

$$\boldsymbol{K} = \frac{\rho g}{\mu} \boldsymbol{k} = \frac{\left(\rho / \rho_0 \right)}{\left(\mu / \mu_0 \right)} \frac{\rho_0 g}{\mu_0} \boldsymbol{k}_s k_r = \frac{\rho / \rho_0}{\mu / \mu_0} \boldsymbol{K}_{so} k_r \tag{4.3}$$

Where, ρ = water density at solute concentration C,

ρ_0 = reference water density corresponding to zero solute concentration,

μ = dynamic viscosity of water at solute concentration C,

μ_0 = reference dynamic viscosity at zero solute concentration,

g = acceleration due to gravity,

$\boldsymbol{k}$ = permeability tensor,

$\boldsymbol{k}_s$ = saturated permeability tensor,

k_r = relative permeability or relative hydraulic conductivity,

$\boldsymbol{K}_{so}$ = reference saturated hydraulic conductivity tensor.

The reference value is usually taken at zero solute concentration. The density (ρ) and dynamic viscosity (μ) of water are functions of solute concentration and are assumed to make the following form,

$$\frac{\rho}{\rho_0} = a_1 + a_2 c + a_3 c^2 + a_4 c^3 \tag{4.4}$$

and

$$\frac{\mu}{\mu_0} = a_5 + a_6 c + a_7 c^2 + a_8 c^3 \tag{4.5}$$

Where $a_1, a_2, a_3, a_4, a_5, a_6, a_7, a_8$ are the parameters used to define concentration dependence of water density and viscosity, and c is the solute concentration.

The Darcy velocity is calculated as given below,

$$\boldsymbol{V} = -\boldsymbol{K}.\left(\frac{\rho_0}{\rho}\nabla h + \nabla z\right) \tag{4.6}$$

4.2.2 Flow initial condition

The appropriate initial condition is to be specified to solve the flow equation (Equation 4.1). The initial condition for the flow equation is given by Equation (4.7):

$$h = h_i\left(x, y, z\right) \text{ in } R \tag{4.7}$$

Where, R is the region of interest, and h_i is the prescribed initial condition, which can be obtained by physical measurements or by solving the steady-state form of Equation (4.1).

4.2.3 Flow boundary condition

The appropriate boundary condition is also to be specified to solve the flow equation. For a steady-state problem, the only boundary condition is required, and for the transient state problem, both initial and boundary conditions are necessary to solve the flow equation. A no-flow boundary condition is considered on all boundaries other than a constant head boundary for the freshwater and saltwater side boundary given by,

$$h = h_d\left(x_b, y_b, z_b, t\right) \text{ on } B_d \tag{4.8}$$

Where, (x_b , y_b , z_b) = spatial coordinate on the boundary,

B_d = Dirichlet boundary,

h_d = head on the Dirichlet boundary.

4.2.4 Transport Equation

The governing equation for transport is derived based on the continuity of mass and flux laws, which is as follows (Lin *et al*., 1997):

$$\theta\frac{\partial C}{\partial t}+\rho_b\frac{\partial S^a}{\partial t}+\boldsymbol{V}.\nabla C-\nabla.\left(\theta\boldsymbol{D}.\nabla C\right)=-\left(\alpha'\frac{\partial h}{\partial t}+\lambda\right)\left(\theta C+\rho_b S^a\right)$$
$$-\left(\theta K_w C+\rho_b K_s S^a\right)+m-\frac{\rho^*}{\rho}qC+ \quad (4.9)$$
$$+\left(F\frac{\partial h}{\partial t}+\frac{\rho_0}{\rho}\boldsymbol{V}.\nabla\left(\frac{\rho}{\rho_0}\right)-\frac{\partial\theta}{\partial t}\right)C$$

Where, ρ_b = bulk density of the porous medium, C = solute concentration in the aqueous phase, S^a = solute concentration in adsorbed phase, t = time, ∇ = del operator, $\boldsymbol{D}$ = dispersion coefficient tensor, α' = compressibility of the porous medium, h = pressure head, λ = decay constant, m = artificial mass rate, q = source rate of water, C_{in} = solute concentration in the source, K_w = first-order biodegradation rate constant through the dissolved phase, K_s = first-order biodegradation rate through the adsorbed phase, F = storage coefficient, ρ = water density at solute concentration C, ρ_0 = reference water density at zero solute concentration, ρ^* = density of either the injection fluid or the withdrawn water. The decay, adsorption, biodegradation, and artificial mass flow are neglected in this study.

The dispersion coefficient $\boldsymbol{D}$ is given by,

$$\boldsymbol{D}=a_T|\boldsymbol{V}|\delta+\left(a_L-a_T\right)\frac{\boldsymbol{VV}}{|\boldsymbol{V}|}+a_m\theta\tau\delta \quad (4.10)$$

Where, $|\boldsymbol{V}|$ = magnitude of $\boldsymbol{V}$, δ = Kronecker delta tensor, a_L = longitudinal dispersivity, a_T = lateral dispersivity, a_m = molecular diffusion coefficient, τ = tortuosity.

4.2.5 Transport initial condition

The appropriate initial condition is to be specified to solve the transport equation (Equation 4.9). The initial condition for the transport equation is given by equation (4.11):

$$c=c_i\left(x,y,z\right)\ \text{in}\ R \quad (4.11)$$

Where, R is the region of interest, and c_i is the prescribed initial condition, which can be obtained by physical measurements.

4.2.6 Transport boundary condition

The appropriate boundary condition is also to be specified to solve the transport equation. For a steady-state problem, the only boundary condition is required, and for the transient state

problem, both initial and boundary conditions are necessary to solve the transport equation. A Dirichlet boundary condition of constant concentration, given by the following, was assigned to the saltwater side boundary;

$$c = c_d\left(x_b, y_b, z_b, t\right) \text{ on } B_d \tag{4.12}$$

Where, (x_b , y_b , z_b) = spatial coordinate on the boundary,

c_d = concentration on the Dirichlet boundary,

B_d = Dirichlet boundary.

The saltwater boundary salinity concentration was assigned as 35 g/L, representing the average salinity level of sea or oceans.

The FEMWATER simulates the flow and transport equations along with the initial and boundary conditions for the variable-density flow and mass transport through saturated-unsaturated porous media. FEMWATER uses the Galerkin finite element method to approximate the flow equation and uses a weighted residual finite element technique to approximate the transport equation. The flow and transport processes represented by equations 4.1 and 4.9 are coupled together by the density coupling coefficient, and Darcy velocities, which makes the saltwater intrusion problems as complex and highly nonlinear.

4.3 Model Development

The numerical model has been built up to simulate the flow, and transport processes for the experimental setup and simulations have been carried out to verify the physical phenomenon for all the laboratory-scale experiments presented in Chapter 3. The main goal of the simulation was to evaluate the consistency of the experimental results with the numerical predictions and to explain the experimental results better. The numerical description of the experimental setup involves a rectangular domain of 45 cm × 30.5 cm, as shown in Figure 4.1.

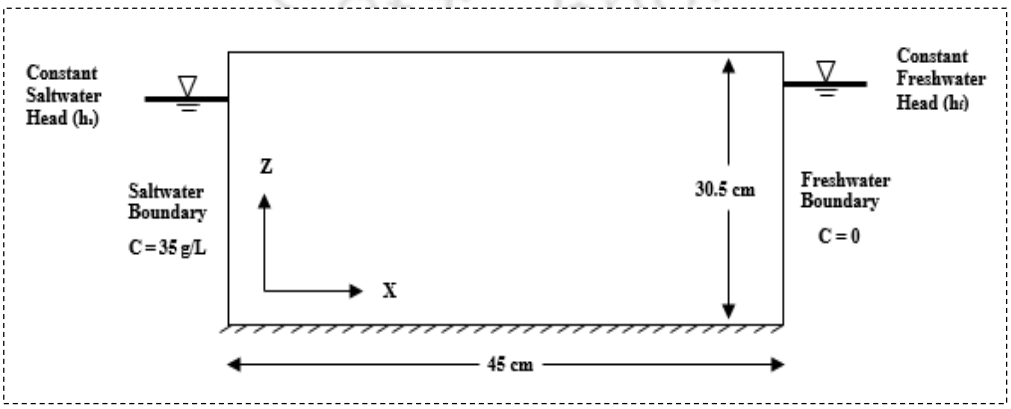

Figure 4.1: Computation domain and boundary conditions used in the numerical model

The left and right side boundaries of the model were assigned as the coastal and inland boundary, respectively. Hydrostatic pressure boundary conditions were applied on the right-side boundary (C = 0%) and to the left-side boundary (C = 100%). A concentration of 35 g/L was specified at the saltwater boundary. Constant-head boundary conditions were imposed at both the freshwater and saltwater side. The base of the domain was bounded by an impervious boundary. A zero mass flux boundary conditions were specified at the top, the front and the backside of the computational domain.

The initial condition used in the numerical model was that of an entirely freshwater aquifer. The freshwater and saltwater boundary conditions were assigned upon the system, and the system was allowed to reach the steady-state condition. The value of time step Δt was set at 60 s in the simulations.

The longitudinal dispersivity (a_L) was fixed for the porous media as the minimal diameter of the glass beads (Luyun *et al*., 2009). A transverse dispersivity (a_T) was assumed to be 1/10 of the longitudinal dispersivity (Goswami and Clement, 2007). The longitudinal dispersivity and transverse dispersivity values were assigned to be 0.057 cm and 0.0057 cm, respectively. The other numerical parameters used in this study are listed in Table 4.1. All other parameters were fixed at the default values in the FEMWATER.

Table 4.1: Parameters of Numerical Simulation

Parameter	Value	Source
Bulk density	1.443 g/cm^3	Measured
Freshwater density	0.997 g/cm^3	Measured
Saltwater density	1.025 g/cm^3	Measured
Viscosity of freshwater	0.00851 g/cm.s	Measured
Viscosity of saltwater	0.00918 g/cm.s	Measured
Molecular diffusion coefficient	1×10^{-5} cm^2/s	Freeze and Cherry (1979)
Porosity	0.43	Measured

The parameters used to define the concentration dependence of water density and viscosity in FEMWATER are listed in Table 4.2. The coefficients described in Table 4.2 are common for all the numerical simulations.

Table 4.2: Parameters used to define the concentration dependence of water density and viscosity

Coefficient	Value
a_1	1
a_2	0.0008821711
a_3	0
a_4	0
a_5	1
a_6	0.01880109
a_7	0
a_8	0

4.4 Numerical Simulations: Results and Discussions

A series of numerical simulations have been carried out using the variable-density flow and transport model FEMWATER (Lin *et al.*, 1997). In this section, all the laboratory-scale experimental results are compared against numerical predictions. The comparison of the numerical and experimental results shows that the numerical prediction is in good agreement with the experimental results. They are presented in the following sections.

4.4.1 Pumping of freshwater

The first numerical investigation has been performed to investigate the effect of pumping on the saltwater intrusion dynamics in a coastal unconfined aquifer. The entire model domain was split into 15008 nodes and 25730 elements with Δx = 1 cm, Δy = 0.85 cm and Δz = 0.984 cm. The constant heads of 28.2 and 27.3 cm was set on the freshwater and saltwater boundary, respectively, in the numerical model as similar to the physical experiment. The simulation of the pump was given through a point source extraction at the node, whereas the pump screen was present in the laboratory experiment, and the flow rate of the extracted water was given as the negative (-) value. The location of the pump in the simulation model was: x = 33 cm, y = 4 cm, and z = 7 cm. The rate of extraction of the pump was 2.52 cm^3/sec within the system, and the subsequent migration pattern of the saltwater intrusion wedge was simulated. The comparison of the numerical and experimental results for the pumping of the freshwater experiment is presented in Figure 4.2.

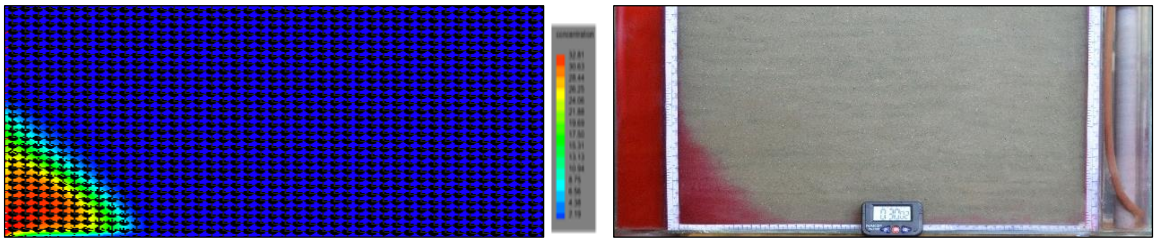

(a) 30 min (Steady State)

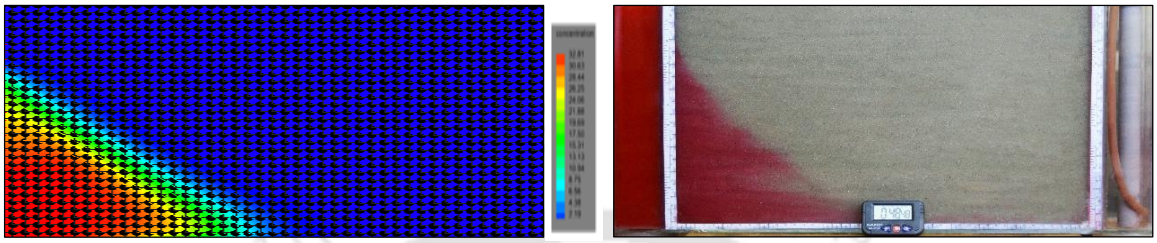

(b) 48 min

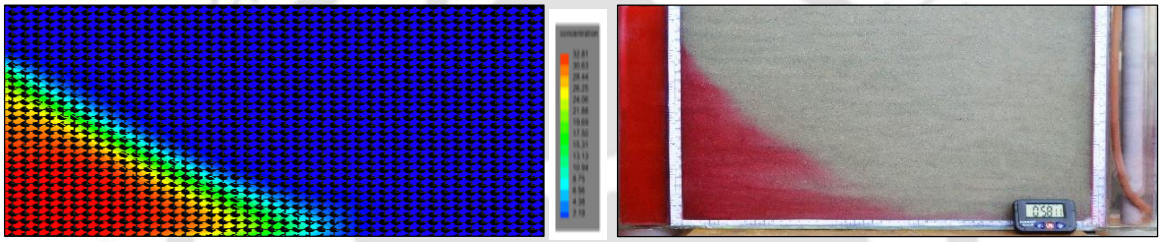

(c) 58 min

Figure 4.2: Comparison of numerical and experimental results for pumping of the freshwater experiment at (a) 30, (b) 48, and (c) 58 min

The observational results at the steady-state are shown in Figure 4.2(a). The steady-state saltwater intrusion wedge was achieved in about 30 min. At the steady-state condition, the toe of the saltwater wedge was 11 cm in both the physical experiment and numerical simulation. The time of starting the pump was at 30 min in the simulation. The results show that the saltwater wedge rapidly advances through the system towards the freshwater boundary after the initiation of the pump [Figure 4.2(b)], as the initiation of pumping establishes a transient flow pattern that leads to a lowering in the water table within the system and thereby causing a slight extension of the toe length of the wedge. After 28 min of pumping [Figure 4.2(c)], the toe of the saltwater wedge was estimated at 26.5 cm in the simulation, as compared to 26 cm in the physical experiment. The simulation result indicates that the intrusion wedge moves towards the pump in a slight cone-shaped formation. It might have eventually reached the pump if the pumping was continued. That could not be observed in the physical experiment. It may be due to the extreme mixing of saltwater and freshwater flows near the interface as a result of pumping. As can be seen from experimental results, the saltwater wedge forms a slight finger-like pattern near the

bottom of the aquifer. It may be due to the non-uniformity of packing of the porous media within the aquifer. The simulated data, however, did not show this pattern.

4.4.2 Injection of freshwater

This numerical simulation was conducted to examine the effects of freshwater injection on the saltwater wedge in unconfined coastal aquifer systems. The model domain was split into 15008 nodes and 25730 elements with Δx = 1 cm, Δy = 0.85 cm and Δz = 0.984 cm. The simulation of the pump was given through a point source injection at the node, whereas the pump screen was present in the physical model, and the flow rate of the injected water was given as the positive (+) value. The constant heads of 28.2 and 27.3 cm was set on the freshwater and saltwater boundary, respectively, in the numerical model. The position of the pump was similar in the previous simulation. The steady-state saltwater intrusion wedge was reached in about 38 min. After steady-state saltwater wedge was attained, the injection pump was then initiated within the system at a rate of 2.5 cm^3/sec. The injection pump was started at 55 min and continued till 89 min in the simulation. Figure 4.3 represents the comparison of observed data with numerical predictions for the injection of the freshwater experiment.

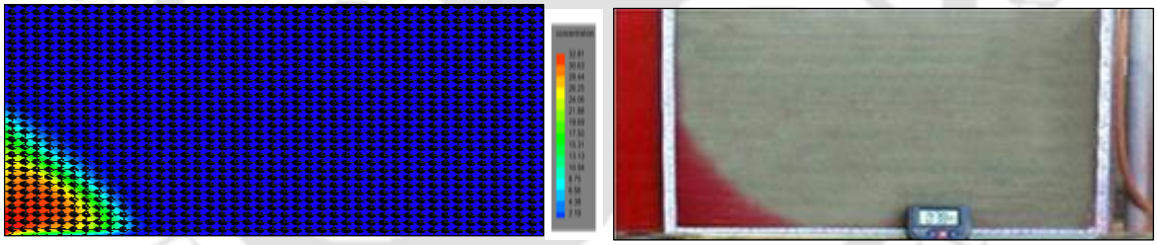

(a) 38 min (Steady State)

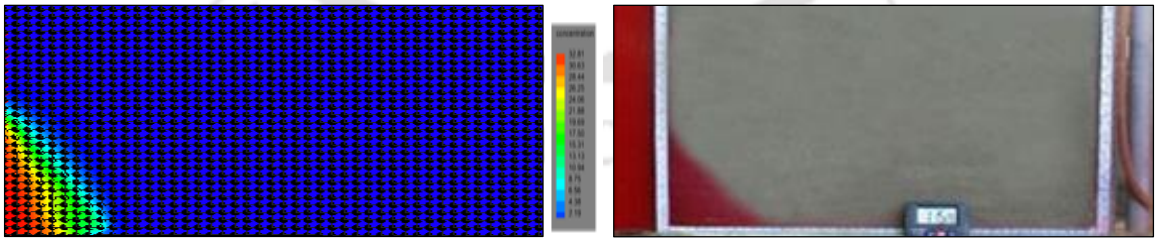

(b) 75 min

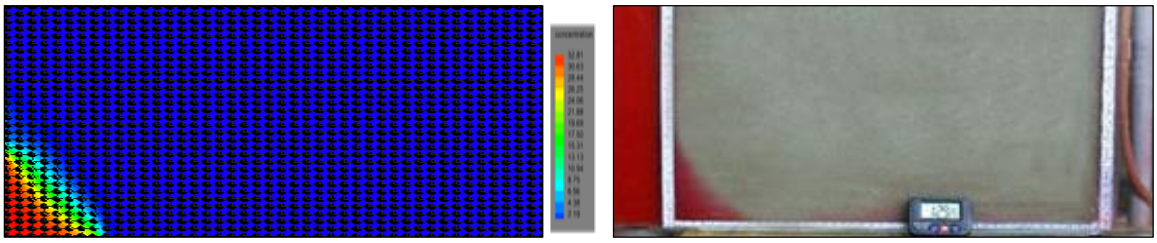

(c) 89 min

Figure 4.3: Comparison of observed data with numerical predictions for the injection of the freshwater experiment at (a) 38, (b) 75, and (c) 89 min

The results shown in Figure 4.3(a) compare the steady-state numerical result predicted by the simulation model against experimental data. At the steady-state, the toe of the saltwater wedge was estimated at 10.8 cm from the coastline in the simulation, as compared to 11 cm in the physical experiment. Figure 4.3(b) and Figure 4.3(c) shows the comparison of numerical and experimental results of the transport patterns of the saltwater wedge from the steady-state. It can be seen in Figures 4.3(b) and 4.3(c) that the saltwater intrusion wedge gradually receded through the system towards the saltwater boundary upon application of the injection of the freshwater. As the initiation of freshwater injection establishes a transient flow pattern that leads to an increase in the water table within the system, and that injected freshwater flow regime drives the wedge towards the saltwater boundary. After 34 min of freshwater injection [Figure 4.3(c)], the toe of the saltwater wedge was measured as 8 cm from the shoreline in the experiment. However, it was 8.6 cm in the numerical simulation. A slight reduction of the saltwater wedge profile has been observed in both numerical simulation and physical experiments. Hence, it could be concluded that the injection of freshwater as a hydraulic barrier can be used for preventing saltwater intrusion in coastal aquifers.

4.4.3 Flow barrier experiment

The purpose of this numerical simulation is to assess the efficiency of bentonite clay slurry on controlling the saltwater intrusion problem. In general, the construction of subsurface flow barriers is one of the most extensively used engineering countermeasures to prevent or mitigate this problem in coastal aquifers. However, the flow barrier was simulated in the numerical model by assigning the hydraulic conductivity as 1.39×10^{-10} cm/s to the elements of interest that correspond to the value measured by experimentally. The width of the flow barrier was imposed to 1.3 cm. Numerical simulation was carried out with the flow barrier set at the location of 10 cm as measured from the coastal boundary. Again, the simulation of the pump was given through a point source extraction at the node, where the pump screen was present in the physical

experiment, and the flow rate of the extracted water was given as the negative (-) value. The location of the pump in the numerical model was: x = 33.5 cm, y = 3.6 cm, and z = 15 cm. The height of water levels on the freshwater and saltwater boundary was also set to 28.3 and 27.3 cm, respectively, yielding a head difference of 1 cm in this simulation. The model domain was split into 12512 nodes and 21204 elements with Δx = 1.125 cm, Δy = 0.85 cm and Δz = 0.984 cm.

The steady-state saltwater intrusion wedge was obtained after about 28 min in both the experimental and numerical results. After reaching the steady-state saltwater wedge, the extraction pump was then started at a rate of 1.52 cm^3/sec, and the subsequent migration pattern of the saltwater intrusion wedge was simulated. The time of beginning the pump was noted as 29 min and stopped at 39 min in the simulation. The flow barrier was introduced at 35 min from starting the simulation. Numerical simulation was continued until 85 min, and simulation results were analyzed at different time intervals. Figure 4.4 indicates the comparison of experimental data with numerical predictions for the flow barrier experiment.

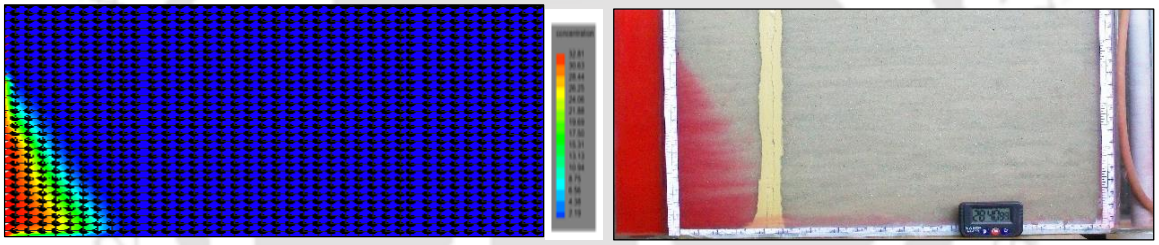

(a) 28 min (Steady State)

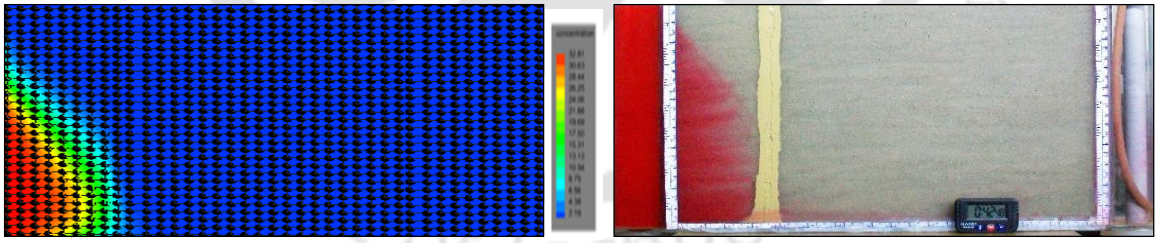

(b) 42 min

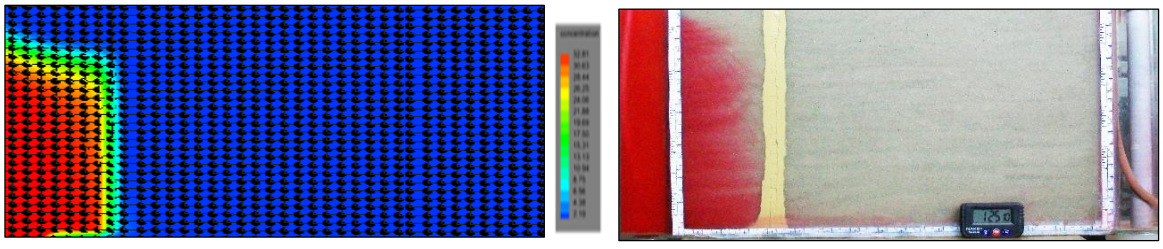

(c) 85 min

Figure 4.4: Comparison of experimental data with numerical predictions for the flow barrier experiment at (a) 28, (b) 42, and (c) 85 min

Figure 4.4(a) represents the transport patterns of the saltwater intrusion wedge at the steady-state condition. At the steady-state, the toe of the saltwater wedge was located at 7.87 cm from the saltwater boundary, and the height of the wedge at the coastline (at x = 0) was 22 cm in the numerical simulation. This agrees well with the 7.5 cm and 22 cm, respectively measured in the laboratory experiment. Figure 4.4(b) and Figure 4.4(c) show the saltwater wedge profile at 42 min and 85 min, respectively. The simulation results demonstrate that the saltwater wedge rapidly advances through the system towards the freshwater boundary after initiation of the extraction pump, similar to that observed in the physical experiment. After 6 min of pumping, the toe and height of the wedge were shifted to 9 cm and 23.3 cm, respectively, in simulation. It could be seen in Figure 4.4(c), the elevation of the saltwater wedge has raised after the barrier implementation. Although the toe of the saltwater intrusion wedge slightly migrated towards the flow barrier, it did not pass through the barrier. The toe and elevation of the saltwater wedge were estimated respectively as 9.4 cm and 26.7 cm (at t = 85 min). Therefore, it reveals that there is no further movement of the saltwater wedge through the barrier towards the freshwater aquifer. The study shows that physical barriers created by bentonite clay slurry can be employed for preventing the movement of the saltwater wedge towards the landward side.

4.4.4 Contaminant transport above a saltwater wedge

This numerical simulation was performed to explore the contaminant transport processes occurring above the saltwater wedge in a coastal groundwater aquifer. The model domain was split into 15008 nodes and 25730 elements with $\Delta x = 1$ cm, $\Delta y = 0.85$ cm and $\Delta z = 0.984$ cm. The constant heads of 28.2 and 27.3 cm were fixed on the freshwater and saltwater boundary, respectively, for the entire simulation. In this simulation, the steady-state condition was achieved in about 37 min. After attaining the steady-state saltwater wedge, a tracer slug was introduced within the system to simulate the contaminant transport patterns. The simulation of tracer slug was given as point boundary condition at the required node. The location of the tracer slug was 22 cm from the coastal boundary and 16 cm above the bottom of the computational domain, whereas it was injected in the laboratory experiment. The tracer plume was allowed to migrate with the freshwater flow, and the simulated results were analyzed at various times. The numerical predictions are compared against the observed data for contaminant transport above a saltwater wedge experiment in Figure 4.5.

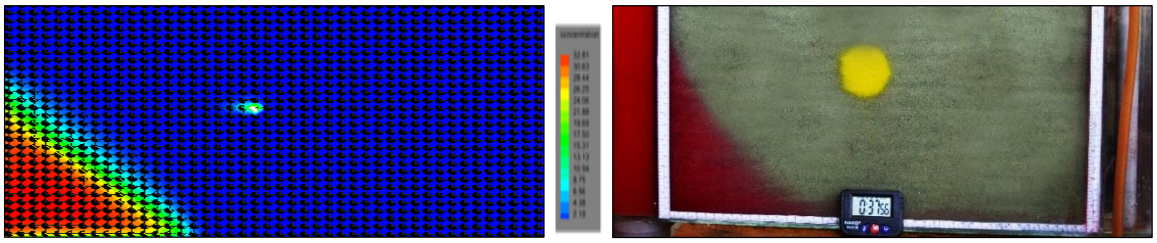

(a) 0 min

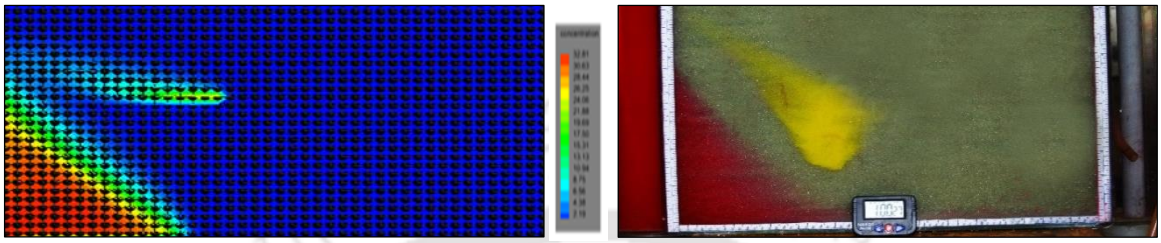

(b) 23 min

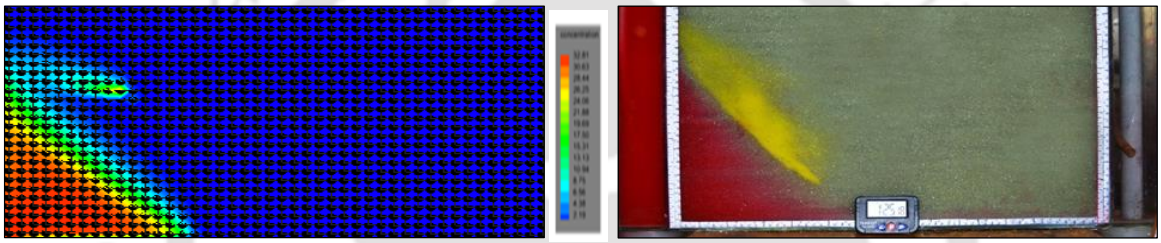

(c) 48 min

Figure 4.5: Comparison of numerical predictions with experimental results for contaminant transport above the saltwater wedge experiment at (a) 0, (b) 23, and (c) 48 min

Figure 4.5(a) shows the numerical and experimental results just after introduce the tracer slug. The toe of the saltwater wedge is located at 14 cm from the saltwater boundary in the simulation, as compared to 13 cm in the experimental observation. As seen in Figure 4.5(a), the initial shape of the tracer slug is almost circular. The laboratory result indicates that the tracer slug initially began to become sink, and this process was continued for about 30 min. The simulation model was not able to replicate this sinking pattern. As the tracer plume approaches the interface, the flow direction changes gradually, and the plume initiate to rise upwards under the influence of the wedge. It is a remarkable observation that the tracer slug traveled vertically along with the saltwater wedge, and the slug eventually discharged at the coastal boundary due to the strong advection-dominated flow condition that takes place near the wedge [Figure 4.5(c)]. This investigation demonstrates that the existence of the saltwater diffusion zone in coastal aquifers plays a vital role in the transport patterns of the contaminant plume.

4.4.5 Contaminant transport above a saltwater wedge under pumping condition

This simulation was designed to study the effects of pumping on the contaminant migration patterns occurring above the saltwater interface. The model domain was split into 15008 nodes and 25730 elements with $\Delta x = 1$ cm, $\Delta y = 0.85$ cm and $\Delta z = 0.984$ cm. The height of water levels on freshwater and saltwater side were set to 28.2 cm and 27.3 cm, respectively, as used in the laboratory model. The steady-state saltwater intrusion wedge was established in about 40 min in this simulation. After reaching the steady-state saltwater wedge, a tracer slug was introduced in the system to simulate the contaminant transport patterns. The location of the tracer slug within the model was: x = 13 cm and z = 23 cm. After a noticeable movement of the tracer plume, the extraction pump was then started at a rate of 2.16 cm^3/sec. As noted, the time of starting the pump was 8 min after introducing the tracer slug, and the location of the pump was: x = 33 cm, y = 4 cm, and z = 9 cm in the model. The simulation of the tracer slug, as well as the pump, was similar to the previous simulations. Similar to the previous simulations, the simulated results are analyzed to investigate the behavior of contaminant migration patterns and presented at different time intervals. The transient datasets for contaminant transport above a saltwater wedge under pumping condition experiment compare with numerical predictions are presented in Figure 4.6.

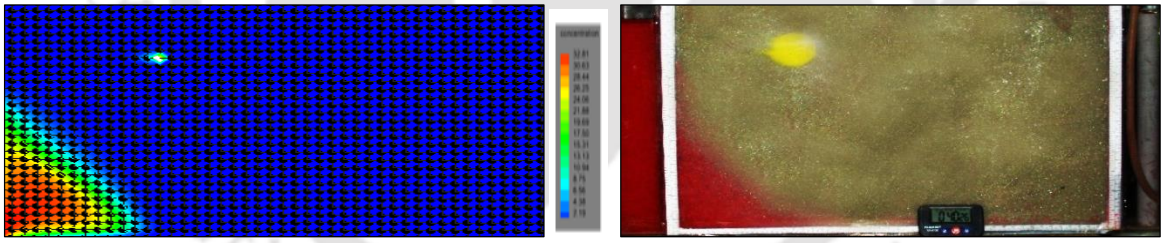

(a) 0 min

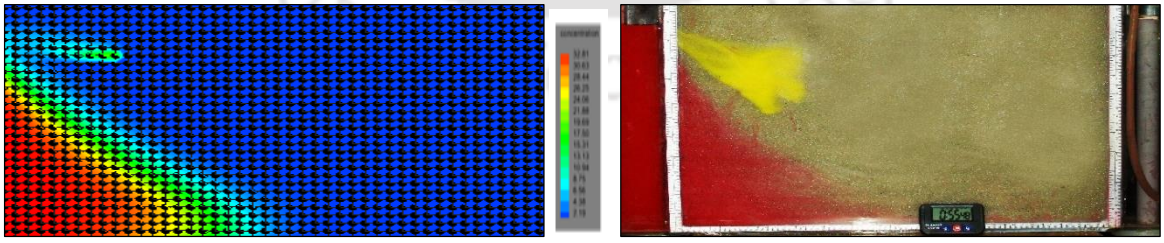

(b) 15 min

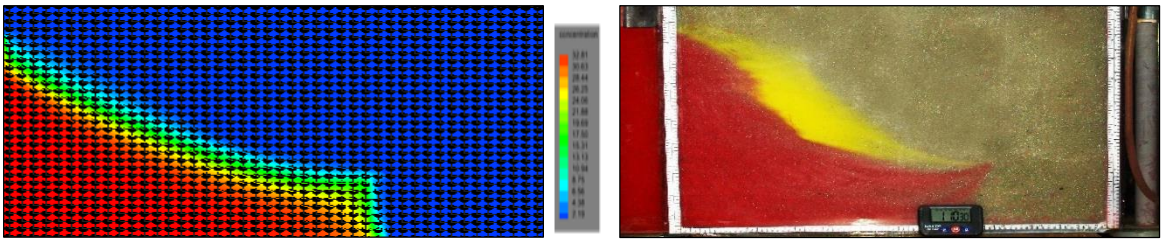

(c) 30 min

Figure 4.6: Comparison of experimental and model-simulated results in the contaminant transport above a saltwater wedge under the pumping condition experiment at (a) 0, (b) 15, and (c) 30 min

Figure 4.6(a) displays the model-simulated and experimental results just after introducing the tracer slug. Analysis of the steady-state results indicates that the toe of the saltwater intrusion wedge was approximately located at 11.3 cm from the coastal boundary in the numerical simulation. In contrast, it was 12 cm in the physical experiment. As could see in Figure 4.6(a), the initial shape of the tracer slug is nearly circular. The experimental result depicts that the tracer slug initially began to become sink, and this process was continued for about 5 min. The simulation model was not capable of replicating this sinking pattern. As the tracer plume approaches the saltwater-freshwater interface, the plume migrates slightly upward owing to the buoyancy forces induce by density contrast between the freshwater and saltwater present within the system [Figure 4.6(b)]. It can be seen in Figure 4.6(c), upon application of the pump, the saltwater wedge rapidly advances through the system towards the freshwater boundary, and the tracer plume is also drawn along with the wedge towards the pump location. As the initiation of pumping establishes a transient flow pattern that leads to a lowering in the water table within the system. Consequently, the plume, along with the wedge moves towards the landward. It is remarkable to note that in the simulation result, an upconing characteristics of the plume along with the saltwater wedge, take place near the pump as a result of pumping, similar to that observed in the laboratory experiment.

4.4.6 Contaminant transport on a saltwater wedge

This numerical simulation was undertaken to simulate the contaminant transport patterns occurring on a saltwater wedge present in an unconfined coastal aquifer. In this simulation, the model domain was split into 15008 nodes and 25730 elements with $\Delta x = 1$ cm, $\Delta y = 0.85$ cm and $\Delta z = 0.984$ cm. The constant heads of 28.2 and 27.5 cm were set on the freshwater and saltwater boundary, respectively. The steady-state saltwater intrusion wedge was attained at

about 34 min in this simulation. Similarly, a tracer slug was introduced at 34 min in the system to simulate the contaminant transport patterns after reaching the steady-state saltwater wedge. The location of the tracer slug was at 9 cm from the saltwater boundary and 7 cm above the bottom boundary of the computational domain. This simulation was terminated at 40 min, after introducing the slug. Figure 4.7 compares the numerical results predicted by the simulation model against experimental data for contaminant transport on a saltwater wedge experiment.

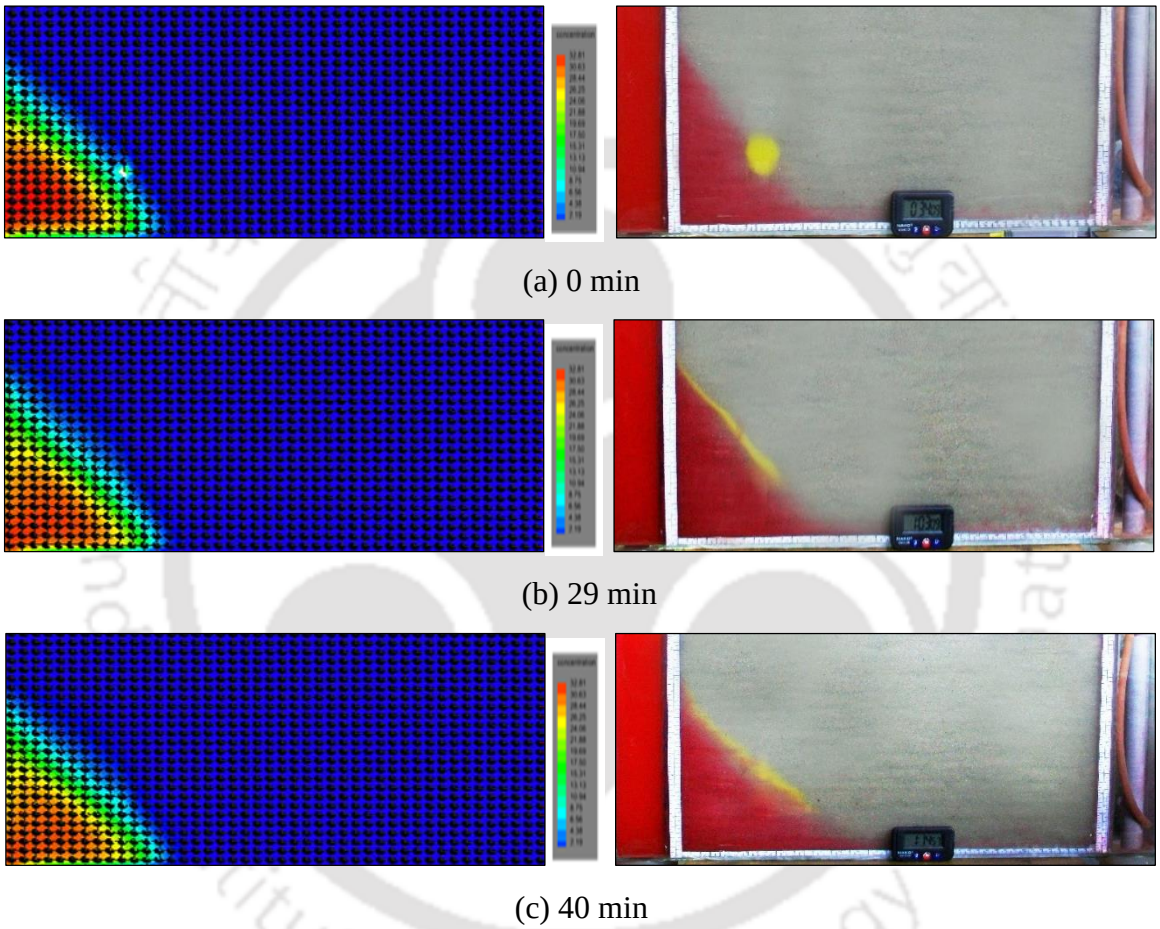

(a) 0 min

(b) 29 min

(c) 40 min

Figure 4.7: Comparison of numerical results predicted by the simulation model with experimental data for contaminant transport on a saltwater wedge experiment at (a) 0, (b) 29, and (c) 40 min

As seen in Figure 4.7(a), the initial shape of the tracer plume is almost circular at t = 0 min. At the steady-state, the toe length of the saltwater wedge is estimated at 13.4 cm in the numerical simulation, as compared to 14 cm in the laboratory experiment. As time progress, the experimental data demonstrates that the circular plume attains an elongated shape due to dispersion effects [Figure 4.7(b)], as a result of higher velocities taking place near the wedge creates a rapid transport of tracer plume mass along the dispersion zone, forming this elongated

shape. This elongated shape, however, could not precisely be observed in the simulation result. That is because of the used numerical model is not quite able to simulate the flow and transport processes of multi-species through saturated-unsaturated porous media. The model that only allows in simulating the flow and transport processes of a single species through porous media. However, it is interesting to note from the experimental result that the tracer slug does not move further seaward through the saltwater intrusion wedge. As could be observed from laboratory data shown in 4.7(c), the tracer plume travels vertically by forming a thin layer over the saltwater wedge and then exits around the coastline because of the active advective flow field present near the wedge. It is assumed the tracer plume follows the same transport path in the simulation that observed in the laboratory experiment.

4.4.7 Contaminant transport on a saltwater wedge under pumping condition

This numerical simulation aims to study the effects of pumping on the behavior of contaminant transport processes occurring on the saltwater interface. This simulation was conducted immediately after the termination of the previous simulation. The extraction pump is then initiated at a rate of 1.45 cm^3/sec in the simulation. The location of the pump was: x = 29 cm, y = 3.2 cm, and z = 7 cm, similar to the laboratory experiment. This numerical simulation was continued until 16 min from starting the simulation, and simulated results were analyzed at different time intervals. The results shown in Figure 4.8 compare the numerical results predicted by the simulation model against experimental data for contaminant transport on a saltwater wedge under the pumping condition experiment.

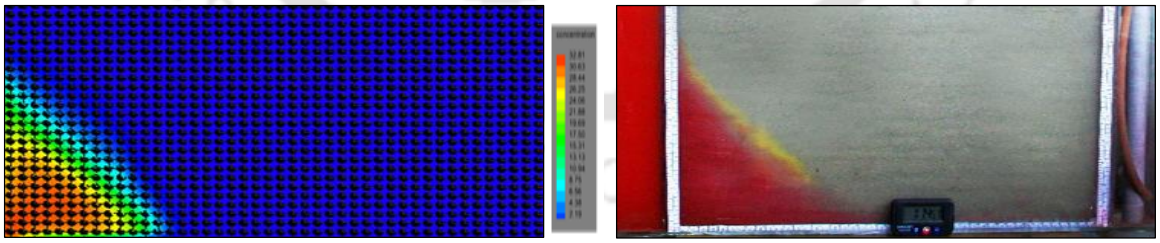

(a) 0 min

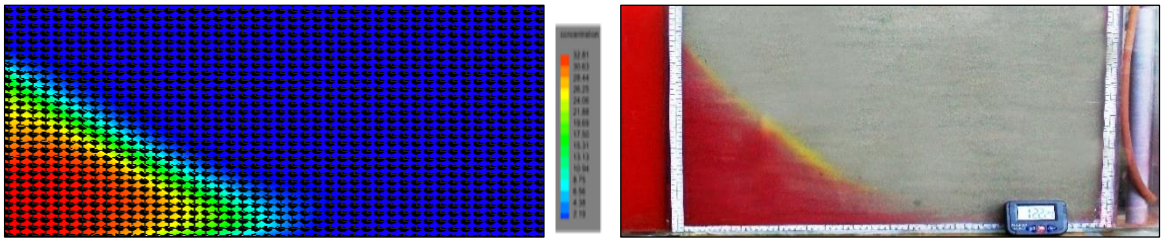

(b) 8 min

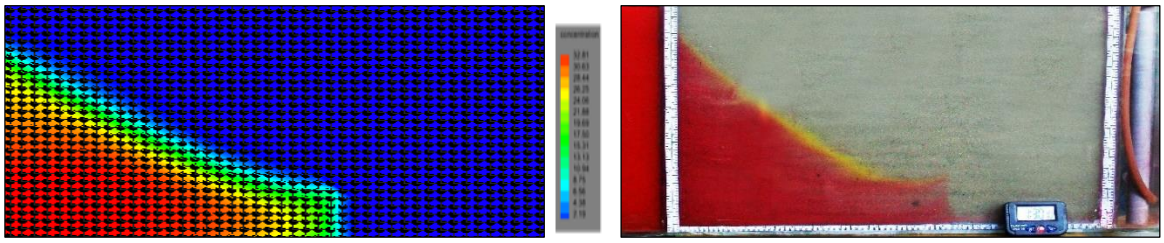

(c) 16 min

Figure 4.8: Comparison of numerical results predicted by the simulation model against experimental data for contaminant transport on a saltwater wedge under the pumping condition experiment at (a) 0, (b) 8, and (c) 16 min

The numerical results are presented at 0, 8, and 16 min after starting the simulation. The results indicate that upon application of the pump, the saltwater wedge starts to advance into the freshwater system rapidly. As time evolves, the results indicate that the tracer plume is drawn along with the saltwater intrusion wedge towards the pump location [Figure 4.8(c)], as the initiation of pumping establishes a transient flow pattern that leads to a lowering in the water table within the system. Consequently, the plume, along with the wedge, moves towards the inland side. It is interesting to note that in the simulation result, an upconing characteristics of the plume along with the saltwater wedge, occur near the pump as a result of pumping, similar to that observed in the laboratory experiment.

4.4.8 Horizontal clay lens experiment

This numerical investigation focuses on studying the flow dynamics in the presence of a horizontal clay lens in an unconfined coastal aquifer system. However, the clay lens was simulated in the numerical model by assigning the hydraulic conductivity as 1.39×10^{-10} cm/s to the elements of interest that correspond to the value measured by experimentally. The thickness of the clay lens is 3 cm. It is prolonged horizontally from the left side of the computational domain to a distance of about 28 cm and at the height of 20 cm from the bottom of the domain. It is covered the entire width of the computational domain. Also, the simulation of the pump was given through a point source extraction at the node, whereas the pump screen was present in the laboratory experiment, and the flow rate of the extracted water was given as the negative (-) value. The location of the pump in the model is: x = 32 cm, y = 2 cm, and z = 25 cm.

The entire model domain was split into 15008 nodes and 25730 elements with Δx = 1 cm, Δy = 0.85 cm and Δz = 0.984 cm. In this simulation, the height of water levels on the freshwater and saltwater boundary was set to 28.5 and 27.5 cm, respectively, yielding a head difference of 1 cm. As simulated, the steady-state saltwater intrusion wedge was achieved in about 37 min.

After reaching the steady-state saltwater wedge, the extraction pump was then started at a rate of 1.8 cm^3/sec, and the subsequent migration pattern of the saltwater intrusion wedge was simulated. The time of starting the pump was noted as 45 min and continued till 89 min. This simulation was terminated at 89 min, and simulated results were analyzed at different time intervals. The comparison of transient variations in the saltwater wedge patterns of simulated results with laboratory data for horizontal clay lens experiment is presented in Figure 4.9.

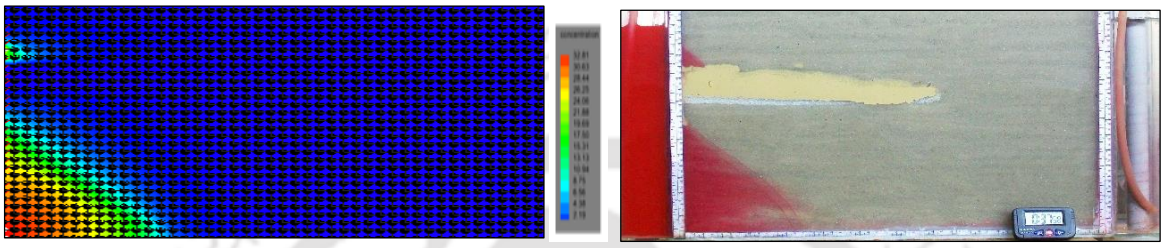

(a) 37 min (Steady State)

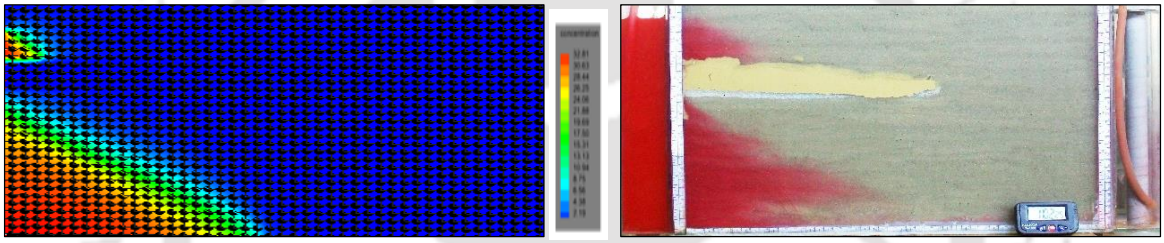

(b) 62 min

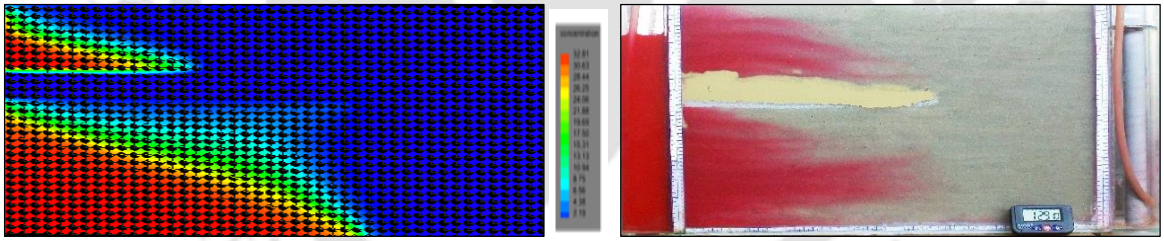

(c) 89 min

Figure 4.9: Comparison of transient variations in the saltwater wedge patterns of simulated results with laboratory data for horizontal clay lens experiment at (a) 37, (b) 62, and (c) 89 min

Figure 4.9(a) shows the model-simulated and experimental results for transport patterns of the saltwater wedge at the steady-state condition. As seen in Figure 4.9(a), there are two saltwater intrusion wedge develops, one at the base of the aquifer, and the other one above the clay lens. Because of the presence of a horizontal stratified layer, it was observed that in addition to the formation of the usual saltwater wedge, there was an additional wedge formed on top of the clay lens. The steady-state simulation result demonstrates that the toe length of the lower and upper wedges from the coastline is at 13 and 2.7 cm, respectively. This agrees well with the 13 and 3

cm, respectively measured in the laboratory-scale experiment. Figure 4.9(b) and Figure 4.9(c) indicates the model-simulated and observed data for transport patterns of the saltwater wedge at 62 min and 89 min, respectively. It can be seen in Figure 4.9(b) that upon application of pumping, both the saltwater intrusion wedges advance rapidly through the system towards the freshwater boundary. As the initiation of pumping establishes a transient flow pattern that leads to a depleting in the water table within the system, and as a result of this, the wedges move towards the landward direction. However, laboratory result shows that finger-like patterns have been observed in both the wedges [Figure 4.9(c)]. These patterns could not be found in the simulated result. Moreover, as can be seen from the simulated result shown in Figure 4.9(c), a slight upconing characteristic occurs in the lower wedge, similar to that observed in the laboratory data. It may be due to the extreme mixing of saltwater and freshwater flows near the interface as a result of pumping. The intruded wedge might have eventually reached the pump if the pumping was continued.

4.4.9 Contaminant transport with horizontal clay lens

This numerical simulation was carried out to investigate the behavior of contaminant migration patterns under the influence of a horizontal clay lens in an unconfined coastal aquifer. It was continued from the previous simulation. After completing the previous simulation, the extraction pump was stopped, and a tracer slug was then introduced within the system to analyze the behavior of contaminant transport patterns. The location of tracer slug in the model is x = 20 cm, and z = 23.5 cm. The tracer slug was allowed to migrate with the ambient freshwater flow, and subsequent simulated results were analyzed at different times. The time of introducing the tracer slug was 35 min from starting the simulation. The comparison of simulated results with experimental data for contaminant transport patterns under the influence of a clay lens experiment is shown in Figure 4.10.

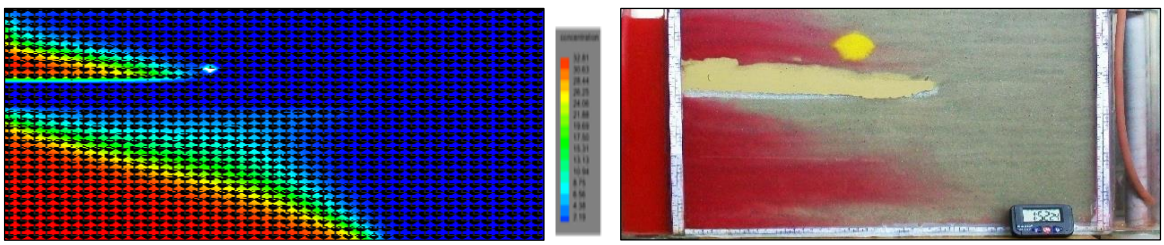

(a) 0 min

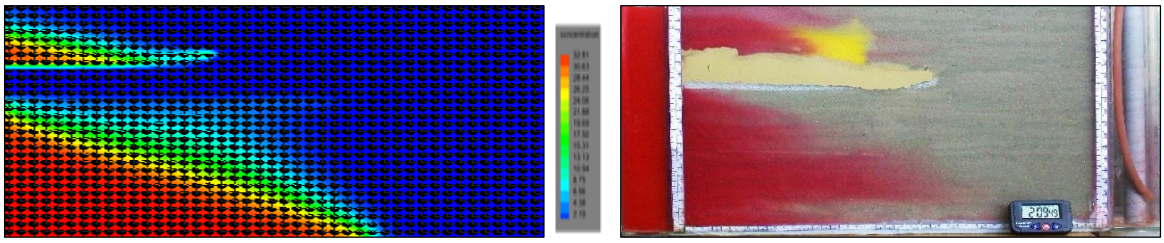

(b) 17 min

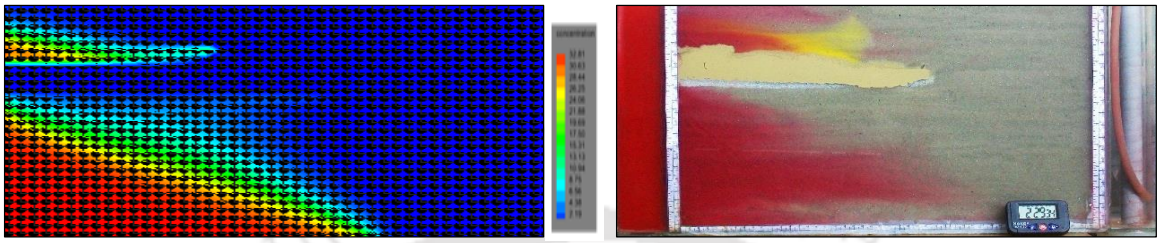

(c) 37 min

Figure 4.10: Comparison of simulated results with experimental data for contaminant transport patterns under the influence of a clay lens experiment at (a) 0, (b) 17, and (c) 37 min

Figure 4.10(a) shows the numerical and experimental results just after introduce the tracer slug, and it indicates that the initial shape of the tracer slug is nearly circular. As time advances, the simulation result depicts that the tracer slug transports toward the saltwater wedge similar to that observed in the experiment [Figure 4.10(b)]. It could see in the experimental result the slug eventually attained an elongated shape when it came closer to the saltwater wedge. Due to the higher level of mixing taking place near the interface, the plume formed an elongated shape as it approached the freshwater-saltwater interface. As stated, the used numerical model is not capable of simulating the flow and transport processes of multi-species through saturated-unsaturated porous media. Therefore, this elongated shape could not precisely be observed in the simulation. However, the laboratory data also indicate that the tracer plume moves vertically along the top surface of the saltwater wedge, and eventually, it discharges at the saltwater boundary [Figure 4.10(c)]. This is because of the active advective flow field present near the saltwater intrusion wedge. It is assumed the tracer plume follows the same transport path in the simulation that observed in the laboratory experiment.

4.5 Summary and Conclusions

Saltwater intrusion is considered a common groundwater contamination problem often exacerbated by overexploitation of coastal aquifers as it not only pollute the available groundwater resources but also adversely affects the social and economic developments of

coastal communities. Therefore, it is necessary to study the dynamics of saltwater intrusion processes in coastal aquifers so as to investigate their transport patterns and work out appropriate remedial countermeasures for sustainable management of coastal aquifer systems. The main goal of this study is to evaluate the consistency of the experimental data with numerical predictions and to explain the experimental results better. In this work, the variable-density flow and transport model FEMWATER has been used to simulate the flow, and transport processes for the experimental setup and simulations have been carried out to verify the physical phenomenon for all the laboratory-scale experiments presented in Chapter 3. The comparison of model-simulated and experimental results demonstrates that the numerical predictions are in good agreement with the experimental results. Little variations in the simulated results are observed, perhaps owing to the packing of aquifer material within the experimental setup and adopted dispersivity coefficients.

The developed numerical model in the present study could be used to simulate groundwater flow and the associated transport processes in unconfined coastal aquifers. The system is able to simulate the constant-head boundary conditions. The insights gained from this study would be useful to understand better the dynamics of saltwater intrusion processes occurring in a coastal unconfined aquifer.

A numerical investigation has successfully been performed to assess the efficiency of bentonite clay slurry on controlling the SI problem in the present study. As simulation results reveal that there is no further movement of the saltwater wedge through the barrier towards the freshwater aquifer after implementation of the barrier. The research suggests that the physical barrier created by bentonite slurry can be employed to retard the movement of the saltwater intrusion in coastal aquifers. The effect of pumping on the saltwater intrusion dynamics has been studied, and results show that the saltwater interface rapidly advances through the system towards the freshwater aquifer after the implementation of pumping. The modeling data implies that the width of the mixing zone has been increased as a result of pumping. Moreover, the influence of the injection of the freshwater on the dynamics of saltwater intrusion processes has also been investigated in this study. This study suggests that the saltwater intrusion wedge gradually recede through the system towards the saltwater boundary upon application of the freshwater injection and could be concluded that the injection of freshwater as a hydraulic barrier can be used for preventing saltwater intrusion problems in coastal aquifers.

However, contaminant transport in coastal groundwater aquifers is a significant concern due to its impact on coastal marine and estuarine environments. The comprehensive understanding

of contaminant transport in coastal aquifers is, therefore, indispensable to manage the contaminant problems effectively. In this work, numerical simulations have been conducted to investigate the contaminant transport processes occurring above and on a saltwater wedge in coastal aquifers under pumping or without pumping conditions. The simulation results indicate that the contaminant travels upward towards the seaward boundary when it approaches the saltwater wedge and then exits around the coastline. It is a remarkable observation that the contaminant plume does not travel further seaward through the saltwater intrusion wedge. This numerical investigation reveals that the existence of the saltwater diffusion zone in coastal aquifers plays a vital role in the transport patterns of the contaminant plume. The simulated results, however, also depict that the tracer plume did not follow the ideal circular flow path. As expected, upon installation of the pump, the saltwater intrusion wedge starts to advance into the freshwater system rapidly, and the contaminant plume is also drawn along with the saltwater wedge towards the pump location.

Moreover, a numerical study has also been undertaken to understand the behavior of contaminant plume in unconfined coastal aquifers under the influence of a horizontal clay lens. The simulated results indicate that there are two saltwater intrusion wedges develop, one at the base of the aquifer, and the other one above the clay lens. Because of the presence of a horizontal stratified layer, it has been observed that in addition to the formation of the usual saltwater wedge, there is an additional wedge form on top of the clay lens. The simulation results also show that the contaminant plume travels vertically along the top surface of the saltwater wedge towards the seaward boundary.

CHAPTER 5

Quantification of concentration profiles in the laboratory flow tank experiments using image analysis

5.1 Introduction

Groundwater is a vital freshwater resource for communities and ecosystems of the coastal regions that are continuously threatened by saltwater intrusion. Saltwater intrusion (SI) is a natural process that defines as the movement of saline water into an aquifer system that is hydraulically connected with the sea or ocean and mainly driven by the density contrast between the denser seawater and the lighter freshwater. Natural events such as sea-level rise due to climate change and overexploitation of coastal aquifers accelerate to further saltwater intrusions. It extensively leads to increase salinity levels in coastal aquifers, thus making it unsuitable for human utilization and further restricts future exploitation of coastal aquifers. Therefore, the sustainable management of groundwater resources in coastal aquifers is necessary to protect them from further contamination by saltwater intrusion.

In general, laboratory-scale flow tank experiments are extensively used in the study of flow and transport phenomena in porous media. In the past years, a variety of laboratory methods have been applied for the qualitative and quantitative determination of solute transport in porous media systems. These are including probe methods (Bear, 1961; Robbins, 1989), tomography techniques (Keller *et al*., 1995; Tidwell and Glass, 1995; Khalili *et al*., 1998), Photoluminescent Volumetric Imaging (Montemagno and Gray, 1995), Nuclear Magnetic Resonance (Majors *et al*., 1991; Grenier *et al*., 1997; Callaghan and Codd, 1998), and dye tracer imaging (Corapcioglu and Fedirchuk, 1999; Huang *et al*., 2002; Goswami *et al*., 2009). However, many researchers based on their studies demonstrate that image analysis techniques of dye tracer movements could be effectively employed to investigate solute transport processes in porous media flow tank experiments. This technique is usually non-invasive and very cheap. Image analysis (IA) captures an optical image property such as pixel intensity, hue or saturation, etc. and the intensity value can be recorded as either light transmission or reflection techniques. In both the methods, the relationship between light intensity and the system property, such as concentration or water content required to be determined by calibration analysis.

Nevertheless, the light reflection technique has previously been used for image analysis in most laboratory flow tank experiments (e.g., Oostom *et al*., 1992; Schincariol *et al*., 1993; Swartz

and Schwartz, 1998; Wildenschild and Jensen, 1999; Simmons *et al*., 2002; Rahman *et al*., 2005; McNeil *et al*., 2006; Konz *et al*., 2008, 2009a, b). The main advantage of this method is that it could be used with non-transparent porous material and thick laboratory flow tanks that avoid light transmission. The usage of this technique to determine the dye concentrations may involve problems with image noise and reflections from the surroundings on measurements. However, in this study, the light reflection technique has been employed to determine the solute concentrations in laboratory-scale flow tank experiments. The main focus of this study is to quantify the spatial and temporal concentration distributions of dyed saltwater flowing through the laboratory aquifer model. This image analysis (IA) technique has been applied in determining the salt concentrations to all the laboratory-scale experimental images presented in Chapter 3. The detailed methodology of the IA technique has been described in the following sections.

5.2 Materials and Methods

5.2.1 Materials

5.2.1.1 Experimental setup

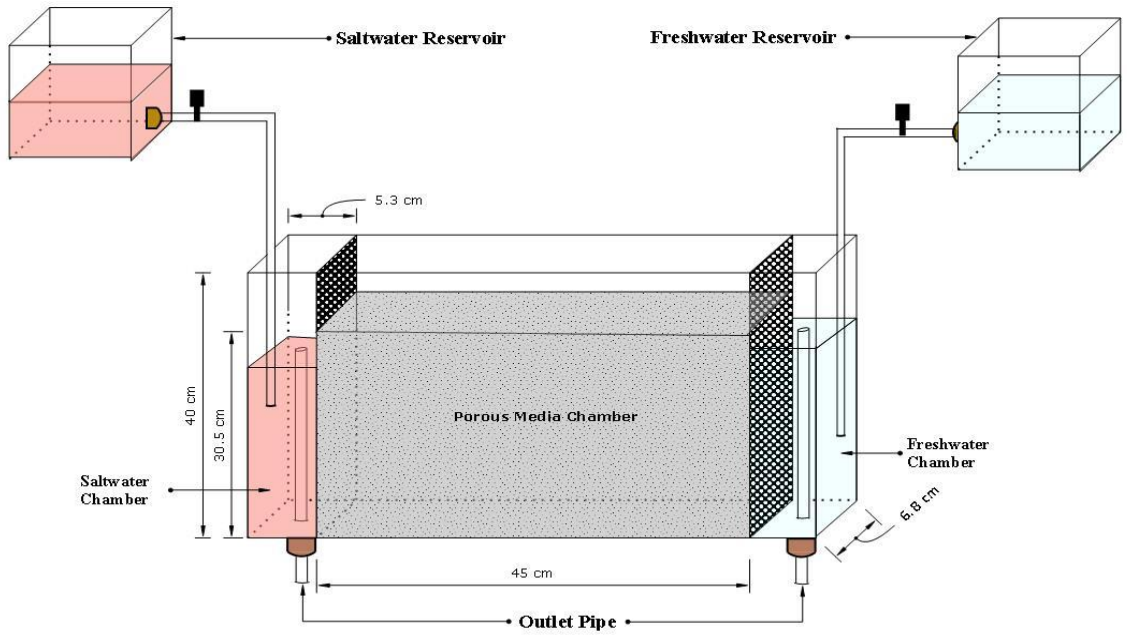

Figure 5.1: Schematic diagram of the experimental setup

Figure 5.1 shows the schematic diagram of the experimental setup. The flow tank was constructed of 6 mm thick glass sheets so that the dyed plume could be distinctly observed. The cross-section of the flow tank was rectangular, with internal dimensions of length 55.6 cm (length) × 40 cm (height) × 6.8 cm (width). The flow tank model is composed of three distinct flow chambers, and the central viewing flow chamber represents the porous media. The central chamber was filled with clear glass beads under fully saturated conditions to simulate an unconfined coastal aquifer. The other two side chambers were used for maintaining constant water heads at the boundary across the flow tank. The left and right chambers were used to feed dyed saltwater and freshwater, representing the coastal and inland boundary, respectively. The hydraulic head at both the side chambers was controlled by vertically adjusted overflow outlets. Both freshwater and saltwater were supplied at constant flow rates into the respective chambers from two overhead reservoirs during the experiments. Both the side chambers are each 5.3 cm long, and each is separated from the central chamber by perforated Plexiglas sheet of thickness 7 mm. That allows water to flow from side chambers to the central chamber. The latter was wrapped by 500-micron fine stainless-steel mesh screens to prevent the passage of porous material from the central chamber to the side ones.

5.2.1.2 Porous matrix

Commercially available glass beads, commonly used for road marking, were chosen to represent the aquifer material in all the experimental runs. In particular, glass beads have been widely used to serve as the porous media as used by various researchers in their research work (Volker *et al*., 2002; Zhang *et al*., 2002; Goswami and Clement, 2007; Abarca and Clement, 2009; Luyun *et al*., 2009, 2011; Chang and Clement, 2012, 2013, etc.) and thereby the clear glass beads have been used to represent the aquifer material in the present study.

Dyed saltwater concentration was correlated with the reflecting light intensity from the porous media chamber that is filled with clear glass beads of an average diameter of 0.57 mm. The glass beads were tamped under fully saturated conditions to avoid entrapment of air bubbles within the porous media. The porosity of the porous media was estimated using the volumetric method and yielded an average value of 0.43.

5.2.1.3 Dye tracer

A red food color dye was used as a tracer. Many researchers have previously been used food color as a dye tracer in variable-density flow tank studies (e.g., Zhang *et al*., 2002; Goswami and Clement, 2007; Luyun *et al*., 2009, 2011; Goswami *et al*., 2012; Kuan *et al*., 2012; Chang and Clement, 2013; Oz *et al*., 2014), and has the benefits of non-sorbing, very cheap and non-reactive. Therefore, 3.125 ml of red food color in a liter of the saltwater solution, yielding an adequate concentration of 3.125 ml/L, was added to discriminate it from freshwater. The saltwater solution was prepared by dissolving 35 g of commercial salt (NaCl) in 1 L of tap water at a concentration of 35 g/L. Tap water was used as a freshwater source in all the experiments. The density of both the freshwater and dyed saltwater was found to be 0.997 g/cm^3 and 1.025 g/cm^3, respectively, as estimated with a specific gravity hydrometer (G8030@JAPSINR). The addition of red food color dye did not produce any measurable change in the density of the saltwater solution (Chang and Clement, 2013; Oz *et al*., 2014).

5.2.1.4 Camera

The images were recorded by using a Nikon D3200 digital camera. The camera is equipped with an 18-55 mm objective lens, having an aperture from f3.5 to f5.6. The camera delivers 8-bit images providing 256 (0-255) intensity levels at each pixel. The camera is about 1 m away from the flow tank to acquire the entire flow tank in the field of view.

5.2.2 Methods

5.2.2.1 Calibration analysis

A calibration dataset is required to relate the recorded image property, light intensity with the system property, concentration. In order to establish the relationship between image intensity and salt concentration, different known concentrations of dyed saltwater solutions were flushed through the entire flow tank, and images were recorded corresponding to a known concentration. The dyed saltwater solutions were filled into the flow tank from a low concentration solution to a high concentration solution. In the present study, different saltwater concentrations, such as 0%, 20%, 40%, 60%, 80%, and 100% have been taken into consideration for the calibration analysis.

However, the calibration of recorded images was undertaken by using the average light intensity method. It is the simplest calibration-regression method, which involves averaging all

the light intensity values across the whole calibration image. The averaged light intensity value represents the entire aquifer domain in the regression analysis. As reported, this procedure works well for uniform lighting conditions usually observed in the homogeneous conditions (Robinson *et al*., 2015). In addition, regression analysis is carried out on the calibration data to acquire a relationship between the light intensity and the saltwater concentration. This relationship is referred to here as the concentration-intensity relationship. A second-order polynomial function is chosen to fit the observed concentration-intensity data points that match well with the measured data points. The calibration data points, along with the regressed fitted curve, are shown in Figure 5.2.

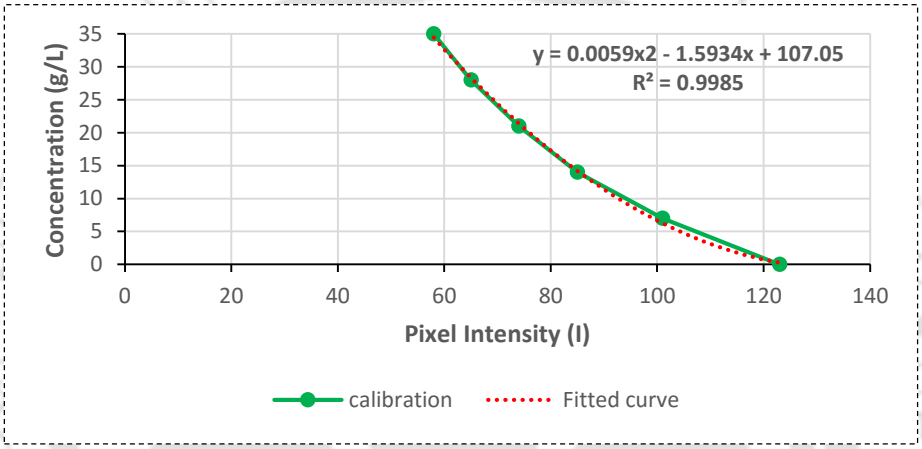

Figure 5.2: Calibration data and the fitted concentration-intensity relationship

The fitted concentration-intensity relationship is then used to measure the concentration distribution profiles in the aquifer domain, and concentration color map images were prepared for all the experimental cases.

5.2.2.2 Spatial domain bounding

An essential prerequisite of IA techniques is to define the aquifer domain boundaries to be investigated. However, considerable variations in intensity value were observed at the edges of calibration images because of edge effects. Many researchers previously removed edges from images in the image analysis (Parker *et al*., 2006; Goswami *et al*., 2009; Robinson *et al*., 2015). Therefore, the cropping method has been adopted to remove edges from the calibration image datasets. This method is also used in image datasets of all the laboratory experiments.

5.2.2.3 Spatial filtering

Median filtering is a well-recognized image processing technique for removing noises. Median filtering has been employed to reduce random noises in calibration images by using MATLAB® function *medfilt2*. In the past years, median filtering has widely been used to reduce noise introduced by non-uniformity lighting and pixel shifting due to camera movement (Schincariol *et al*., 1993; McNeil *et al*., 2006; Konz *et al*., 2008; Goswami *et al*., 2009; Robinson *et al*., 2015). In this study, median filtering with a pixel width of nine has been applied on calibration datasets in order to maintain a spatial resolution of one porous media grain diameter (Goswami *et al*., 2009; Robinson *et al*., 2015). After filtering, the color images have been converted to grayscale images for the analysis. All the laboratory-scale experimental photographs are processed through the same methodology that has been employed for processing the calibration datasets.

5.2.2.4 Error estimation

The IA techniques may involve several types of errors as similar to other measurement techniques. Non-uniformity of lighting is the most common source of error that can be both spatial and temporal (Tidwell and Glass, 1994; Detwiler *et al*., 1999). There could also be introduced some errors in data acquisition and processing because of hardware and software problems (Hansen *et al*., 2006). Moreover, as the regression relationship is not known, the selection of the best fit function for the calibration datasets would also include errors. It is only selected based on the regression statistics. Hence, the estimated concentration values using the fitted relationship would have some error. In this study, all these errors have been classified into two categories, such as:

- Calibration relationship error (CRE): The error introduces in fitting regression relationship to the calibration datasets. The error associated with the calibration relationship can be estimated using the equation (Taylor, 1997):

$$\sigma_{calib}=\sqrt{\frac{\sum_{i=1}^{N}(C_m\text{-}C)2}{N\text{-}p}} \tag{5.1}$$

Where σ_{calib} is an estimate is for CRE calculated from regression statistics, C_m is the actual measured concentration, C is the predicted concentration based on regression analysis, N is the

number of data points in the calibration, and p is the number of coefficients used to define the regression relationship.

It represents the average residual error along the curve and also known as the root mean square error (RMSE).

- Experimental error (EE): The error generates by the noise in light intensity of the calibration images due to some experimental factors including non-uniformity of lighting, light scattering, etc. The experimental error can be estimated using the relationship (Taylor, 1997):

$$\sigma_{exp} = \left| \frac{dC}{dI} \sigma_I \right| \tag{5.2}$$

Where σ_{exp} is the error in concentration due to noise in pixel intensity values, $\frac{dC}{dI}$ is the slope of the concentration-intensity relationship, σ_I is the standard deviation of light intensity in the calibration image.

The total error for the calibration is estimated by adding both the errors in quadrature (Taylor, 1997):

$$\sigma_{total} = \sqrt{\sigma_{calib}^2 + \sigma_{\exp}^2} \tag{5.3}$$

Both the errors have been estimated in order to assess the reliability of the method and to quantify the error associated with the measurements. Table 5.1 summarises the errors computed in the IA technique for the calibration images.

Table 5.1: Error analysis results for the IA method

Error type	Concentration of dyed saltwater solution (g/L)					
	0	7	14	21	28	35
Estimated concentration	0.32	6.3	14.23	21.44	28.4	34.48
σ_{calib}	0.18	0.4	0.13	0.25	0.23	0.3
σ_{exp}	8.39	8.58	8.86	9.36	10.02	10.9
σ_{total}	8.39	8.58	8.86	9.36	10.02	10.9

5.2.3 Experimental procedure

A series of saltwater intrusion experiments have been carried out in a laboratory-scale flow tank model (Figure 5.1). All the laboratory-scale experiments were recorded at various time intervals using a Nikon digital camera. A digital timer is used to record the experimental timing. The left bottom corner of the porous media chamber was considered as the origin to record experimental images.

Prior to each laboratory experiment, the porous chamber of the flow tank was filled with clear glass beads to simulate a coastal unconfined aquifer. The glass beads were tamped under fully saturated conditions to avoid air entrapment within the aquifer. The glass beads were packed to a height of 30.5 cm in layers of about 5 cm and carefully compacted within the flow tank to achieve a homogenous packing condition after each layer was complete. After filling the aquifer, the entire system was initially flushed with tap water at a constant rate from the overhead freshwater reservoir through a fixed hydraulic head gradient. This hydraulic gradient was large enough to transmit fresh water through the system toward the saltwater chamber. The freshwater and saltwater heads in the respective chambers were measured from the bottom of the flow tank. The system was then allowed to continue until it reaches a steady-state flow. After the freshwater flow stabilized, the in situ method similar to that applied by Goswami and Clement (2007) was adopted to estimate the hydraulic conductivity of the porous media. The average value was determined to be 0.251 cm/s.

After a steady-state flow was established, the saltwater chamber was then fed quickly with the red-dyed saltwater solution from the overhead saltwater reservoir through the bottom to replace freshwater, and once the saltwater attained a constant level, the saltwater began to intrude the entirely freshwater aquifer. The saltwater intrusion process was then allowed to progress through the system until an equilibrium saltwater wedge position was obtained. As the saltwater intrusion process advanced, the intruding wedge was captured through digital images at different times. All the laboratory-scale experiments were performed after the establishment of the steady-state saltwater wedge.

5.3 Laboratory-scale experiments

A series of saltwater intrusion experiments have been conducted in a laboratory-scale flow tank model. The detailed description of all the laboratory-scale experiments has been presented in Chapter 3.

5.4 Calculation of toe length and width of the mixing zone

Toe length (TL) and width of the mixing zone (WMZ) are the typical parameters used to define a saltwater intrusion wedge. As reported, TL can be defined as the distance between the seaward boundary and whereas the 50% saltwater concentration isoline intersects the bottom boundary of the aquifer (Robinson *et al*., 2015, 2016). Also, WMZ is defined as the average of the vertical distance between 25% and 75% saltwater concentration isolines in the range between 0.2×(TL) and 0.8×(TL). A reference diagram for how intrusion parameters are calculated is shown in Figure 5.3.

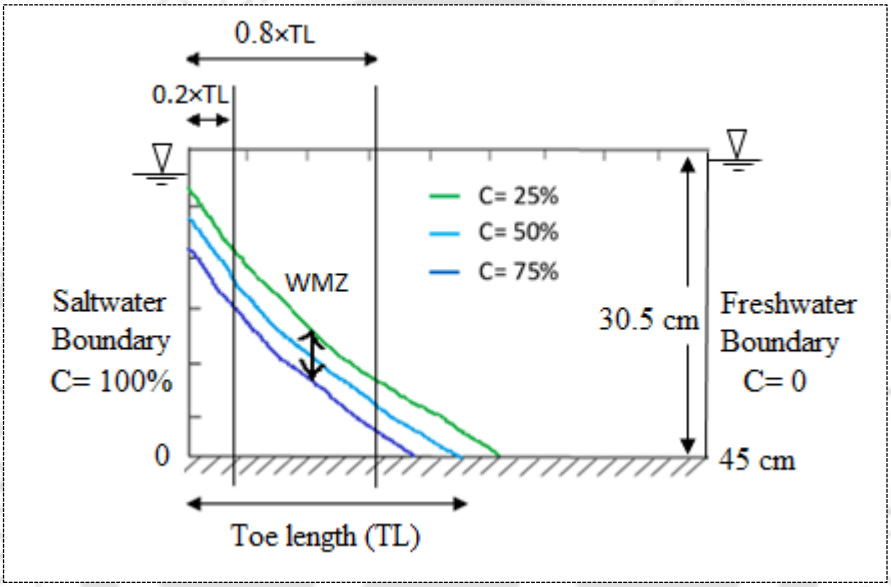

Figure 5.3: Reference diagram for analyzed the intrusion parameters ers

However, to estimate the TL and WMZ, the most typical concentration isolines are isolated, and other isolines are considered as noise and ignored. The concentration isolines are calculated using the following rules (Robinson *et al*., 2015):

- The concentration isoline needs to have a z coordinate at the bottom boundary of the aquifer domain. The concentration isoline must intersect the bottom boundary as this is how TL is computed.
- The concentration isoline must have an x coordinate at the saltwater boundary. The most typical concentration isoline must initiate at the saltwater boundary and should be present along the entire saltwater wedge.
- Unless x coordinate present at the saltwater boundary, the longest spanning isoline turns into the most representative isoline.

When the concentration isolines are located, the TL is defined as where the 50% concentration isoline intersects the bottom boundary of the aquifer domain. Also, the WMZ is computed by sampling across the 25% and 75% concentration isolines and estimating the locations of corresponding x coordinates. Once these corresponding x coordinates fall within the range of 0.2×(TL) and 0.8×(TL), the difference in z coordinates is determined and averaged across the entire wedge, thus providing the final value for WMZ.

5.5 Results and Discussions

5.5.1 Pumping of freshwater

This laboratory-scale experiment has been carried out to investigate the effect of pumping on the saltwater intrusion dynamics in a coastal unconfined aquifer. The height of water levels on the freshwater and saltwater boundary was set to 28.2 and 27.3 cm, respectively, yielding a head difference of 0.9 cm in this experiment. The steady-state saltwater intrusion wedge was achieved in about 30 min. The concentration color map image at the steady-state for the pumping of freshwater experiment is presented in Figure 5.4.

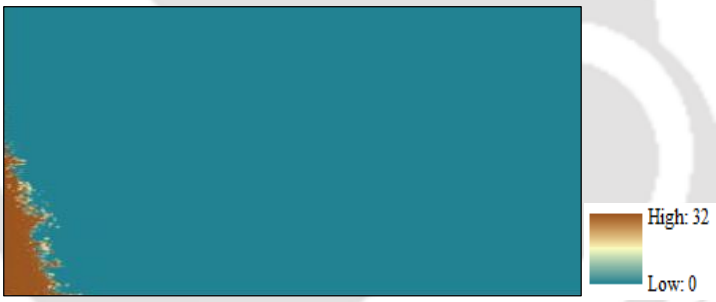

Figure 5.4: Steady-state concentration distribution profiles for the pumping of freshwater experiment

At the steady-state, the toe length (TL) and width of the mixing zone (WMZ) are calculated as 8.5 and 3.5 cm, respectively. The transient experimental TL and WMZ results are shown in Figure 5.5 and compared with the numerically simulated results. The details of the numerical simulation and results are presented in Chapter 4.

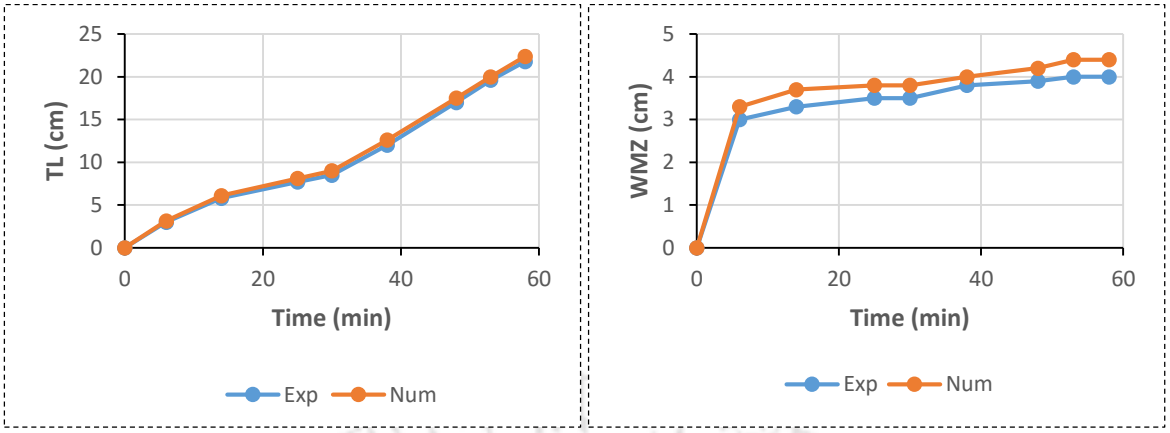

(a) (b)

Figure 5.5: Comparison of transient experimental and numerical results for the pumping of the freshwater experiment of (a) TL and (b) WMZ

As expected, after the initiation of pumping, the saltwater wedge advances through the system towards the freshwater boundary and results in an increase in TL and WMZ. This could be seen in Figure 5.5. With the pumping, the freshwater pressure head decreasing within the system that induces a landward movement of the saltwater intrusion wedge. As can be seen in Figure 5.4, the non-uniformity of the saltwater wedge has been observed. It may be due to the non-uniformity of the packing of the porous media within the flow tank.

5.5.2 Injection of freshwater

This experiment was conducted to examine the effects of freshwater injection on the saltwater wedge in unconfined coastal aquifer systems. The height of water levels on the freshwater and saltwater boundary was set as similar to the previous experiment. In this experiment, the steady-state saltwater intrusion wedge was reached after about 38 min. The concentration color map image at the steady-state is shown in Figure 5.6.

Figure 5.6: Steady-state concentration profiles for the injection of freshwater experiment

The steady-state TL and WMZ have been computed as 9 and 4.8 cm, respectively. The comparison of experimental and numerical results of transient TL and WMZ is presented in Figure 5.7.

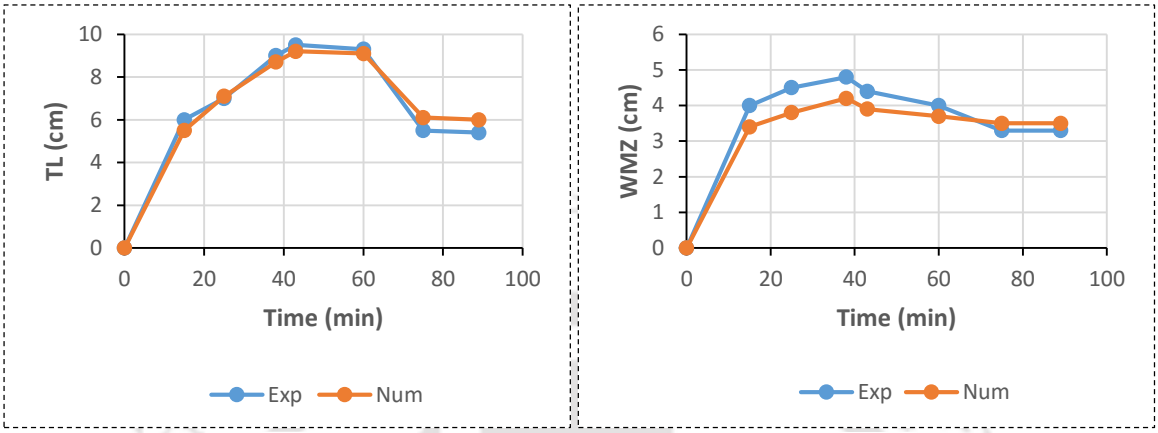

(a) (b)

Figure 5.7: Comparison of transient experimental and numerical results for the injection of the freshwater experiment of (a) TL and (b) WMZ

As expected, upon application of the injection pump, the saltwater wedge starts to recede through the system towards the saltwater boundary. It results in a decrease in TL and WMZ (Figure 5.7). With the injection of freshwater, the freshwater pressure head increasing within the system that induces a seaward movement of the saltwater intrusion wedge and drives the toe further towards the coastline. This study demonstrates that the injection of freshwater as a hydraulic barrier can be used for preventing the saltwater intrusion towards the inland side.

5.5.3 Flow barrier experiment

The purpose of this experiment is to assess the efficiency of bentonite clay slurry on controlling the saltwater intrusion problem. In general, the construction of subsurface flow barriers is one of the most extensively used engineering countermeasures to prevent or mitigate this problem in coastal aquifers. However, the constant heads of 28.3 and 27.3 cm were fixed on the freshwater and the saltwater boundary, respectively, in this laboratory-scale experiment. As noted, the steady-state saltwater intrusion wedge is obtained in about 28 min. Figure 5.8 presents the concentration color map image at the steady-state for the flow barrier experiment.

Figure 5.8: Steady-state concentration distributions profile for the flow barrier experiment

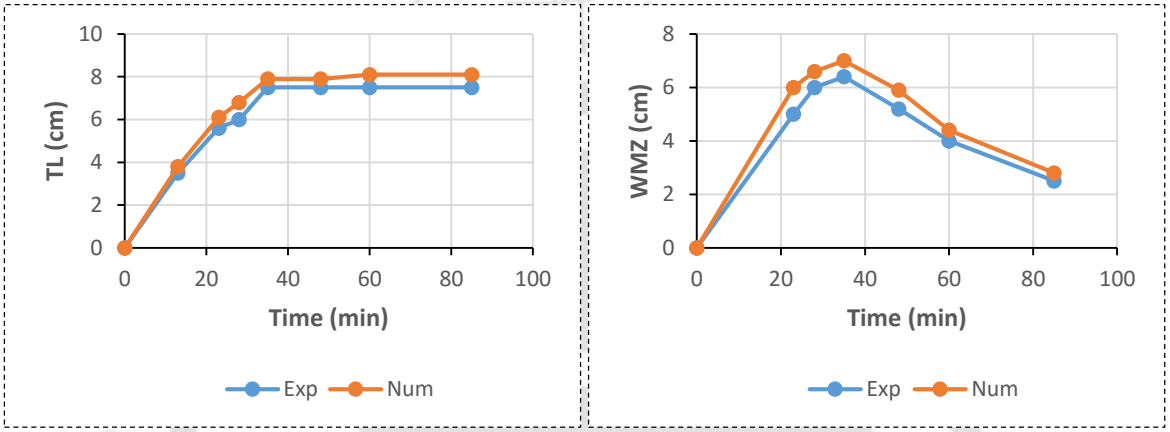

(a) (b)

Figure 5.9: Comparison of transient experimental and numerical results for the flow barrier experiment of (a) TL and (b) WMZ

The comparison of experimental and numerical results of transient TL and WMZ is shown in Figure 5.9. At the steady-state, both toe length (TL) and width of the mixing zone (WMZ) are estimated as 6 cm. In this experiment, the extraction pump was initiated within the system after establishing the steady-state saltwater wedge. Upon application of pumping, the saltwater wedge advances through the system towards the landward side. As a result of this, TL and WMZ have slightly increased in the experiment, similar to that observed in numerical simulation. It has been found in the experimental result [Figure 5.9(a)] that TL of the wedge was remaining the same as before after barrier implementation. Although the slight extension has been observed towards the flow barrier in the simulation result, it did not pass through the barrier. Therefore, it reveals that there is no further movement of the saltwater wedge through the barrier towards the freshwater aquifer. As could be seen in Figure 5.9(b), WMZ has gradually been decreased after the barrier implementation. This is observed in both the experimental and simulation results. The present study shows that physical barriers created by bentonite clay slurry can be employed for preventing the movement of the saltwater wedge towards the inland side.

5.5.4 Contaminant transport above a saltwater wedge

This experiment was performed to explore the contaminant transport processes occurring above the saltwater wedge in a coastal groundwater aquifer. The main objective of this experiment is only to determine the saltwater concentration distributions profile in the laboratory aquifer domain. In the present study, the contaminant concentration has not been taken into consideration for the analysis. The overflow outlet pipes were adjusted to maintain constant heads of 28.2 and 27.3 cm on the freshwater and saltwater boundary, respectively, in this experiment. This hydraulic gradient allowed to transmit freshwater towards the saltwater boundary. The steady-state saltwater intrusion wedge was achieved after about 37 min.

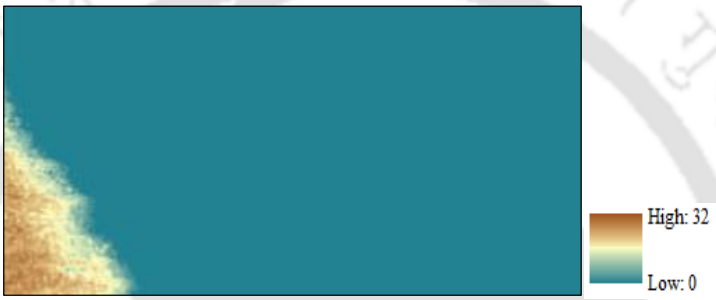

Figure 5.10: Steady-state concentration distributions profile for the contaminant transport above a saltwater wedge experiment

The concentration color map image prepared using the IA technique at the steady-state for the contaminant transport above a saltwater wedge experiment is shown in Figure 5.10. At the steady-state condition, both toe length (TL) and width of the mixing zone (WMZ) have been computed and found to be 12.7 and 3.5 cm, respectively. The comparison of numerical predictions with transient experimental TL and WMZ results for contaminant transport above the saltwater wedge experiment is presented, as shown in Figure 5.11.

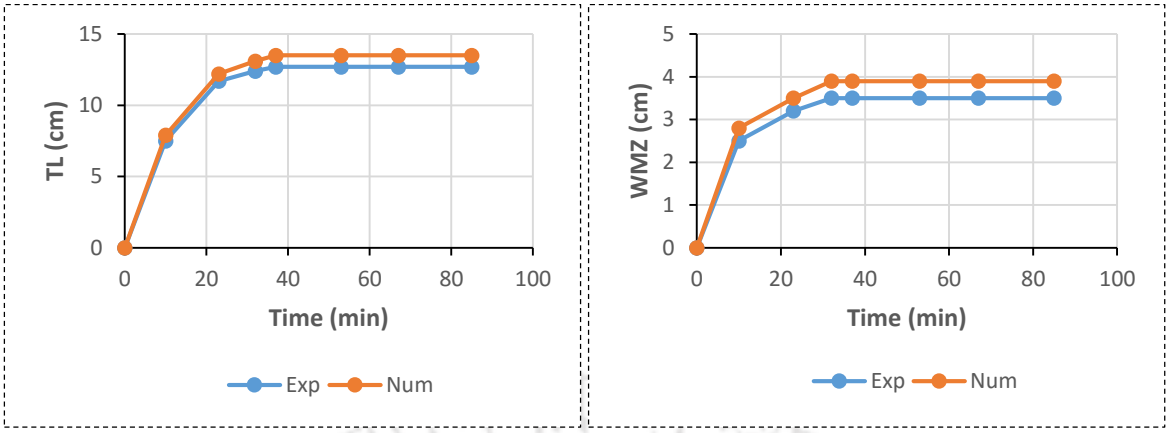

(a) (b)

Figure 5.11: Comparison of numerical predictions with transient experimental results for contaminant transport above the saltwater wedge experiment of (a) TL and (b) WMZ

It could see in Figure 5.11, the TL and WMZ gradually increase before reaching the steady-state condition. After establishing the steady-state condition, both TL and WMZ remained constant throughout the experiment, as similar to that observed in the numerical simulation.

5.5.5 Contaminant transport above a saltwater wedge under the pumping condition

This laboratory experiment was designed to study the effects of pumping on the contaminant migration patterns occurring above the saltwater interface. The height of water levels on freshwater and saltwater side were fixed to 28.2 cm and 27.3 cm, respectively as used in the previous experiment. The steady-state saltwater intrusion wedge was achieved in about 40 min. The concentration color map image prepared using the IA technique at the steady-state for the contaminant transport above a saltwater wedge under the pumping condition experiment is presented in Figure 5.12.

Figure 5.12: Steady-state concentration distributions profile for the contaminant transport above a saltwater wedge under the pumping condition experiment

Analysis of the steady-state results indicates that the TL and WMZ were approximately 11.5 and 3.3 cm in the experiment, whereas in the numerical simulation, it was 10.8 and 2.8 cm, respectively. The transient experimental TL and WMZ for the contaminant transport above a saltwater wedge under pumping condition experiment compare with numerical predictions is presented in Figure 5.13.

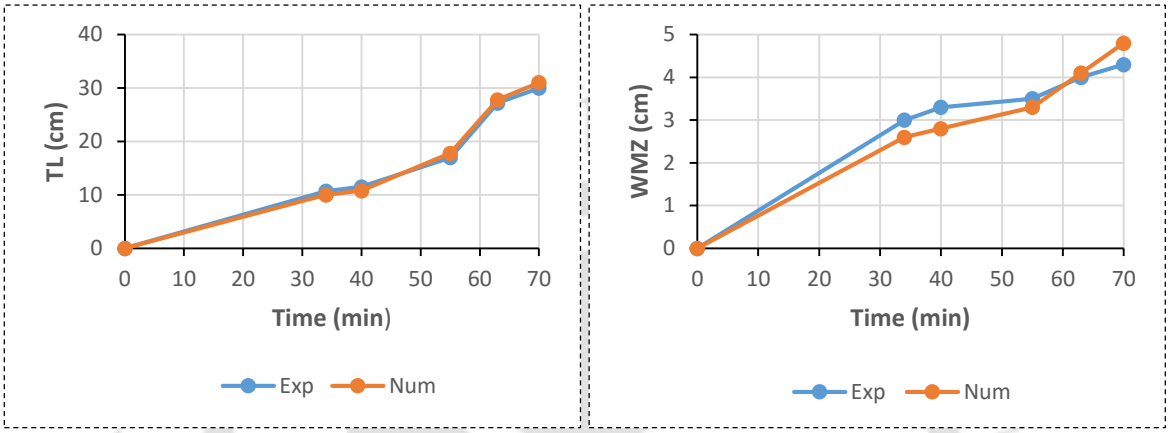

(a) (b)

Figure 5.13: Comparison of transient experimental and model-simulated results in the contaminant transport above a saltwater wedge under the pumping condition experiment of (a) TL and (b) WMZ

Similar to the previous experimental cases, upon application of the pump, the saltwater intrusion wedge starts to advance through the system towards the freshwater boundary. As the initiation of pumping establishes a transient flow pattern that leads to a lowering in the water table within the system, and consequently, the wedge moves further landward direction. Both TL and WMZ has increased due to pumping in both experiment and simulated results.

5.5.6 Contaminant transport on a saltwater wedge

This laboratory-scale experiment was undertaken to simulate the contaminant transport patterns occurring on a saltwater wedge present in an unconfined coastal aquifer. However, the constant heads of 28.2 and 27.5 cm were set on the freshwater and saltwater boundary, respectively, in this experiment. As observed, the steady-state saltwater intrusion wedge is achieved at about 34 min. Figure 5.14 represents the concentration color map image at the steady-state condition for the contaminant transport on a saltwater wedge experiment.

Figure 5.14: Concentration color map image at the steady-state condition for the contaminant transport on a saltwater wedge experiment

At the steady-state condition, both toe length (TL) and width of the mixing zone (WMZ) have been calculated and found to be 13 and 4 cm, respectively. Figure 5.15 compares the transient TL and WMZ numerical results predicted by the simulation model against experimental data for contaminant transport on a saltwater wedge experiment.

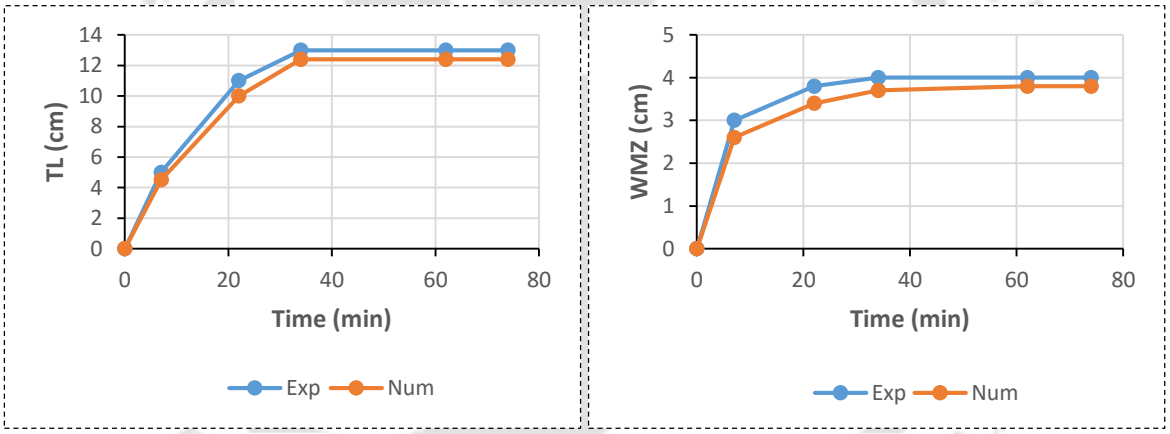

(a) (b)

Figure 5.15: Comparison of transient numerical results predicted by the simulation model with experimental data for contaminant transport on a saltwater wedge experiment of (a) TL and (b) WMZ

As could be seen in Figure 5.15, TL and WMZ gradually increase before attainment of the steady-state. It can also see in the numerical result (Figure 5.15) that both TL and WMZ were remaining constant after it reached the steady-state condition. This agrees well with the experimental result.

5.5.7 Contaminant transport on a saltwater wedge under pumping condition

This experiment aims to study the effects of pumping on the behavior of contaminant transport processes occurring on the saltwater interface. This laboratory-scale experiment was performed immediately after the completion of the previous experiment. The pump was then initiated within the system, and the subsequent migration patterns of saltwater intrusion wedge were observed. This experiment was continued until 16 min from the beginning of the experiment. The results shown in Figure 5.16 compare the transient TL and WMZ numerical results predicted by the simulation model against the experimental data for contaminant transport on a saltwater wedge under the pumping condition experiment.

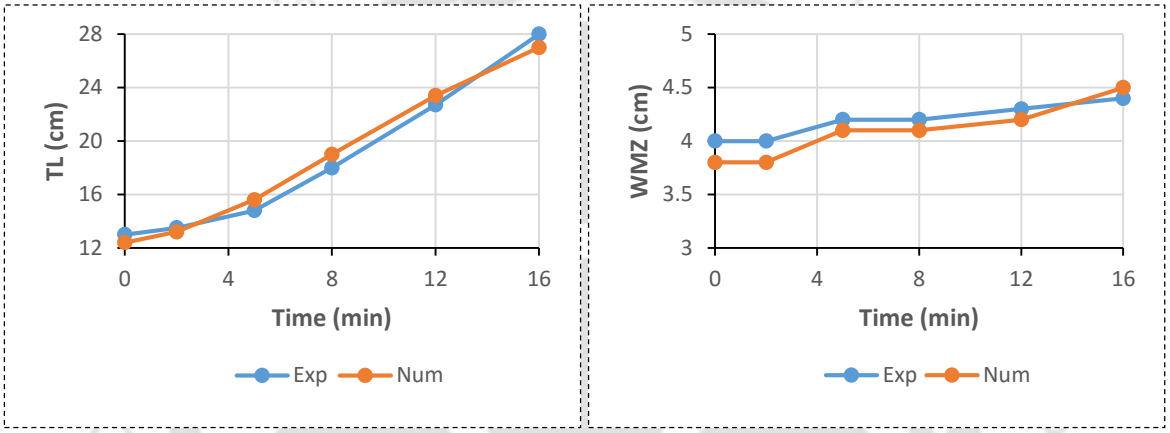

(a) (b)

Figure 5.16: Comparison of transient numerical results predicted by the simulation model against experimental data for contaminant transport on a saltwater wedge under the pumping condition experiment of (a) TL and (b) WMZ

As expected, upon initiation of the pumping, the saltwater wedge further advances into the aquifer and thus increasing to TL and WMZ. This could be observed in Figure 5.16. With the application of pumping, the freshwater pressure head is decreasing within the aquifer that induces a landward movement of the saltwater intrusion wedge.

5.5.8 Horizontal clay lens experiment

This experiment focuses on studying the flow dynamics in the presence of a horizontal clay lens in an unconfined coastal aquifer system. In this experiment, the height of water levels on the freshwater and saltwater boundary was set to 28.5 and 27.5 cm, respectively, yielding a head difference of 1 cm. The steady-state saltwater intrusion wedge was reached in about 37 min in

the experiment. The concentration color map image at the steady-state for the horizontal clay lens experiment is shown in Figure 5.17.

Figure 5.17: Steady-state concentration distributions profile for the horizontal clay lens experiment

As could be seen in Figure 5.17, there are two saltwater intrusion wedge develops, one at the base of the aquifer, and the other one above the clay lens. Because of the presence of a horizontal stratified layer, it was observed that in addition to the formation of the usual saltwater wedge, there was an additional wedge formed on top of the clay lens. In order to calculate TL and WMZ, only the lower saltwater intrusion wedge has been considered. At the steady-state condition, TL and WMZ have been estimated to be 11.8 and 3.9 cm, respectively, in the experiment, as compared to 12 and 4.2 cm, in the simulation.

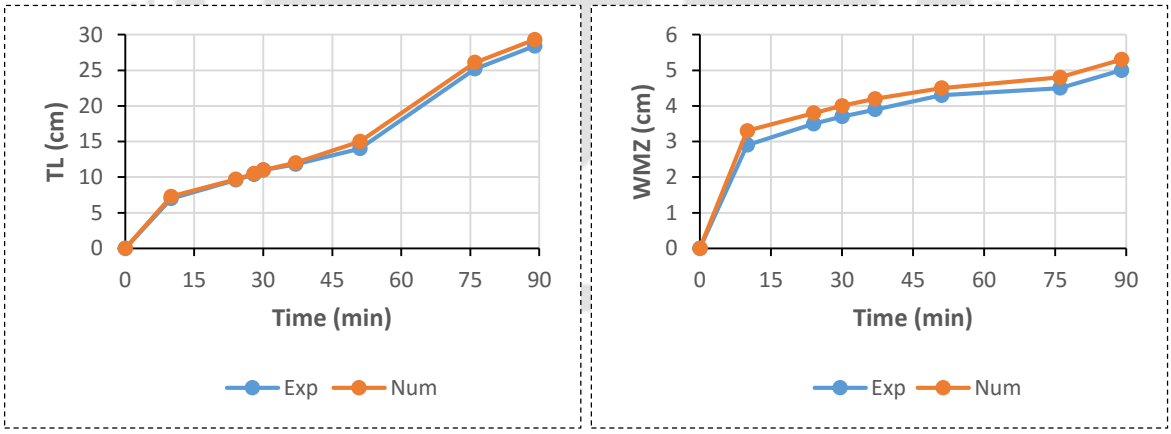

(a) (b)

Figure 5.18: Comparison of transient simulated results with experimental data for horizontal clay lens experiment of (a) TL and (b) WMZ

The comparison of transient TL and WMZ simulated results with experimental data for horizontal clay lens experiment is presented in Figure 5.18. Similar to the previous experiment,

upon application of the pumping, both the saltwater intrusion wedges advance rapidly through the system towards the freshwater boundary. As the initiation of pumping establishes a transient flow pattern that leads to a depleting in the water table within the system, and as a result of this, the wedges move towards the landward direction. Therefore, an increasing pattern of TL and WMZ has been observed in both the laboratory and numerical experiments.

5.5.9 Contaminant transport with horizontal clay lens

This experiment was performed to investigate the behavior of contaminant migration patterns under the influence of a horizontal clay lens in an unconfined coastal aquifer. This laboratory-scale experiment was continued from the previous experiment. After completing the previous experiment, the extraction pump was then stopped, and the tracer slug was injected into the aquifer. However, the main focus of this experiment is to estimate the saltwater concentration distributions profile within the aquifer using the IA technique. The contaminant concentration has not also been taken into consideration in this experiment. The transient TL and WMZ numerical predictions are compared against the observed data for contaminant transport with a horizontal clay lens experiment in Figure 5.19.

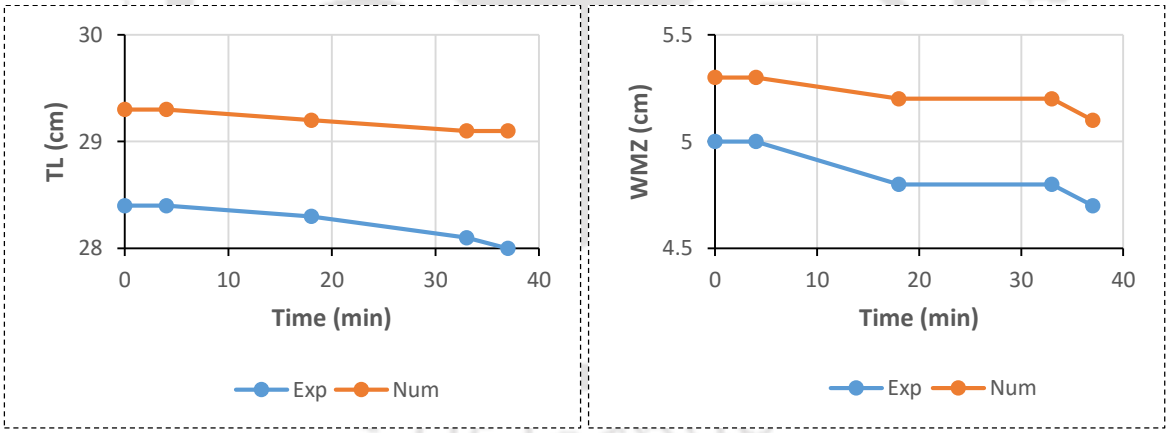

(a) (b)

Figure 5.19: Comparison of transient numerical predictions with experimental results for contaminant transport with a horizontal clay lens experiment of (a) TL and (b) WMZ

As can be seen in Figure 5.19, TL was almost the same in different time intervals. A slight variation has been observed in transient TL. Similarly, a slight deviation of transient WMZ has also been observed in both laboratory and numerical experiments.

5.6 Summary and Conclusions

Saltwater intrusion (SI) into coastal aquifers is the most widespread groundwater contamination problem that has become a considerable prominent concern around the globe. Therefore, the study on saltwater intrusion processes in coastal aquifers is tending to be of increasing interest worldwide with the growing populations and rapid development of coastal regions. The overall aim of this study is to determine the solute concentrations in laboratory-scale flow tank experiments. An image analysis (IA) technique has been presented in the present study that can efficiently measure the salt concentration distributions profile in a laboratory-scale aquifer model. In this effort, a series of saltwater intrusion experiments have been carried out in a laboratory-scale flow tank model, and the IA technique has been applied to all the laboratory-scale experimental cases in estimating the salt concentration distributions. A statistics-based error analysis method is undertaken to assess the reliability of the method and to quantify the error associated with the measurements. Moreover, the typical saltwater intrusion parameters such as the toe length (TL) and width of the mixing zone (WMZ) have been computed using the IA technique, and results are compared with the numerical predictions. The IA technique is capable of tracking both spatial and temporal variations in a saltwater wedge in laboratory-scale experiments.

However, the calibration technique in order to establish the relationship between light intensity and dyed saltwater concentration have been reported, and this relationship presents a non-linear behavior at high concentrations that is in good agreement with the results demonstrated in the published literature.

Furthermore, experimental results indicate that a more significant increase in the TL and WMZ has been observed after the initiation of pumping within the aquifer as similar to that found in numerical simulations. Because of pumping, the freshwater pressure head is decreasing within the system that induces a landward movement of the saltwater intrusion wedge. As expected, upon application of the injection pump, the saltwater wedge starts to recede through the system towards the saltwater boundary and results in a decrease in TL and WMZ. The steady-state experimental results demonstrate that TL and WMZ gradually increase before the attainment of the steady-state. After establishing the steady-state condition, both TL and WMZ remained constant throughout the experiment. This agrees well with the simulated results.

This study shows the IA technique could be effectively used for quantification of the solute concentration distributions profile in laboratory-scale flow tank experiments. The presented IA technique is non-invasive and of relatively lower cost as compared to the other methods.

CHAPTER 6

Development of Management Strategy to control Saltwater Intrusion

6.1 Introduction

Coastal regions are considered to be the most vulnerable areas around the world, as almost half of the world's population dwells within 100 km of the shoreline (Dose *et al*., 2014) and rely on freshwater aquifers for their survival. However, coastal aquifers play a pivotal role all over the world due to the availability as well as the high quality of groundwater resources they provide. Nevertheless, the quality and quantity of groundwater resources of most of these aquifers are deteriorating extensively because of saltwater intrusion. Saltwater intrusion is already emerged as a common groundwater contamination problem often exacerbated by overexploitation of coastal aquifers. The overexploitation of coastal aquifers is thus inevitable to meet the ever-increasing demands for freshwater in coastal regions as it not only leads to increasing salinity levels in coastal aquifers, thus making it unsuitable for human utilization but also further restricts future exploitation of coastal aquifers. Furthermore, it also adversely affects the social and economic developments of coastal communities. Once the aquifer gets highly contaminated by saltwater intrusion, its restoration is challenging and expensive to remediate the saltwater intruded coastal aquifers. Therefore, efficient planning and management strategies should be implemented in coastal aquifer systems to protect them and for continued utilization of groundwater resources on a sustainable basis under the threat of saltwater intrusion.

The deterioration of groundwater quality from saltwater intrusion in most of the coastal areas around the world has motivated the researchers to emphasize controlling saltwater intrusion and develop the most effective management strategies to mitigate the problem. The issue is not only to protect the groundwater resources for the human being, but also the remediation strategy should be a cost-efficient one. However, several management strategies have been proposed to prevent or mitigate saltwater intrusion problems and to secure groundwater reserves in coastal aquifers (Todd, 1959; Dam, 1999; Oude Essink, 2001) over the past decades. As reported, the earlier controlling methods have some limitations (Abd-Elhamid and Javadi, 2008). Most of these approaches are too expensive, and some of them are not applicable in some instances. The effective strategy to control saltwater intrusion is so far not developed that could efficiently manage this problem in coastal and island environments. As such, a reliable and cost-effective

strategy is, therefore, required for mitigating the problems and protecting coastal groundwater resources from further contamination by saltwater intrusion.

In the present study, an effort has been made to investigate the effect of a groundwater circulation well (GCW) on controlling saltwater intrusion in coastal aquifers using both experimental and numerical approaches. The main focus of this study is not only to cease the further migration of saltwater wedge towards inland but also to extract partially some percentage of water for human needs. The details of the laboratory experiment and numerical simulation have been presented in the following sections.

6.2 Experimental Approach

6.2.1 Laboratory Setup

A laboratory-scale experiment was conducted in a two-dimensional rectangular flow tank model with internal dimensions of length 55.6 cm, width 6.8 cm, and a total height of 40 cm, representing a homogenous and unconfined coastal aquifer (Figure 6.1).

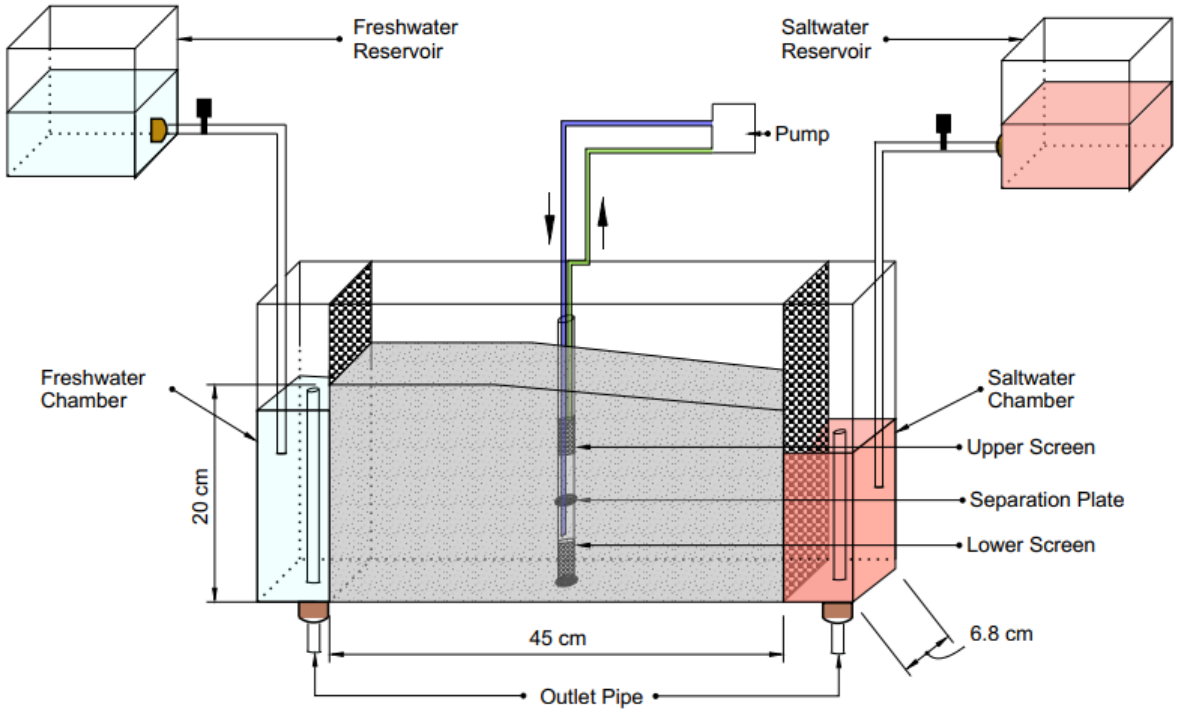

Figure 6.1: Schematic diagram of the laboratory setup

The experimental aquifer model was made using 6 mm thick glass sheets so that the experiment could be distinctly observed. As shown in Figure 6.1, the flow tank model is divided into three distinct sections, and the middle section represents the porous media (the unconfined

aquifer). The middle section of the flow tank was filled with clear glass beads under fully saturated conditions to simulate an unconfined coastal aquifer. The other two side sections were used for maintaining constant water heads at the boundary across the flow tank. The left and right side sections were used to feed freshwater and saltwater, representing the inland and coastal boundary, respectively. The hydraulic head at both the side chambers was controlled by vertically adjusted overflow outlets. Both freshwater and saltwater were supplied at constant flow rates into the respective chambers from two overhead reservoirs throughout the experiment. Both the side chambers are each 5.3 cm long, and each is separated from the porous media chamber by perforated Plexiglas sheet of thickness 7 mm. That allows water to flow from side chambers to the porous media chamber. The latter was wrapped by 500-micron fine stainless-steel mesh screens to hinder the passage of porous material from the porous media chamber to the side ones.

6.2.2 Materials Used

Commercially available glass beads, commonly used for road marking, were chosen to represent the aquifer material in the experiment (Figure 6.2). In particular, glass beads have been widely used to serve as the porous media as used by various researchers in their research work (Volker *et al*., 2002; Zhang *et al*., 2002; Goswami and Clement, 2007; Abarca and Clement, 2009; Luyun *et al*., 2009, 2011; Chang and Clement, 2012, 2013, etc.) and thereby the clear glass beads have been used to represent the aquifer material in the present study.

Figure 6.2: Sample of glass beads used in the study

The samples of glass beads were sieved to determine their grain-size distributions (Figure 6.3), and the median grain size (D_{50}) was estimated to be 0.57 mm. A uniformity coefficient (D_{60}/D_{10}) was also determined as 1.78, indicating that the grain size distribution of the glass

beads is relatively uniform (Simmons *et al*., 2002). The granulometric properties of aquifer material are listed in Table 6.1.

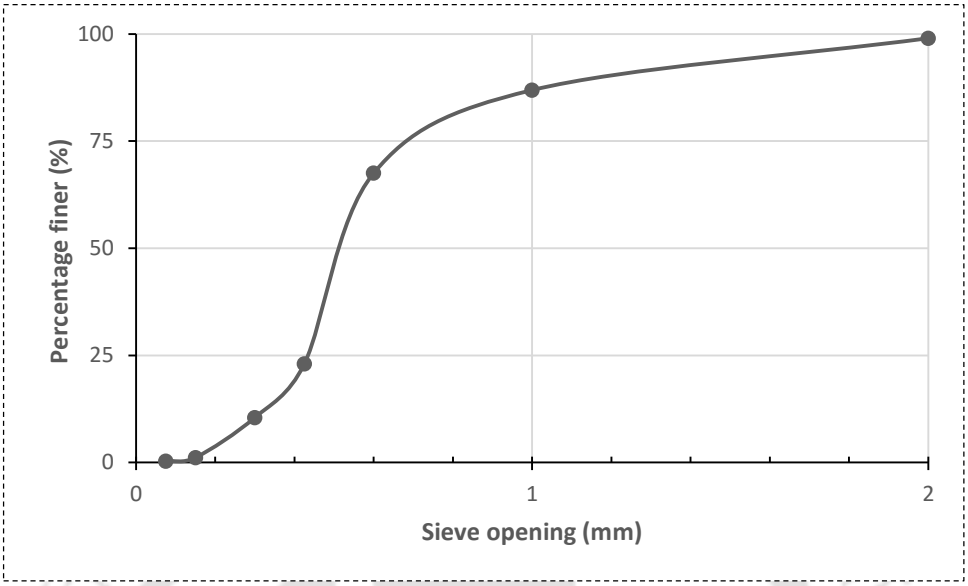

Figure 6.3: Grain size distributions of glass beads used in the present study

Table 6.1: Error analysis results for the IA method

Parameter	Value
D_{10}, mm	0.359
D_{30}, mm	0.488
D_{50}, mm	0.575
D_{60}, mm	0.642
C_u (= D_{60}/D_{10})	1.788
C_c {= $(D_{30})^2/D_{10}\times D_{60}$}	1.033

The saltwater solution was prepared before the laboratory experiment by dissolving 35 g of commercial salt (NaCl) in 1 L of tap water at a concentration of 35 g/L. Many researchers have previously been used food color as a dye tracer in variable-density flow tank studies (e.g., Zhang *et al*., 2002; Goswami and Clement, 2007; Luyun *et al*., 2009, 2011; Goswami *et al*., 2012; Kuan *et al*., 2012; Chang and Clement, 2013; Oz *et al*., 2014), and has the benefits of non-sorbing, very cheap and non-reactive. Therefore, 3.125 ml of red food color in a liter of the saltwater solution, yielding an effective concentration of 3.125 ml/L, was added to visualize the freshwater-saltwater mixing zone. Tap water was used as a freshwater source throughout the experiment. The density of both the freshwater and dyed saltwater was found to be 0.997 g/cm^3 and 1.025 g/cm^3, respectively, as estimated with a specific gravity hydrometer

(G8030@JAPSINR). The addition of red food color dye did not produce any measurable change in the density of the saltwater solution (Chang and Clement, 2013; Oz *et al*., 2014). The laboratory-scale experiment was performed at room temperature of 27^0C.

In addition, prior to the laboratory experiment, both the extraction and injection screens in the GCW were made of a 500-micron stainless-steel mesh of length of 2 cm. The internal diameter of the extraction/injection screens is 3 cm each. Both the screens are isolated with a separable plate provided in between the impermeable casing. This isolation of screens does not allow the accumulated water at the lower screen of the well to move upward. Hence, a small pinhole is provided in the separation plate through which the pump is connected either to extract the water from the lower section of the well or to inject in the lower section of the well. The diameter of the augured hole provided in the separation plate is 0.3 mm. The impermeable casing is constructed by a PVC pipe of the length of 7 cm. In this study, a 12V micropump having a maximum discharge rate of 7 cm^3/s has been used for extraction or injection.

Figure 6.4: Groundwater circulation well (GCW) used in the present study

6.2.3 Experimental Procedures

The laboratory-scale experiment was recorded at various intervals using a Nikon digital camera. A digital timer is used to record the experimental timing. The right bottom corner of the porous chamber was considered as the origin to record experimental observations. The recorded images were cropped and presented at a suitable scale to provide better visualization.

Prior to the laboratory experiment, the groundwater circulation well (GCW) was initially emplaced in the middle of the porous media chamber within the flow tank. It allowed for starting the GCW at any phase of the experiment without disturbing the aquifer media. The GCW was located at x = 22.5 cm, and y = 3.4 cm from the saltwater boundary and had a height of 12 cm (i.e., z = 12) from the bottom boundary of the flow tank. After placing the GCW, the porous

section of the flow tank was filled with clear glass beads to simulate an unconfined coastal aquifer. The glass beads were packed under fully saturated conditions to avoid entrapment of air bubbles within the porous media. The glass beads were packed to a height of 20 cm in layers of about 5 cm within the flow tank. Each of the layers was prudently compacted to satisfy a homogenous condition. After filling the porous media chamber, the entire system was initially flushed with tap water at a constant rate from the overhead freshwater reservoir. The overflow outlets were adjusted to maintain a constant head of 15.5 cm and 14.5 cm in the freshwater and saltwater chamber, respectively, yielding a head difference of 1 cm. These head values were estimated from the bottom of the flow tank. This hydraulic gradient allowed to transmit freshwater through the system towards the saltwater boundary. The system was then allowed to continue until it reaches a steady-state flow. After a steady freshwater flow established, a similar procedure to that used by Goswami and Clement (2007) was employed to determine the hydraulic conductivity of the porous media, and the average value was found to be 0.172 cm/s. The porosity of the porous media was calculated using the volumetric method and yielded an average value of 0.43. Table 6.2 presents the geometrical and hydraulic properties of porous media.

Table 6.2: Properties of the porous media

Parameter	Value
Average grain size, mm	0.57
Average bulk density, g/cm^3	1.443
Specific gravity	2.49
Average hydraulic conductivity, cm/s	0.172
Porosity	0.43

After establishing a steady-state flow, the red-dyed saltwater solution was then introduced quickly from the overhead saltwater reservoir into the saltwater chamber to replace freshwater. Once the saltwater reached a constant level, the saltwater intrusion process was initiated. The system was then allowed to progress for some time until the steady-state saltwater wedge was achieved. As the saltwater intrusion process advanced, the location of the toe of the intruding wedge was determined and captured through digital images at different times. After the establishment of the steady-state wedge, the extraction of water from the aquifer was initiated for 5 min at the rate of 1.25 cm^3/sec, and the subsequent migration pattern of saltwater intrusion wedge was observed. The GCW was then introduced within the system after 5 min of extraction, and the entire system was allowed to continue until the end of the experiment.

6.3 Laboratory-scale experiment: Results and Discussions

The laboratory-scale experiment has been performed to investigate the effect of a groundwater circulation well (GCW) on controlling saltwater intrusion in unconfined coastal aquifers. Figure 6.5 represents the transport patterns of saltwater intrusion wedge in the flow tank. The photographs were taken at 5, 15, 32, and 47 min after starting the experiment. The color image taken from the flow tank experiment at the steady-state (SS) is shown in Figure 6.5(d). The steady-state saltwater wedge was achieved after about 47 min. At the steady-state condition, the toe of the saltwater wedge was located at 8.75 cm from the coastline, and the elevation of the wedge at the saltwater boundary (at x = 0) was 11 cm.

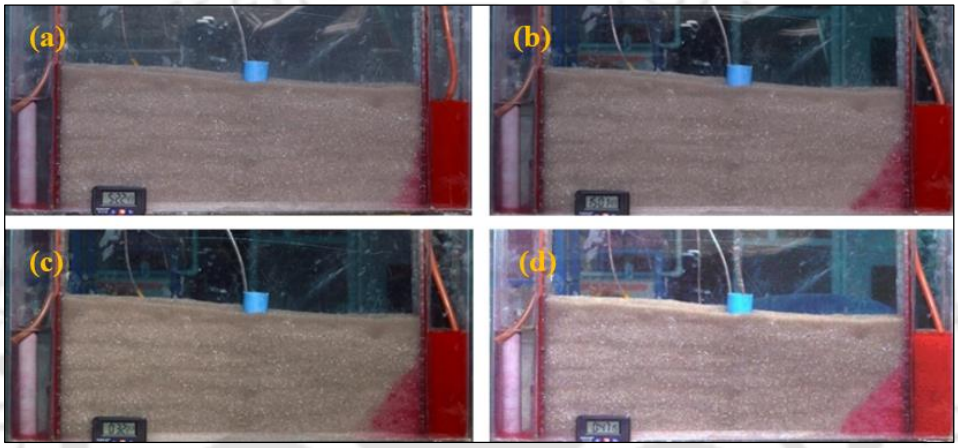

Figure 6.5: Transport patterns of saltwater intrusion wedge at (a) 5 min, (b) 15 min, (c) 32 min, and (d) 47 min

After reached the steady-state saltwater wedge, the extraction pump was started at a rate of 1.25 cm^3/s, and the subsequent migration pattern of the saltwater intrusion wedge was observed.

Figure 6.6: The experimental result after 5 min of extraction over the steady-state position at 47 min

To observe the better effect of the GCW on the saltwater intrusion dynamics, the extraction pump has initially been used within the aquifer. The time of beginning the extraction pump was noted as 47 min. As could be seen in Figure 6.6, after the extraction pump was initiated, the saltwater wedge rapidly advanced through the system towards the freshwater boundary. From

the experimental data, it can be observed that a considerable mixing of saltwater and freshwater flows during the intrusion period. The mixing takes place due to the advection occurs as a result of pumping.

The GCW was then initiated within the system at 52 min and continued till 2 hrs 40 min. After starting the GCW, it can be observed that the position of the wedge is shifted towards the seaward boundary, and the groundwater circulation well (GCW) has been acting as a hydraulic barrier (Figure 6.7). The toe of the saltwater wedge was measured as 6.5 cm from the coastline at 2 hrs 40 min.

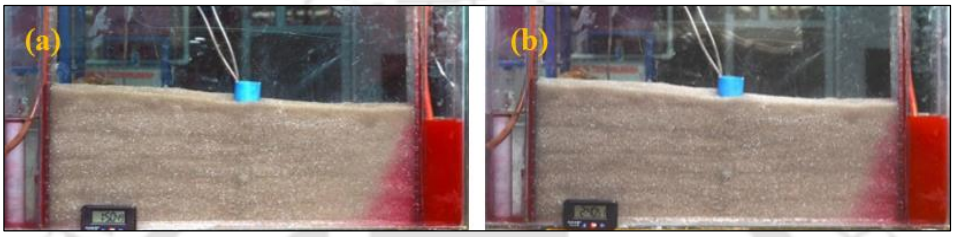

Figure 6.7: Effect of GCW on the saltwater wedge at (a) 1 hr 50 min, and (b) 2 hrs 40 min

For a better understanding of the phenomenon, a GCW system with partial extraction was employed to push the saltwater intrusion wedge towards the saltwater boundary. For better visualization of the movement of recirculated water, food color (blue) dye was injected on the lower screen of GCW with 10% partial extraction through the injection pump. The time of injection of blue-colored dye was recorded as 2 hrs 45 min. The observational results are presented in Figure 6.8. The toe of the saltwater wedge was measured at 3 hrs 17 min as 7.56 cm from the coastline.

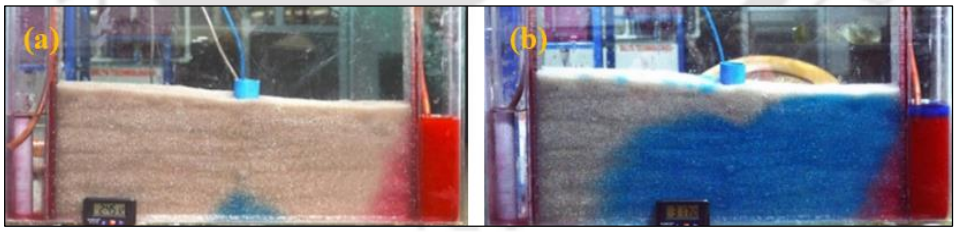

Figure 6.8: Experimental results for 10% partial extraction at (a) 2 hrs 45 min, and (b) 3 hrs 17 min

It can be seen in Figure 6.8, the blue color plume initially formed a circulation cell due to the presence of an extraction pump at the upper screen and then moved towards the seaward boundary. It was also seen that as it approached closer to the interface, it moved over the freshwater-saltwater interface, and eventually, the plume discharged at the saltwater chamber. It

proves that even after partial extraction of water, there was no further migration of saltwater wedge towards the well. Hence, GCW can act as a hydraulic barrier in controlling saltwater intrusion in coastal aquifers. Simultaneously, some water can be extracted from the aquifer through the well for different domestic, agricultural, or industrial needs.

6.4 Numerical Approach

The variable-density flow and transport model FEMWATER (Lin *et al*., 1997) is adopted to simulate the flow and transport processes for the laboratory-scale experiment conducted in this study. It is a three-dimensional finite-element model that can simulate the density-dependent flow and mass transport through saturated-unsaturated porous media. The detailed description of the governing equations for flow and transport processes is already presented in Chapter 4. The main goal of the simulation was to evaluate the consistency of the experimental result with the numerical prediction. Once the numerical model is validated, the model can be used for creating different saltwater intrusion management scenarios using GCW. The details of the numerical simulation model have been presented in the following sections.

6.4.1 Description of the Model

The numerical description of the experimental setup involves a rectangular domain of 45 cm × 20 cm, as shown in Figure 6.9. The entire model domain was split into 7749 nodes and 12800 elements with $\Delta x = 1.125$ cm, $\Delta y = 0.85$ cm and $\Delta z = 1$ cm.

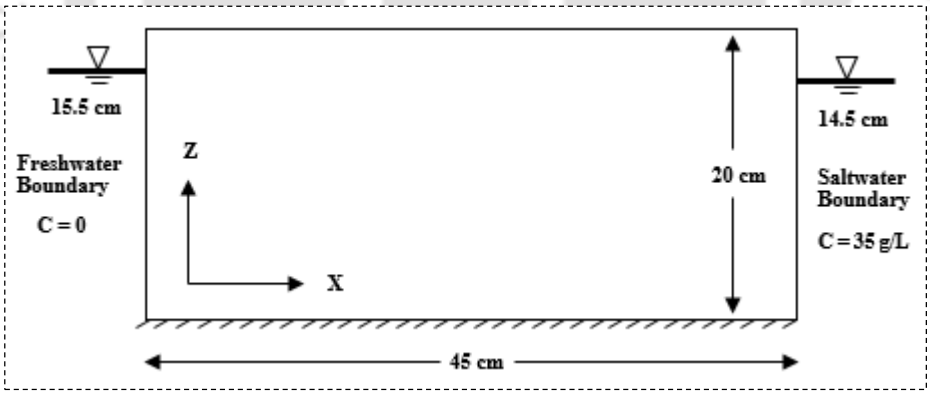

Figure 6.9: Computation domain and boundary conditions used in the numerical model

The left and right side boundaries of the model were assigned as the inland and coastal boundary, respectively. Hydrostatic pressure boundary conditions were applied on the left-side boundary (C = 0%) and to the right-side boundary (C = 100%). A concentration of 35 g/L was used for the saltwater boundary. The constant head of 15.5 cm was set on the freshwater boundary while that was fixed at 14.5 cm on the saltwater boundary, yielding a head difference of 1 cm for the entire numerical simulation. The base of the domain was bounded by an

impervious boundary. No flow boundary conditions were specified at the top, the front and the backside of the computational domain.

The initial condition used in the model was that of a totally freshwater aquifer. The freshwater and saltwater boundary conditions were assigned upon the system, and the system was allowed to reach the steady-state condition. The value of time step Δt was set at 60 s in the simulation.

To simulate a GCW in the model, two wells have been used to represent extraction/ injection at the same location in a horizontal direction. The location of both extraction and injection wells center was at x = 22.5 cm and y = 3.4 cm but in different model layers. Also, the flow rate of the extracted water is given as the negative (-) value as well as it is given as the positive (+) value for the injection. The longitudinal dispersivity (a_L) was estimated using the method described in Xu and Eckstein (1995), and the transverse dispersivity (a_T) was assumed to be 1/10 of the longitudinal dispersivity (Goswami and Clement, 2007). The longitudinal dispersivity and transverse dispersivity values were assigned to be 7 cm and 0.7 cm, respectively. The density of freshwater and saltwater was set into the numerical model to be 0.997 g/cm^3 and 1.025 g/cm^3, respectively. The other numerical parameters used in this study are listed in Table 6.3. All other parameters were fixed at the default values in the FEMWATER.

Table 6.3: Parameters of Numerical Simulation

Parameter	Value	Source
Bulk density	1.443 g/cm^3	Measured
Hydraulic conductivity	0.172 cm/s	Measured
Pumping rate	1.25 cm^3/s	Measured
Molecular diffusion coefficient	1×10^{-5} cm^2/s	Freeze and Cherry (1979)
Porosity	0.43	Measured

6.5 Numerical Simulation: Results and Discussions

The numerical model has been built up to simulate the flow and transport processes for the experimental setup, and simulations have been carried out to verify the physical phenomenon of saltwater intrusion dynamics under the effect of a groundwater circulation well (GCW). In this section, the experimental results are compared against numerical predictions.

The experimental results indicate that there is further movement of the saltwater wedge towards the well due to the extraction of water. Even though recirculating the freshwater by using the GCW, the saltwater wedge was subsidized and pushed towards the saltwater boundary to achieve a new steady state. At the steady-state condition, the toe of the saltwater wedge was 8.75

cm in the physical model, whereas in the numerical simulation, it was 8.98 cm. Later, a new steady-state wedge position was achieved at 6.5 cm and 6.75 cm, respectively, in the laboratory experiment and numerical simulation using the GCW. Also, partial extraction of 10% was recirculated as such the toe of the saltwater wedge has shifted to 7.56 cm and 7.88 cm respectively in the laboratory experiment and numerical simulation. The comparison of the numerical and experimental results shows that the numerical prediction is in good agreement with the experimental results (Figure 6.10).

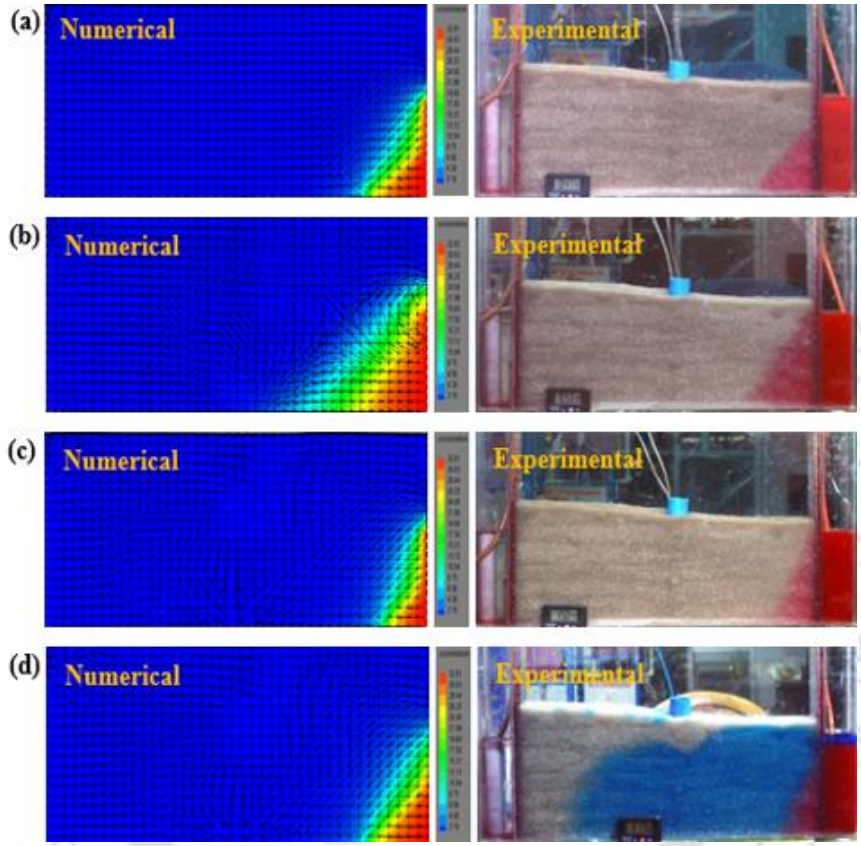

Figure 6.10: Comparison of numerical and experimental results for (a) Steady State, (b) 5 min extraction, (c) GCW with 0% partial extraction and (d) GCW with 10% partial extraction

It can be observed from Figure 6.10 that due to the presence of groundwater circulation well (GCW), the saltwater intrusion wedge has been pushed toward the coast, and the groundwater circulation well has been acted as a hydraulic barrier.

Prior to the development of reverse circulation flow GCW, a standard flow GCW was modeled with extraction at lower screen and injection at the upper screen, keeping the same parameters as it was considered in the physical model. Figure 6.11 shows the simulation result for the steady-state condition.

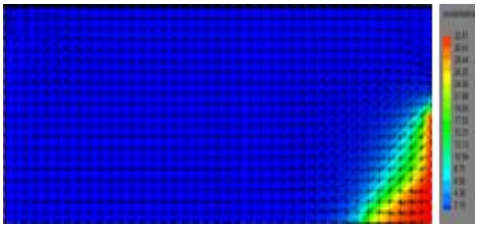

Figure 6.11: Simulation result for steady-state (SS) condition

To evaluate the effect of partial extraction from the GCW on the saltwater intrusion wedge, a numerical simulation has been conducted with different partial extraction between 0% to 50%. The simulation results of this scenario are presented, as shown in Figure 6.12.

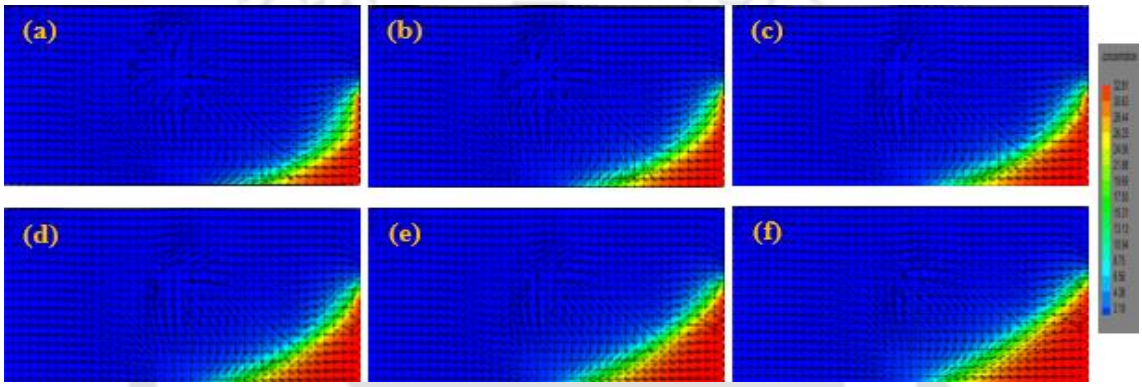

Figure 6.12: Standard flow GCW for (a) 0% partial extraction, (b) 10% partial extraction, (c) 20% partial extraction, (d) 30% partial extraction, (e) 40% partial extraction and (f) 50% partial extraction

From the simulation results, it was found that for most of the cases of partial extraction (0%-50%), the saltwater intrusion wedge migrated near the GCW. It may be observed from Figure 6.12 that the saltwater wedge is moving towards the inland side with an increase in the partial extraction rate. However, the wedge has not touched the GCW. As such, proper care has to be taken if it is necessary to go for a partial extraction from the well.

The results of the new steady-state (SS) saltwater wedge position of Standard flow for different percentages of partial extraction are compared with the initial steady-state (SS) saltwater wedge in Figure 6.13.

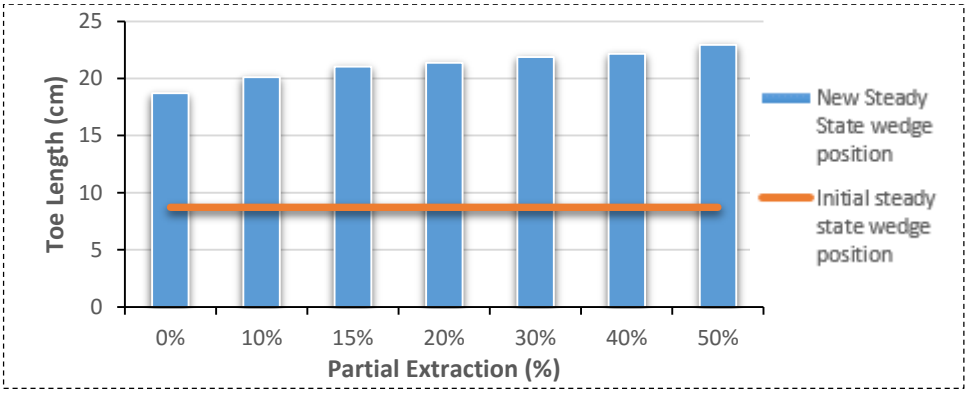

Figure 6.13: Comparison of the new steady-state wedge position of Standard flow for different percentages of partial extraction with the initial steady-state wedge

As could be seen in Figure 6.12, the saltwater intrusion wedge migrates to near the GCW for most of the cases of partial extractions (0%-50%). Therefore, it has been decided not to choose standard flow GCW for further analysis in this study. Hence, reverse circulation flow GCW was selected for both the physical experiment and numerical simulation model.

6.6 Scenarios Development

To obtain the optimal percentage of the partial extraction, different scenarios have numerically been developed, and the model was simulated for all the scenarios. Firstly, it was developed for 0%, 10%, 20%, 30%, 40%, 50% of partial extractions with different screen lengths. Also, scenarios for different anisotropy values and different discharges for recirculation were developed. Table 6.4 and Table 6.5 shows the different scenarios developed in this study. The optimal percentage of extraction and screen length are finally obtained by conducting a thorough analysis of these scenarios. The detailed analysis of these scenarios has been presented in the following sections.

Table 6.4: Scenarios developed for different screen length

Scenarios	Partial extractions (for Q = 1.25 cm^3/s and K_x/K_z = 1)					
	0%	10%	20%	30%	40%	50%
Scenario 1	Screen length 3 cm, Distance between screens 9 cm					
Scenario 2	Screen length 4 cm, Distance between screens 8 cm					
Scenario 3	Screen length 5 cm, Distance between screens 7 cm					
Scenario 4	Screen length 6 cm, Distance between screens 6 cm					

Table 6.5: Scenarios developed for different discharge and anisotropy value

Scenarios	Partial extractions (for screen length 4 cm and distance between screens of 8 cm)					
	0%	10%	20%	30%	40%	50%
Scenario 5	Discharge (Q = 0.625 cm^3/s), Anisotropy (K_x/K_z = 1)					
Scenario 6	Discharge (Q = 1.25 cm^3/s), Anisotropy (K_x/K_z = 2)					
Scenario 7	Discharge (Q = 0.625 cm^3/s), Anisotropy (K_x/K_z = 4)					

6.6.1 Scenario 1

As demonstrated above, scenario 1 represents the case of upper and lower screens length as 2 cm and 1 cm with a spacing of 9 cm. The model was simulated for different percentages of partial extraction with discharge (Q = 1.25 cm^3/s) and anisotropy (K_x/K_z = 1). The total simulation time was 4 hrs. Figure 6.14 represents the simulation result for the initial steady-state condition, and the initial steady-state saltwater wedge was at 8.67 cm from the saltwater boundary. From the analysis, it was observed that the new steady-state wedge positions were established at 6.27, 7.74, 8.49, 9.32, 11.71, 13.83, and 15.9 cm respectively, for 0%, 10%, 20%, 30%, 40%, and 50% partial extraction. The numerical simulation results are displayed in Figure 6.15. Hence, it is cleared that if the partial extraction is nearly below or equal to 15%, the horizontal extents of the new steady-state wedge position are under the initial steady-state position. Therefore, at least 15-20% of water can be extracted from GCW without preventing the initial steady-state. It is cleared that there is no problem in extracting 30% of the water from the GCW since the location of GCW is 22.5 cm from the coastline. Figure 6.16 shows the partial extraction possible under the initial steady-state wedge position for a 3 cm screen length.

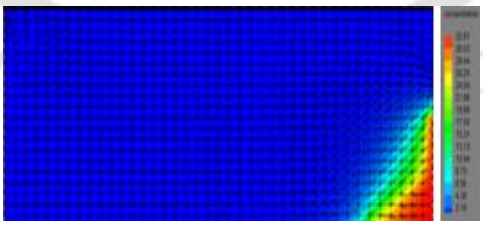

Figure 6.14: Simulation result for initial steady-state (SS) condition

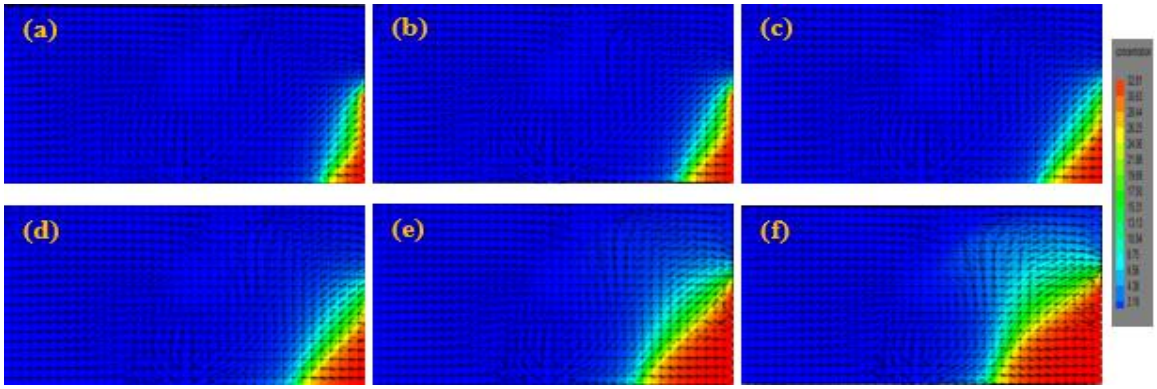

Figure 6.15: Reverse GCW with 3 cm screen for (a) 0% partial extraction, (b) 10% partial extraction, (c) 20% partial extraction, (d) 30% partial extraction, (e) 40% partial extraction and (f) 50% partial extraction

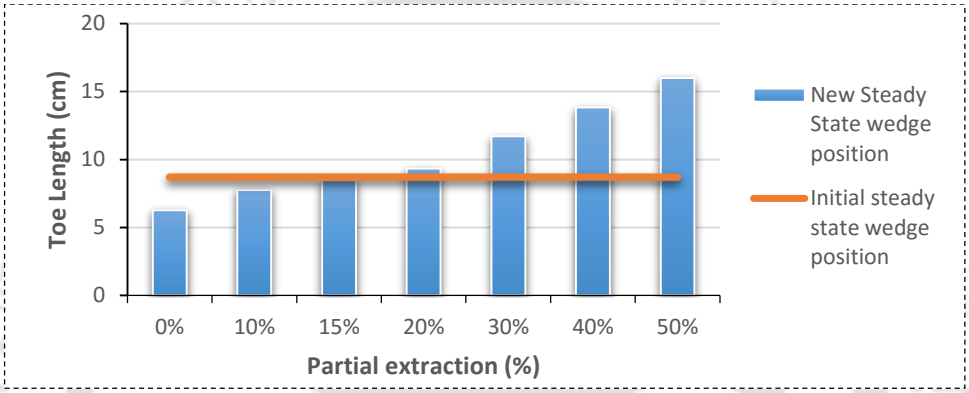

Figure 6.16: Graph showing the partial extraction possible under the initial steady-state wedge position for 3 cm screen length

6.6.2 Scenario 2

In this scenario, the impact of screen length and distance between the screens has been examined on the behavior of the saltwater intrusion wedge pattern. In this effort, the model was simulated by considering the upper and lower screen's length of 2 cm and the spacing between the screens of 8 cm. The other parameters, such as discharge and anisotropy value, was kept constant as it was considered in scenario 1. The total simulated time was 4 hrs. The new steady-state saltwater wedge position was observed at 6.37, 7.76, 8.93, 9.31, 11.7, 13.97 and 16.1 cm for the partial extraction of 0%, 10%, 20%, 30%, 40% and 50%, respectively as shown in Figure 6.17. As mentioned above, the initial steady-state wedge position was at 8.67 cm from the coastline. Nevertheless, the horizontal extent of the new steady-state wedge position exceeds the initial one for 15% partial extraction. Thus, it has become clear from the analysis that when the partial extraction is in between 10-15%, there is a possibility to reach its initial steady-state condition.

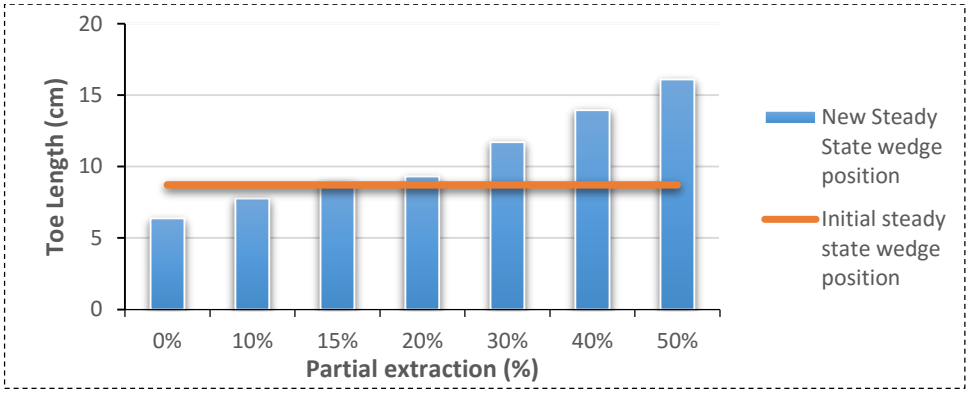

Figure 6.17: Graph showing the partial extraction possible under the initial steady-state wedge position for 4 cm screen length

6.6.3 Scenario 3

In this scenario, the screen length of upper and lower sections is kept as 3 cm and 2 cm, respectively, with a spacing of 7 cm. The other parameters, such as discharge and anisotropy value, was kept constant as it was considered in scenario 1. Once the model is simulated for a period of 4 hrs, it is perceived that the new steady-state wedge position has slightly deviated as it was observed in scenario 2. The new steady-state position was found to be as 6.44, 7.74, 8.72, 9.32, 11.55, 13.97, and 16.13 cm, respectively for partial extraction of 0%, 10%, 20%, 30%, 40%, and 50%. The observational results are shown in Figure 6.18.

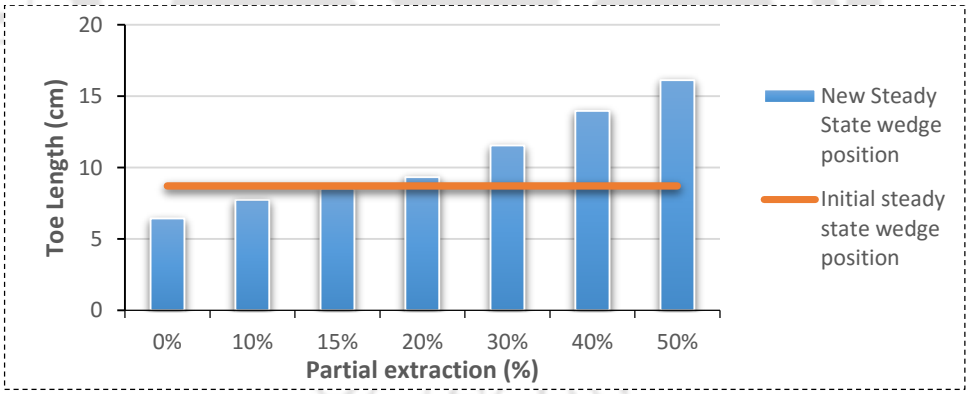

Figure 6.18: Graph showing the partial extraction possible under the initial steady-state wedge position for 5 cm screen length

6.6.4 Scenario 4

In this scenario, the model was simulated by considering the length of each upper and lower screens 3 cm with spacing in between of 6 cm. The other parameters, such as discharge and anisotropy value, was kept constant as it was considered in scenario 1. From the simulation

results, it is observed that the new steady-state position of the saltwater intrusion wedge was almost similar, as it was seen in scenario 3 (Figure 6.19).

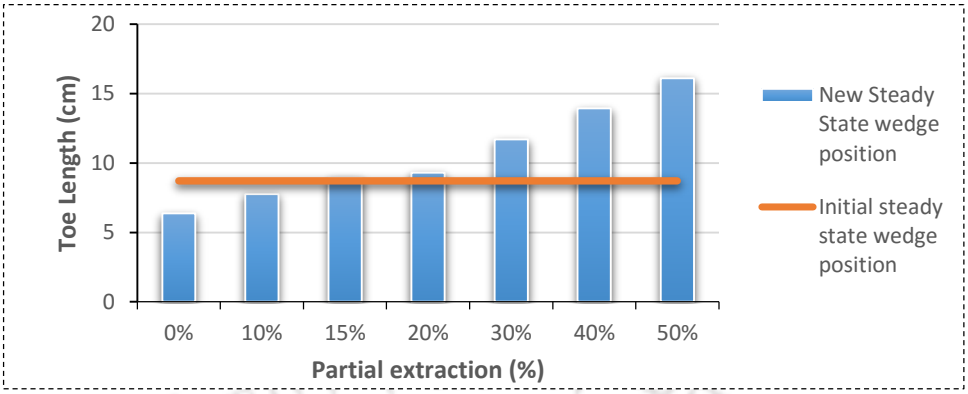

Figure 6.19: Graph showing the partial extraction possible under the initial steady-state wedge position for 6 cm screen length

From the above four scenarios, it could be concluded that if the screen length is smaller and non-uniform with upper screen length greater than lower screen length, most of the new saltwater steady-state wedge position is under the initial one. Moreover, more amount of water can be extracted from GCW through partial extraction to satisfy different human needs in coastal zones.

6.6.5 Scenario 5

Scenario 5 demonstrates the case of screen length of 4 cm, and the distance between the screens of 8 cm with discharge (Q = 0.625 cm^3/sec). The model was simulated for different percentages of partial extraction with an anisotropy value of 1 (K_x/K_z = 1). The initial steady-state result for this scenario is shown in Figure 6.20. The results for steady-state wedge position for different partial extractions are as follows 8.16, 8.95, 9.8, 10.81, 11.96, and 13.32 cm corresponding to 0%, 10%, 20%, 30%, 40%, and 50% (Figure 6.21 and Figure 6.22). Though the steady-state wedge position for the 0% is comparatively higher than the above four scenarios, even 50% of water can be partially extracted from GCW. There is no significant horizontal movement of the saltwater intrusion wedge. The range of fluctuation of the migration wedge is limited to 5 cm, whereas, in the case of the above four scenarios, it was found to be approximately 10 cm. Hence, it could be suggested that as a coastal area having less population with little requirement of water, a low discharge of GCW can be established to mitigate the saltwater intrusion problem. At the same time, partial extraction up to 20% can likely be possible.

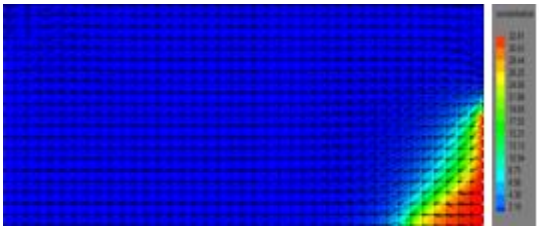

Figure 6.20: Simulation result for initial steady-state (SS) condition

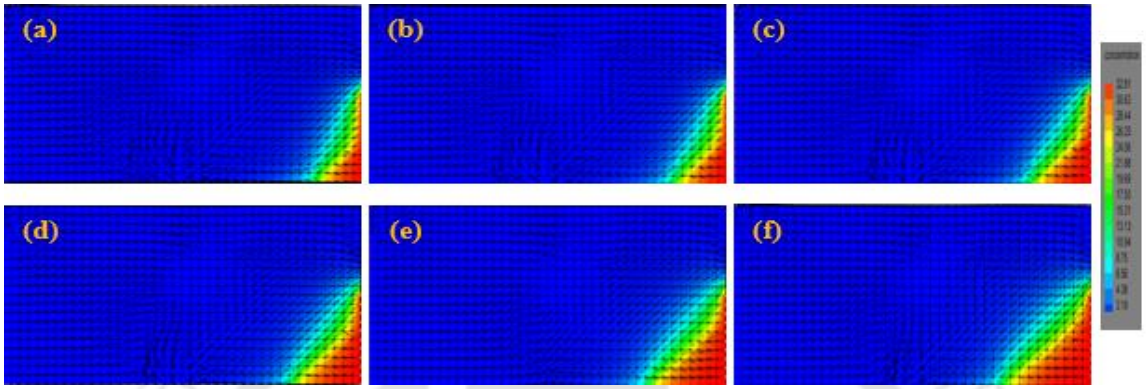

Figure 6.21: Reverse GCW with discharge, Q = 0.625 cm^3/sec for (a) 0% partial extraction, (b) 10% partial extraction, (c) 20% partial extraction, (d) 30% partial extraction, (e) 40% partial extraction and (f) 50% partial extraction

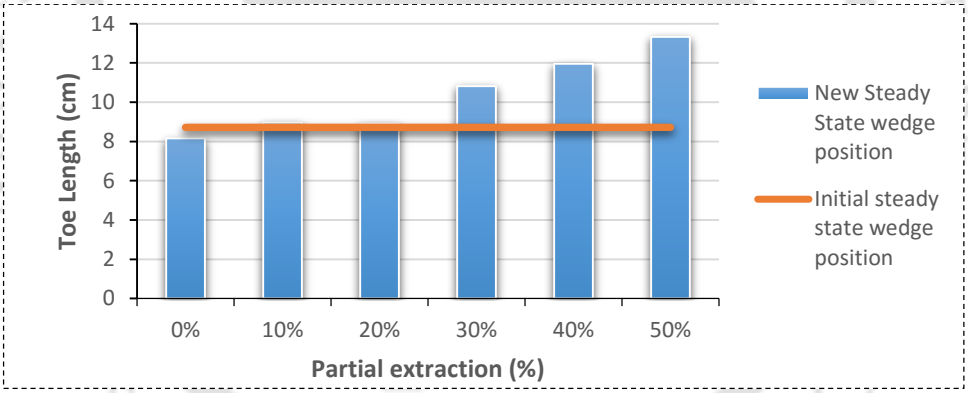

Figure 6.22: Graph showing the partial extraction possible under initial steady-state wedge position for Q = 0.625 cm^3/sec

6.6.6 Scenario 6

In this scenario, anisotropy value (K_x/K_z) was considered to be 2, keeping as the discharge of 1.25 cm^3/sec and screen length 4 cm. The initial steady-state wedge position was achieved at 7.07 cm from the coastal boundary, and the result is presented in Figure 6.23. For the different partial extractions of 0%, 10%, 20%, 30%, 40% and 50%, the new steady-state wedge positions were 3.98, 4.4, 5.1, 6.7, 8.83 and 11.01 cm, respectively. Figure 6.24 represents the simulation results for the partial extractions of 0%, 10%, 20%, 30%, 40%, and 50%. It could be inferred from the results that the horizontal extent of the saltwater intrusion wedge is limited to 11 cm

from the seaward boundary, which is comparatively smaller than the other scenarios. Hence, nearly 30-35% of partial extraction could be possible. In a practical situation, this scenario is efficient in providing a large amount of discharge in terms of partial extraction from GCW to a well-developed coastal area. Figure 6.25 shows the partial extraction possible under the initial steady-state wedge position for Q = 1.25 cm^3/sec and K_x/K_z = 2.

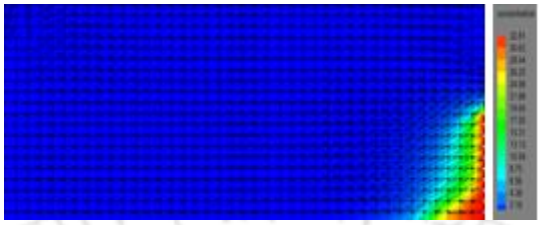

Figure 6.23: Simulation result for the steady-state condition

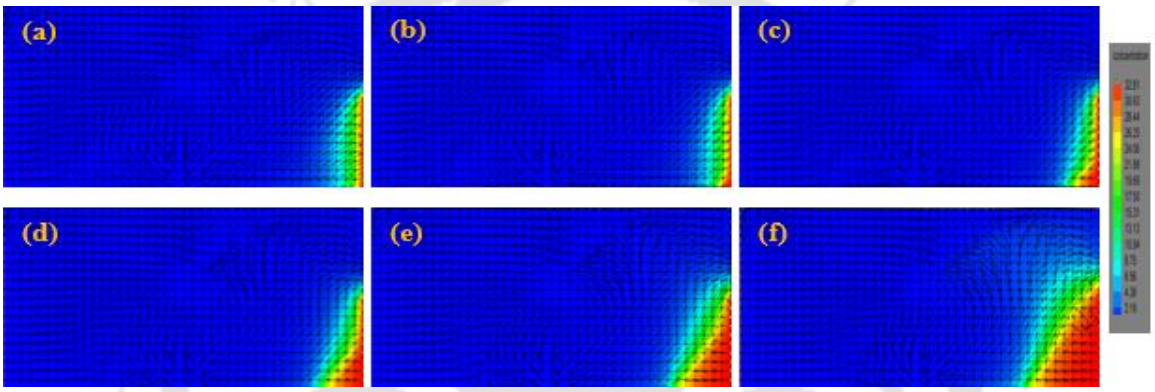

Figure 6.24: Reverse GCW with discharge, Q = 1.25 cm^3/sec and Kx/Kz = 2 for (a) 0% partial extraction, (b) 10% partial extraction, (c) 20% partial extraction, (d) 30% partial extraction, (e) 40% partial extraction and (f) 50% partial extraction

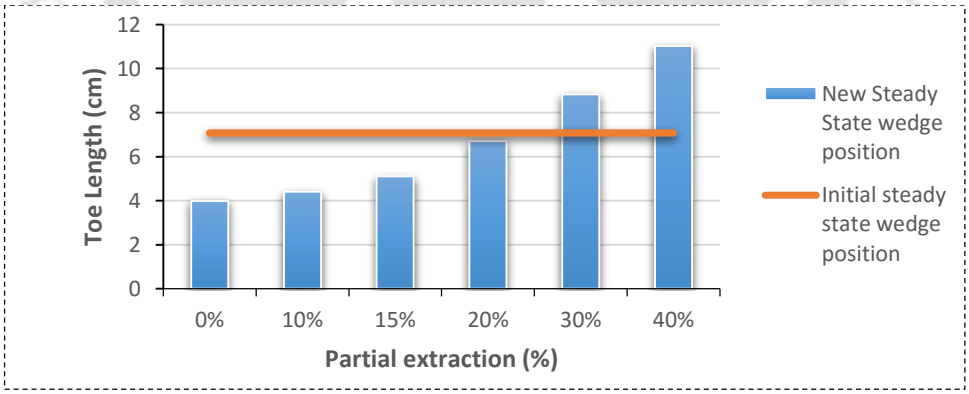

Figure 6.25: Graph showing the partial extraction possible under initial steady-state wedge position for Q = 1.25 cm^3/sec and Kx/Kz = 2

6.6.7 Scenario 7

The situation with anisotropy value as assumed to be 4 and a discharge value of 0.625 cm^3/sec has been considered in this scenario. The screen length of both the screens was kept to

be 4 cm, and the distance between the screens as 8 cm. In this case, the initial steady-state wedge position was observed at 5.63 cm, and the steady-state simulation result is shown in Figure 6.26. The new steady-state wedge position for 0%, 10%, 20%, 30%, 40%, and 50% partial extractions was found to be 5.16, 5.52, 5.18, 4.73, 4.4 and 5.09 cm, respectively. Numerical simulation results of new steady-state wedge position for 0%, 10%, 20%, 30%, 40%, and 50% partial extraction is presented in Figure 6.27. Figure 6.28 represents the partial extraction possible under initial steady-state wedge position for Q = 0.625 cm^3/sec and K_x/K_z = 4.

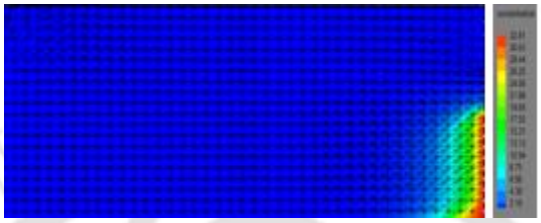

Figure 6.26: Simulation result for the steady-state condition

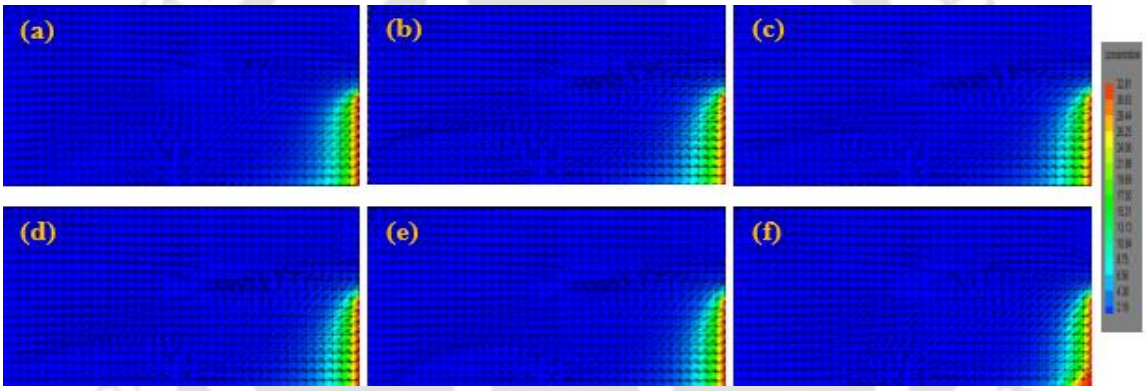

Figure 6.27: Reverse GCW with discharge, Q = 0.625 cm^3/sec and Kx/Kz = 4 for (a) 0% partial extraction, (b) 10% partial extraction, (c) 20% partial extraction, (d) 30% partial extraction, (e) 40% partial extraction and (f) 50% partial extraction

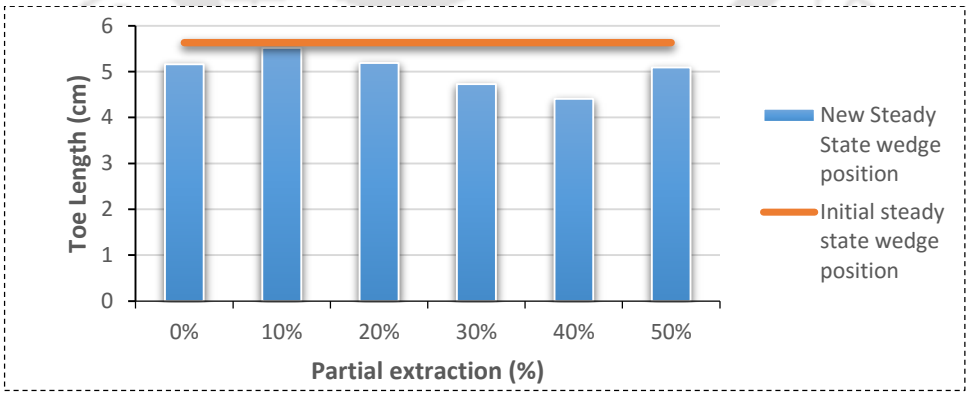

Figure 6.28: Graph showing the partial extraction possible under initial steady-state wedge position for Q = 0.625 cm^3/sec and Kx/Kz = 4

Therefore, it could be interpreted from the above results that there is hardly any change in the pattern and behavior of the steady-state wedge position. The fluctuation of the horizontal extent of the saltwater wedge is in the range of 1 cm. It could be achieved by up to 50% partial extraction from GCW.

6.7 Summary and Conclusions

The control of saltwater intrusion is a common environmental problem worldwide encountered in coastal groundwater hydrology. The issue is not only to protect the groundwater resources for the human being, but also the remediation strategy should be a cost-efficient one. As such, a reliable and cost-effective strategy is, therefore, required for mitigating the problems and protecting coastal groundwater resources from further contamination by saltwater intrusion in coastal and island environments. In this study, an effort has been made to investigate the behavior of saltwater intrusion dynamics under the effect of a groundwater circulation well (GCW) using both the experimental and numerical approaches. The physical experiment has successfully been conducted in a laboratory-scale flow tank model under constant water head boundary conditions. A numerical model has been built up to simulate the flow and transport processes for the experimental setup, and simulations have been carried out to further study the dynamics of saltwater intrusion with different scenarios under a GCW.

The experimental results show that a considerable mixing of saltwater and freshwater flows is observed during the initial intrude period. After starting the extraction pump, the saltwater wedge starts rapidly to advance towards the inland. The evaluation of the results also indicates that the position of the wedge is shifted towards the coastline as GCW is initiated in the system. Hence, GCW can act as a hydraulic barrier for controlling saltwater intrusion in coastal aquifer systems.

However, for all the developed scenarios, it is seen that the initial steady-state wedge position is pushed at least 15% towards the seaward boundary. Hence, no further saltwater intrusion is possible around the sphere of influence of the well. Furthermore, the simulation results suggest that almost 30% partial extraction is likely to be possible from the GCW if screen length is smaller and non-uniform. That is because to pass the same amount of water through a smaller screen area. The increase in the recirculating water velocity near the lower screen location leads to the rise in elliptical circulation cell influence in a downward direction. Moreover, a comparatively more amount of water can also be extracted to meet different domestic, agricultural, or industrial needs in coastal zones.

The purpose of the present study is not only to cease the further migration of saltwater wedge towards inland but also to extract some percentages of water for human needs partially. Simultaneous abstracting of water from the GCW also proves to be effective in mitigating the saltwater intrusion problem in coastal aquifers. Except for 50%, partial extraction in scenarios 1-4, every case is suitable and efficient for continuously extracting water up to 40%. Out of all the above-developed scenarios, scenario 6 shows the optimal condition as approximately 40% of partial extraction can be achieved, without crossing the initial steady-state wedge position. The present study reveals the GCW with partial extraction can effectively mitigate the saltwater intrusion problem in coastal regions and could be considered as one of the most efficient management strategies for controlling the problem. Moreover, this strategy is very cost-effective, has a less environmental impact, and could be employed for sustainable development of water resources in coastal zones.

CHAPTER 7

Summary, Conclusions, and Recommendations for Future work

7.1 Summary

Saltwater intrusion (SI) into coastal aquifers is the most widespread groundwater contamination problem that has become a considerable prominent concern faced by water resource planners worldwide as it not only leads to the depletion of available water resources but also adversely affects the social and economic developments of coastal communities. Coastal aquifers play a vital role all over the world due to the availability as well as the high quality of groundwater resources they provide. In the last few decades, with the growing global population and the tendency of people to live in the coastal areas, the demand for freshwater has been accelerating at an alarming rate and also has increased excessive groundwater pumping to satisfy their daily water requirements for coastal communities. The indiscriminate and overexploitation of coastal aquifers has led to SI problems and consequently deteriorates groundwater quality in coastal subsurface systems. Moreover, catastrophic events such as tsunamis, hurricanes, and droughts could result in severe saltwater intrusion into coastal aquifers. The interest in better understanding the mechanism of saltwater intrusion processes in coastal aquifers is, therefore, garnering increased attention worldwide in the past few years. In particular, physical models are valuable and efficient research tools to understand as well as visualize the processes and also for verifying the analytical and numerical models. In the present study, a series of physical experiments have been carried out in a laboratory-scale aquifer model to develop a better scientific understanding of the dynamics of saltwater intrusion processes in coastal aquifers. Furthermore, the density-dependent flow and transport simulation model FEMWATER is used to simulate the flow and transport processes for the experimental setup, and simulations have been conducted to verify the observed phenomena for all the physical experiments. The main goal of these simulations was to evaluate the consistency of the experimental results with the numerical predictions and to explain the experimental results better.

In addition, image analysis (IA) techniques have widely been employed to quantify the spatial and temporal concentration distribution profiles in laboratory-scale flow tank experiments. In this study, the IA technique is used to measure the saltwater concentration field in the laboratory-scale aquifer model domain. A statistics-based error analysis method is also

undertaken to assess the reliability of the method and to quantify the error associated with the measurements. As the toe length (TL) and width of the mixing zone (WMZ) are the typical parameters used to define a saltwater intrusion wedge, therefore, these parameters have been calculated using the IA technique for all the laboratory-scale experimental cases, and results are compared with the numerical predictions.

Groundwater circulation well (GCW) is one of the most promising in-situ remedial techniques of groundwater. In this work, an effort has been made to investigate the behavior of saltwater intrusion dynamics under a GCW with partial extraction of water using both experimental and numerical approaches. The main focus is not only to cease the further migration of saltwater wedge towards inland but also to extract some percentage of water partially for human needs. As such, different scenarios have numerically been developed, and the model was simulated for all the scenarios in order to obtain the optimal percentage of the partial extraction.

7.2 Conclusions

The following conclusions can be drawn from the present study.

- ***Investigation of the dynamics of saltwater intrusion processes in an unconfined coastal aquifer using laboratory and numerical approaches***

  The overall goal of this work is to perform physical and numerical experiments with regard to develop a better scientific understanding of the dynamics of saltwater intrusion processes in a coastal unconfined aquifer. In this effort, a series of physical experiments have been carried out in a laboratory-scale aquifer model to have a better understanding of the dynamics of this phenomenon under different scenarios. The variable-density flow and transport model FEMWATER is used to simulate the flow and transport processes for the experimental setup on the same scale, and simulations have been carried out to verify the observed phenomena for all the physical experiments. The main goal of these simulations was to evaluate the consistency of the experimental results with the numerical predictions and to explain the experimental results better. It has been found that the numerical predictions are in good agreement with all the experimental results.

  An investigation has successfully been conducted to assess the efficiency of bentonite clay slurry on controlling the SI problem in the present study. The results reveal that there is no further movement of the saltwater intrusion wedge towards the inland side after implementation of the barrier. The research also suggests that the physical barrier created by bentonite slurry can be employed for preventing the movement of saltwater intrusion

in coastal aquifer systems. Further, the effect of pumping on the saltwater intrusion dynamics has been studied, and results show that the saltwater interface rapidly advances through the system towards the freshwater aquifer after the application of pumping. Also, the influence of the injection of the freshwater on the dynamics of saltwater intrusion processes has been investigated in this study. The evaluation of the results suggests that the saltwater wedge gradually recede through the system towards the saltwater boundary upon injection of freshwater and could be concluded the injection of freshwater as a hydraulic barrier can be used in impeding saltwater intrusion in coastal aquifers.

The saltwater diffusion zone present within the coastal aquifer system plays a significant role in the transport and fate of contaminants. This study examines the behavior of contaminant transport patterns in saltwater intruded aquifer with and without pumping conditions. The results demonstrate that the contaminant travels upward towards the seaward boundary when it approaches the saltwater intrusion wedge and then exits around the coastline. It is a remarkable observation that the contaminant plume does not travel further seaward through the saltwater intrusion wedge. Upon installation of a pump, the wedge advances rapidly into the freshwater system, and the contaminant plume is also drawn along with the wedge towards the pump location. It has been observed that the contaminant plume did not follow the ideal circular flow path. Due to the effect of advection, the circular plume forms an elongated shape as it approaches the saltwater wedge. Moreover, the behavior of contaminant plume under the influence of a horizontal clay lens has also been investigated, and it has been observed that there are two saltwater intrusion wedges develop, one at the base of the aquifer, and the other one above the clay lens. The results also indicate that the contaminant plume travels vertically along with the saltwater wedge towards the seaward boundary. The findings from the present study would be useful to understand better the saltwater intrusion processes occurring in a coastal unconfined aquifer.

- ***Quantification of concentration distributions profile in the laboratory-scale flow tank experiments using an image analysis technique***

  An image analysis technique has been employed to determine the solute concentrations in laboratory-scale flow tank experiments. The main focus of this study is to quantify the spatial and temporal concentration distributions profile of dyed saltwater flowing through

the laboratory aquifer model. The presented IA technique is capable of tracking both spatial and temporal variations in a saltwater wedge in laboratory-scale experiments.

The calibration technique in order to establish the relationship between light intensity and dyed saltwater concentration has been reported. The relationship shows non-linear behavior at high concentrations that is in good agreement with the results demonstrated in the published literature.

Furthermore, experimental results indicate that a more significant increase in the TL and WMZ has been observed after the initiation of pumping within the aquifer as similar to that found in numerical simulations. Because of pumping, the freshwater pressure head is decreasing within the system that induces a landward movement of the saltwater intrusion wedge. As expected, upon application of the injection pump, the saltwater wedge starts to recede through the system towards the saltwater boundary and results in a decrease in TL and WMZ. The steady-state experimental results demonstrate that TL and WMZ gradually increase before attainment of the steady-state, and after establishing the steady-state, both TL and WMZ remained constant throughout the experiment. This agrees well with the simulated results.

This study shows the IA technique could be effectively used for quantification of the solute concentration distributions profile in laboratory-scale flow tank experiments. The presented IA technique is non-invasive and of relatively lower cost as compared to the other methods.

- ***Development of a management strategy to control saltwater intrusion in coastal aquifer systems***

In the present study, an effort has been made to investigate the effect of a groundwater circulation well (GCW) on controlling saltwater intrusion in coastal aquifers using both experimental and numerical approaches. The physical experiment has successfully been conducted in a laboratory-scale flow tank model under constant water head boundary conditions. A numerical model has been built up to simulate the flow and transport processes for the experimental setup, and simulations have been carried out to study further the dynamics of saltwater intrusion with different scenarios under a GCW.

The experimental results show that a considerable mixing of saltwater and freshwater flows is observed during the initial intrude period. After the application of pumping, the saltwater wedge advances rapidly towards the inland side. The evaluation of the results

also indicates that the position of the wedge is shifted towards the coastline as GCW is initiated in the system. Hence, GCW can act as a hydraulic barrier for controlling saltwater intrusion in coastal aquifer systems.

However, for all the developed scenarios, it has been observed that the initial steady-state wedge position is pushed at least 15% towards the seaward boundary. Hence, no further saltwater intrusion is possible around the sphere of influence of the well. Furthermore, the evaluation of the results suggests that almost 30% partial extraction is likely to be possible if the screen length of GCW is shorter and non-uniform. That is because to pass the same amount of water through a smaller screen area. The increase in the recirculating water velocity near the lower screen location leads to the rise in elliptical circulation cell influence in a downward direction. Moreover, a comparatively more amount of water can also be extracted to meet different domestic, agricultural, or industrial needs in coastal zones.

The purpose of the present study is not only to cease the further migration of saltwater wedge towards inland but also to abstract partially some percentages of water for human needs. Simultaneous extracting of water from GCW also proves to be effective in mitigating the saltwater intrusion problem. Except for 50% partial extraction in scenarios 1-4, every case is suitable and efficient for continuously extracting water up to 40%. Out of all the generated scenarios, scenario 6 shows the optimal condition as approximately 40% of partial extraction can be achieved, without crossing the initial steady-state wedge position. The present study reveals the GCW with partial abstraction can effectively mitigate the saltwater intrusion problem in coastal regions and could be considered as one of the most efficient management strategies for controlling the problem. Moreover, this strategy is very cost-effective, has a less environmental impact, and could be employed for sustainable development of water resources in coastal zones.

7.3 Recommendations for future work

Based on the concepts established in this thesis, the following research efforts can be accomplished for future work:

- In this study, laboratory and numerical experiments have been carried out to investigate the dynamics of saltwater intrusion processes in unconfined coastal aquifers under homogeneous conditions. However, future studies can be conducted to study the

saltwater intrusion processes in coastal groundwater aquifers under confined and heterogeneous conditions.

- The present study is mainly based on laboratory, and numerical experimental results could be verified in the field study impacted by climate change effects.
- This study examines the behavior of contaminant transport patterns in saltwater intruded aquifer without tidal fluctuations. Future research needs to be carried out to investigate the contaminant transport patterns in coastal aquifers subject to tidal fluctuations.
- In the present study, bentonite clay slurry has been employed as a subsurface barrier in controlling the saltwater intrusion problem in coastal aquifers. The efficacy of different materials (e.g., cement slurry), as well as their locations to prevent or mitigate the problem in coastal aquifer systems that could be investigated.
- The light reflection technique has been employed to determine the spatial and temporal salt concentration distributions profile in laboratory-scale flow tank experiments. Moreover, the light transmission technique could be used in quantifying the salt concentration distributions profile in laboratory-scale saltwater intrusion experiments.
- Groundwater circulation well (GCW) has been used in controlling saltwater intrusion problems in coastal aquifers in the present study. However, the GCW was located in the middle of the aquifer in this study. The effects of variation of the GCW location on the dynamics of saltwater intrusion processes in coastal subsurface systems could be examined.

References

Abarca, E., and Clement, T. P. (2009). A novel approach for characterizing the mixing zone of a saltwater wedge. *Geophysical Research Letters*, 36(6), L06402.

Abd-Elhamid, H. F., and Javadi, A. A. (2008). Mathematical models to control saltwater intrusion in coastal aquifer. *Proceeding of GeoCongress*, New Orleans, Louisiana, USA.

Abd-Elhamid, H. F., and Javadi, A. A. (2011a). A density-dependant finite element model for analysis of saltwater intrusion in coastal aquifers. *Journal of Hydrology*, 401, 259-271.

Abd-Elhamid, H. F., and Javadi, A. A. (2011b). A cost-effective method to control seawater intrusion in coastal aquifers. *Water Resources Management*, 25(11): 2755-2780.

Abdollahi-Nasab, A., Boufadel, M. C., Li, H., and Weaver, J. W. (2010). Saltwater flushing by freshwater in a laboratory beach. *Journal of Hydrology*, 386(1-4), 1-12.

Abdoulhalik, A., Ahmed, A., and Hamill, G. A. (2017). A new physical barrier system for seawater intrusion control. *Journal of Hydrology*, 549, 416-427.

Acosta, A. B., and Donado, L. D. (2015). Laboratory scale simulation of hydraulic barriers to seawater intrusion in confined coastal aquifers considering the effects of stratification. *Procedia Environmental Sciences*, 25, 36-43.

Allmon, W. E., Everett, L. G., Lightner, A. T., Alleman, B., Boyd, T. J., and Spargo, B. J. (1999). Groundwater circulating well technology assessment. *Rep. No. NRL/PU/6115-99-384*, Naval Research Laboratory, Washington, D.C.

Allow, K. (2012). The use of injection wells and a subsurface barrier in the prevention of seawater intrusion: a modelling approach. *Arabian Journal of Geosciences*, 5(5): 1151-1161.

Anders, R., Mendez, G. O., Futa, K., and Danskin, W. R. (2014). A geochemical approach to determine sources and movement of saline groundwater in a coastal aquifer. *Groundwater*, 52, 756-768.

Ataie-Ashtiani, B., Volker, R. E., and Lockington, D. A. (1999). Tidal effects on sea water intrusion in unconfined aquifers. *Journal of Hydrology*, 216, 17-431.

Barlow, P. (2003). Ground Water in Freshwater-Saltwater Environments of the Atlantic Coast. *Circular 1262*, U.S. Department of the Interior, U.S. Geological Survey.

Barlow, P. M., and Reichard, E. G. (2010). Saltwater intrusion in coastal regions of North America. *Hydrogeology Journal*, 18, 247-260.

Barrocu G., Cau, P., Muscas, L., Soddu, S., and Uras, G. (2004). Predicting groundwater salinity changes in the coastal aquifer of Arborea (central-western Sardinia). *Proceeding of the 18th Salt Water Intrusion Meeting*, Cartagena, Spain.

Bear, J. (1961). Some experiments in dispersion. *J. Geophys. Res.*, 66: 2455-2467.

Bear, J. (1979). *Hydraulics of Groundwater*. McGraw-Hill Publishing Company, Inc., New York; 569.

Bear, J., and Cheng, A. H. -D. (2010). *Modeling Groundwater Flow and Contaminant Transport*. Springer, p. 834.

Bear, J., Cheng, A. H. -D., Sorek, S., Ouazar, D., and Herrera, I. (1999). *Seawater Intrusion in Coastal Aquifers-Concepts, Methods and Practices*, Kluwer, Dordrecht, Netherlands.

Bear, J., and Dagan, G. (1964). Some exact solutions of interface problems by means of the hydrograph method. *J. Geophys. Res.*, 69, 1563-1572.

Bear, J., and Zhou, Q. (2007). Sea water intrusion into coastal aquifers. In: Delleur, J. W. (ed.), *The handbook of groundwater engineering*. Second ed. Boca Raton, Florida: CRC Press, Taylor & Francis Group.

Bhattacharjya, R. K., and Datta, B. (2005). Optimal Management of Coastal aquifer Using Linked Simulation Optimization Approach. *Water Resour. Manag.*, 19(3) 295-320.

Bhattacharjya, R. K., and Datta, B. (2009). ANN-GA-Based Model for Multiple Objective Management of Coastal Aquifers. *Journal of Water Resources Planning and Management*, 135(5): 314-322.

Bhattacharjya, R. K., Datta, B., and Satish, M. G. (2009). Artificial Neural Network Model for Simulating Saltwater Intrusion Process in Coastal Aquifers with Noisy Training Data. *KSCE Journal of Civil Engineering*, 13(3), 205-215.

Boufadel, M. C. (2000). A mechanistic study of nonlinear solute transport in a groundwater-surface water system under steady state and transient hydraulic conditions. *Water Resources Research*, 36(9), 2549-2565.

Brovelli, A., Mao, X., and Barry, D. A. (2007). Numerical Modeling of tidal influence on density-dependent contaminant transport. *Water Resources Research*, 43, W10426.

Bruington, A. E. (1972). SALTWATER INTRUSION INTO AQUIFERS. *JAWRA Journal of the American Water Resources Association*, 8(1): 150-160.

Callaghan, P. T., and Codd, S. L. (1998). Generalised calculation of NMR imaging edge effects arising from restricted diffusion in porous media. *Magn. Reson. Imaging*, 16, 471-478.

Cary, L., Petelet-Giraud, E., Bertrand, G., *et al.* (2015). Origins and processes of groundwater salinization in the urban coastal aquifers of Recife (Pernambuco, Brazil): a multi-isotope approach. *Sci. Total Environ.*, 530, 411-429.

Chang, S. W., and Clement, T. P. (2012). Experimental and numerical investigation of saltwater intrusion dynamics in flux-controlled groundwater systems. *Water Resources Research*, 48(9), W09527.

Chang, S. W., and Clement, T. P. (2013). Laboratory and numerical investigation of transport processes occurring above and within a saltwater wedge. *Journal of Contaminant Hydrology*, 147, 14-24.

Chen, K. P., and Jiao, J. J. (2007). Seawater intrusion and aquifer freshening near reclaimed coastal area of Shenzhen. *Water Science and Technology: Water Supply*, 7: 137-145.

Cheng, A. H. D., Halhal, D., Naji, A., and Ouazar, D. (2000). Pumping optimization in saltwater-intruded coastal aquifers. *Water Resources Research*, 36(8): 2155-2165.

Cheng, A. H. -D., and Ouazar, D. (2003). *Coastal Aquifer Management-Monitoring, Modeling, and Case Studies*. Lewis Publ., p. 280.

Cheng, J., Chen, C., and Ji, M. (2004). Determination of aquifer roof extending under the sea from variable-density flow modeling of groundwater response to tidal loading: case study of the Jahe River Basin, Shandong Province, China. *Hydrogeology Journal*, 12, 408-423.

Cherubini, C., and Pastore, N. (2011). Critical stress scenarios for a coastal aquifer in southeastern Italy. *Nat. Hazards Earth Syst. Sci.*, 11(5): 1381-1393.

Cooper, H., Kohout, F., Henry, H., and Glover, R. (1964). Sea Water in Coastal Aquifers. *US Geological Survey Water-Supply Paper*, 1613-C.

Corapcioglu, M. Y., and Fedirchuk, P. (1999). Glass bead micromodel study of solute transport. *J. of Contam. Hydrol.*, 36, 209-230.

Dagan, G., and Bear, J. (1968). Solving the problem of interface upconing in a coastal aquifer by the method of small perturbations. *J. of Hydraul. Res.*, 6(1), 15-44.

Dam, J. C. van (1999). *Seawater intrusion in coastal aquifers-concepts, methods and practices*. In: Bear, J., Cheng, A.H.-D., Sorek, S., Ouazar, D., Herrera, I. (Eds.), Theory and Applications of Transport in Porous Media, vol. 14. Kluwer, Academic Publishers., Dordrecht, The Netherlands.

Dausman, A., and Langevin, C. (2005). Movement of the saltwater interface in the Surficial Aquifer System in response to hydrologic stresses and water-management practices. Broward County, Florida: *USGS Scientific Investigations Report: SIR 2004-5256Rep.*

Das, A., and Datta, B. (1999). Development of Multiobjective Management Models for Coastal Aquifers. *Journal of Water Resources Planning and Management*, 125(2): 76-87.

Das, A., and Datta, B. (2001). Simulation of seawater intrusion in coastal aquifers: Some typical responses. *Sadhana*, 26(4): 317-352.

Datta, B., Vennalakanti, H., and Dhar, A. (2009). Modeling and control of saltwater intrusion in a coastal aquifer of Andhra Pradesh, India. *Journal of Hydro-environment Research*, 3 (3): 148-159.

Detwiler, R.L., Pringle, S. E., and Glass, R. J. (1999). Measurement of fracture aperture fields using transmitted light: An evaluation of measurement errors and their influence on simulations of flow and transport through a single fracture. *Water Resources Research*, 35(9), 2605-2617.

Diersch, H. J. (1988). Finite element modelling of recirculating density-driven saltwater intrusion processes in groundwater. *Advances in Water Resources*, 11(1): 25-43.

Don, N. C., Hang, N. T. M., Araki, H., Yamanishi, H., and Koga, K. (2006). Effect of Groundwater Pumping on Saltwater Intrusion in a Coastal Plain. *International Commission of Agricultural Engineering*, 8.

Dose, E. J., Stoeckl, L., Houben, G. J., Vacher, H. L., Vassolo, S., Dietrich, J., and Himmelsbach, T. (2014). Experiments and modeling of freshwater lenses in layered aquifers: Steady state interface geometry. *Journal of Hydrology*, 509, 621-630.

Drizin, C. B., Hoban, K. P., Hannaleck, J. A., and Chaney, J. (2008). In Situ Remediation of MTBE in a Multilevel Aquifer by Integrating Air Sparging and Groundwater Circulation. *Proceedings of the Sixth International Conference on Remediation of Chlorinated and Recalcitrant Compounds*, Monterey, CA.

Elmore, A. C., and Graff, T. (2002). Best available treatment technologies applied to groundwater circulation wells, *Remediation*, 12(13), 63-80.

Fadili, A., Najib, S., Mehdi, K., Riss, J., Makan, A., Boutayeb, K., and Guessir, H. (2016). Hydrochemical features and mineralization processes in coastal groundwater of Oualidia, Morocco. *Journal of African Earth Sciences*, 116, 233-247.

Feseker, T. (2007). Numerical studies on saltwater intrusion in a coastal aquifer in northwestern Germany, *Hydrogeology Journal*, 15(2), 267-279.

Fetter, C. W. (2001). *Applied Hydrogeology*, Prentice Hall, N.J.

Freeze, R. A., and Cherry, J. A. (1979). *Groundwater*. Englewood Cliffs, Prentice-Hall, Inc., N.J., pp. 435.

Galeati, G., Gambolati, G., and Neuman, S. P. (1992). Coupled and partially coupled Eulerian-Lagrangian Model of freshwater-seawater mixing. *Water Resources Research*, 28(1): 149-165.

Gambolati, G., Putti, M., and Paniconi, C. (1999). Three-Dimensional Model of Coupled Density-Dependent Flow and Miscible Salt Transport. *In:* Bear, J., Cheng, A. D., Sorek, S., Ouazar, D. & Herrera, I. (eds.) *Seawater Intrusion in Coastal Aquifers-Concepts Methods and Practices.* Springer Netherlands.

Gonen, O., and Gvirtzman, H. (1997). Laboratory-scale analysis of aquifer remediation by in-well vapor stripping: 1. Laboratory results. *J. of Contam. Hydrol.*, 29, 23-39.

Goswami, R. R., Ambale, B., and Clement, T. P. (2009). Estimating errors in concentration measurements obtained from image analysis. *Vadose Zone Journal*, 8(1), 108-118.

Goswami, R. R., and Clement, T. P. (2007). Laboratory-scale investigation of saltwater intrusion dynamics. *Water Resources Research*, 43(4), W04418.

Goswami, R. R., Clement, T. P., and Hayworth, J. H. (2012). Comparison of numerical techniques used for simulating variable-density flow and transport experiments. *Journal of Hydrologic Engineering*, 17(2), 272-282.

Gotovac, H., Andricevic, R., Gotovac, B., Kozulic, V., and Vanjes, M. (2003). An improved collocation method for solving the Henry problem. *Journal of Contaminant Hydrology*, 64, 129-149.

Grenier, A., Schreiber, W., Brix, G., and Kinzelbach, W. (1997). Magnetic resonance imaging of paramagnetic tracers in porous media: quantification of flow and transport parameters. *Water Resour. Res.*, 33, 1461-1473.

Guo, H., and Jiao, J. J. (2007). Impact of Coastal Land Reclamation on Ground Water Level and the Sea Water Interface. *Ground Water*, 45(3): 362-367.

Guo, H., and Jiao, J. J. (2009). *Coastal Groundwater System Changes in Response to Large-scale Land Reclamation*, New York, Nova Science Publishers,Inc.

Guo, W., and Langevin, C. D. (2002). *User's guide to SEAWAT: A computer program for simulation of three-dimensional variable-density ground-water flow*. US Geol. Surv. (USGS), Techniques of Water Resour. Invest. Book 6, Chapter A7.

Guvanasen, V., Wade, S. C., and Barcelo, M. D. (2000). Simulation of regional groundwater flow and saltwater intrusion in Hernando Country, Florida. *Ground Water*, 38(5), 722-783.

Gvirtzman, H., and Gorelick, S. M. (1992). The concept of in-situ vapour stripping for removing VOCs from groundwater. *Transp. Porous Media*, 8, 71-92.

Halihan, T., and Zlotnik, V. A. (2000). Asymmetric dipole-flow test in a fractured carbonate aquifer. *Ground Water*, 40, 491-499.

Hansen, P. C., Nagy, J. G., and O'Leary, D. P. (2006). Deblurring Images: Matrices, Spectra and Filtering. *Society for Industrial and Applied Mathematics*, Philadelphia, PA.

Harne, S., Chaube, U. C., Sharma, S., Sharma, P., and Parkhya, S. (2006). Mathematical modelling of salt water transport and its control in groundwater. *Natural and science*, 4: 32-39.

Held, R., Attinger, S., and Kinzelbach, W. (2005). Homogenization and effective paremeters for the Henry problem in heterogeneous formations. *Water Resour. Res.*, 41, W11420.

Henry, H. R. (1959). Saltwater intrusion into coastal aquifers. *J. of Geophys. Res.*, 64, 1911-1919.

Herrling, B., and Buermann, W. (1990). UVB-Verfahren-Grundprinzip und Messungen. *Untergrundsanierung mittels Bodenluftabsaugung und in-situ-strippen Schriftenr*, P. Bock *et al*., eds., Angew Geologie Karlsruhe, Karlsruhe, Germany, 275-290.

Herrling, B., Buermann, W., and Stamm J. (1990). In-situ Beseitigung leichtfluechtiger Schadstoffe aus dem Grundwasserbereich mit dem UVB-Verfahren. *Neuer Stand der Sanierungstechniken von Atlasten, IWS-Schriftenreihe*, H.-P. Luehr *et al*., eds., Erich Schmidt, Berlin, 71-99.

Herrling, B., Buermann, W., and Stamm, J. (1991). In situ groundwater remediation of strippable or volatile contamination using the UVB method. *Proc., European Conf. Advances in Water Resources Technology*, G. Tsakiris, eds., Athens, 315-321.

Herrling, B., and Stamm, J. (1993). Numerische untersuchungen zum unterdruck-verdampfer-brunnen (UVB) and zum grundwasserzirkulationsbrunnen (GZB). *Rep. No. 702*, Institute for Hydromechanics, Univ. of Karlsruhe, Germany.

Hong, S., Park, N., Bhopanam, N., and Han, S. (2004). Verification of optimal model of coastal pumping with sand-tank experiment. *Proceeding of the 18th Salt Water Intrusion Meeting*, Cartagena, Spain.

Hu, L., and Jiao, J. J. (2010). Modeling the influences of land reclamation on groundwater systems: A case study in Shekou peninsula, Shenzhen, China. *Engineering Geology*, 114 (3-4): 144-153.

Huang, W., Smith, C. C., Lerner, D. N., Thornton, S. F., and Oram, A. (2002). Physical modelling of solute transport in porous media: evaluation of an imaging technique using UV excited fluorescent dye. *Water Res.*, 36(7), 1843-1853.

Hussain, M. S., Javadi, A. A., Ahangar-Asr, A., and Farmani, R. (2015). A surrogate model for simulation-optimization of aquifer systems subjected to seawater intrusion. *Journal of Hydrology*, 523(0): 542-554.

Huyakorn, P. S., Andersen, P. F., Mercer, J. W., and White, H. O. (1987). Saltwater intrusion in aquifers: Development and testing of a three-dimensional finite element model. *Water Resources Research*, 23(2): 293-312.

Illangasekare, T., *et al*. (2006). Impacts of the 2004 tsunami on groundwater resources in Sri Lanka, *Water Resources Research*, 42(5).

Indelman, P., and Zlotnik, V. (1997). Average steady non-uniform flow in stratified formations. *Water Resour. Res*., 33(5), 927-934.

Jakovovic, D., Werner, A. D., and Simmons, C. T. (2011). Numerical modeling of saltwater up-coning: Comparison with experimental laboratory observations. *Journal of Hydrology*, 402(3-4), 261-273.

Japan Green Resources Agency (2004). Technical Reference for Effective Groundwater Development.

Javadi, A. A., Abd-Elhamid, H. F., and Farmani, R. (2012). A simulation-optimization model to control seawater intrusion in coastal aquifers using abstraction/recharge wells. *International Journal for Numerical and Analytical Methods in Geomechanics*, 36(16): 1757-1779.

Javadi, A., Hussain, M., Sherif, M., and Farmani, R. (2015). Multi-objective optimization of different management scenarios to control seawater intrusion in coastal aquifers. *Water Resources Management*, 29(6): 1843-1857.

Kabala, Z. J. (1993). The Dipole Flow Test: A New Single-Borehole Test for Aquifer Characterization, *Water Resour. Res.*, 29, 99-107.

Kaleris, V. K., and Ziogas, A. I. (2013). The effect of cutoff walls on saltwater intrusion and groundwater extraction in coastal aquifers. *Journal of Hydrology*, 476(0): 370-383.

Kallioras, A., Pliakas, F.-K., Schuth, C., and Rausch, R. (2013). Methods to countermeasure the intrusion of seawater into coastal aquifer systems. In: Sharma, S. K. & Sanghi, R. (eds.) *Wastewater Reuse and Management*, Springer Netherlands.

Keller, A. A., Paul, V. R., and Peter, K. K. (1995). Prediction of single phase transport parameters in a variable aperture fracture. *Geophys. Res. Lett.*, 22, 1425-1428.

Khalili, A., Basu, A. J., and Pietrzyk, U. (1998). Flow visualization in porous media via Positron Emission Tomography. *Phys. Fluid.*, 10, 1031-1033.

Kim, K., Seong, H., Kim, T., Park, K., Woo, N., Park, Y., Koh, G., and Park, W. (2006). Tidal effects on variations of fresh-saltwater interface and groundwater flow in a multilayered coastal aquifer on a volcanic island (Jeju Island, Korea). *Journal of Hydrology*, 330, 525-542.

Kirubaharan, S. C., Eldho, T. I., and Mohrlok, U. (2008). Simulation of Three Dimensional Circulation Flow Field for Groundwater Pollution Remediation. The 12th *International Association for Computer Methods and Advances in Geomechanics (IACMAG)*, 1-6 October, Goa, India.

Knox, R. C., Sabatini, D. A., Harwell, J. H., Brown, R. E., West, C. C., Blaha, F., and Griffin, C. (1997). Surfactant remediation field demonstration using a vertical circulation well. *Ground Water*, 35(6), 948-953.

Konz, M., Ackerer, P., Meier, E., Huggenberger, P., Zechner, E., and Gechter, D. (2008). On the measurement of solute concentrations in 2D flow tank experiments. *Hydrology and Earth System Sciences*, 12(3), 727-738.

Konz, M., Younes, A., Ackerer, P., Fahs, M., Huggenberger, P., and Zechner, E. (2009a). Variable-density flow in heterogeneous porous media-Laboratory experiments and numerical simulations. *Journal of Contaminant Hydrology*, 108(3-4), 168-175.

Konz, M., Ackerer, P., Younes, A., Huggenberger, P., and Zechner, E. (2009b). Two-dimensional stable-layered laboratory-scale experiments for testing density-coupled flow models. *Water Resources Research*, 45(2), W02404.

Kourakos, G., and Mantoglou, A. (2013). Development of a multi-objective optimization algorithm using surrogate models for coastal aquifer management. *Journal of Hydrology*, 479(0): 13-23

Koussis, A. D., Georgopoulou, E., Kotronarou, A., Lalas, D. P., Restrepo, P., *et al*. (2010a). Cost-efficient management of coastal aquifers via recharge with treated wastewater and desalination of brackish groundwater: general framework. *Hydrological Sciences Journal*, 55(7): 1217-1233.

Koussis, A. D., Georgopoulou, E., Kotronarou, A., Mazi, K., Restrepo, P., *et al*. (2010b). Cost-efficient management of coastal aquifers via recharge with treated wastewater and desalination of brackish groundwater: application to the Akrotiri basin and aquifer, Cyprus. *Hydrological Sciences Journal*, 55(7): 1234-1245.

Kouzana, L., Benassi, R., Ben Mammoua, A., and Sfarfelfoul, M. (2010). Geophysical and hydrochemical study of the seawater intrusion in Mediterranean semi arid zones: Case of

the Korba coastal aquifer (Cap-Bon, Tunisia). *Journal of African Earth Sciences*, 58, 242-254.

Kuan, W. K., Jin, G., Xin, P., Robinson, C., Gibbes, B., and Li, L. (2012). Tidal influence on seawater intrusion in unconfined coastal aquifers. *Water Resources Research*, 48(2), W02502.

Lester, B. (1991). SWICHA. A three-dimensional finite element code for analysing seawater intrusion in coastal aquifers. Version 5.05. *GeoTrans., Inc., Sterling, Virginia, USA, IGWMC, International Ground Water Modeling Center, Delft, the Netherlands*.

Li, F., Chen, X., Liu, C., Lian, Y., and He, L. (2018). Laboratory tests and numerical simulations on the impact of subsurface barriers to saltwater intrusion. *Natural Hazards*, 91(3), 1223-1235.

Li, H., Boufadel, M. C., and Weaver, J. W. (2008). Tide-induced seawater-groundwater circulation in shallow beach aquifers. *Journal of Hydrology*, 352(1-2), 211-224.

Li, H., and Jiao, J. J. (2003a). Influence of the tide on the mean watertable in an unconfined, anisotropic, inhomogeneous coastal aquifer. *Advances in Water Resources*, 26(1), 9-16.

Li, H., and Jiao, J. J. (2003b). Tide-induced seawater-groundwater circulation in a multi-layered coastal leaky aquifer system. *Journal of Hydrology*, 274(1-4), 211-224.

Li, L., Barry, D. A., Stagnitti, F., and Parlange, J. Y. (1999). Submarine groundwater discharge and associated chemical input to a coastal sea. *Water Resour. Res.*, 35(11), 3253-3259.

Liles, M., Thomas, S., and Sovich, T. (2001). Saltwater intrusion in orange country, California: planning for the future. *Proceeding of the 1st international conference and workshop on saltwater intrusion and coastal aquifers, monitoring, modelling, and management*, Morocco.

Lin, H. -C. J., Richards, D. R., Yeh, G. -T., Cheng, J. -R., Cheng, H. -P., and Jones, N. L. (1997). FEMWATER: *A three-dimensional finite element computer model for simulating density-dependent flow and transport in variably saturated media*. U.S. Army Corps of Engineer.

Loáiciga, H. A., Pingel, T. J., and Garcia, E. S. (2011). Sea Water Intrusion by Sea-Level Rise: Scenarios for the 21st Century, *Ground Water*, no-no.

Lu, C., Chen, Y., Zhang, C., and Luo, J. (2013). Steady-state freshwater-seawater mixing zone in stratified coastal aquifers. *Journal of Hydrology*, 505, 24-34.

Lu, C., Kitanidis, P. K., and Luo, J. (2009). Effects of kinetic mass transfer and transient flow conditions on widening mixing zones in coastal aquifers. *Water Resources Research*, 45 (12): W12402.

Lu, C., and Luo, J. (2010). Dynamics of freshwater-seawater mixing zone development in dual domain formations. *Water Resour. Res.*, 46, W11601.

Lu, C., Shi, W., Xin, P., Wu, J., and Werner, A. D. (2017). Replenishing an unconfined coastal aquifer to control seawater intrusion: Injection or infiltration?. *Water Resources Research*, 53, 4775-4786.

Luyun Jr., R., Momii, K., and Nakagawa, K. (2009). Laboratory-scale saltwater behavior due to subsurface cutoff wall. *Journal of Hydrology*, 377, 227-236.

Luyun Jr., R., Momii, K., and Nakagawa, K. (2011). Effects of recharge wells and flow barriers on seawater intrusion. *Ground Water*, 49, 239-249.

Maekawa, K., Karasaki, K., and Takasu, T. (2007). Laboratory Experiments for Seawater Intrusion into Freshwater Aquifer with Heterogeneity. *AGU*, 88(52), Fall Meet. Suppl., Abstract H23G-1702.

Mahesha, A. (1996). Steady-State Effect of Freshwater Injection on Seawater Intrusion. *Journal of Irrigation and Drainage Engineering*, ASCE, 122:149-154.

Maimone, M., and Fitzgerald, R. (2001). Effective modelling of coastal aquifers systems. *Proceeding of the 1st international conference and workshop on saltwater intrusion and coastal aquifers, monitoring, modelling, and management*, Morocco.

Majors, P. D., Smith, D. M., and Davis, P. J. (1991). Effective diffusivity measurement in porous-media via Nmr radial imaging. *Chem. Eng. Sci.*, 46, 3037-3043.

Mantoglou, A., and Papantoniou, M. (2008). Optimal design of pumping networks in coastal aquifers using sharp interface models. *Journal of Hydrology*, 361, 52-63.

McCarty, P. L., Goltz, M. N., Hopkins, G. D., Dolan, M. E., Allan, J. P., Kawakami, B. T., and Carrothers, T. J. (1998). Full scale evaluation of in situ cometabolic degradation of trichloroethylene in groundwater through toluene injection. *Environ. Sci. Tecnol.*, 32(1), 88-100.

McNeil, J. D., Oldenborger, G. A., and Schincariol, R. A. (2006). Quantitative imaging of contaminant distributions in heterogeneous porous media laboratory experiments. *J. of Contam. Hydrol.*, 84, 36-54.

Mehdizadeh, S. S., Werner, A. D., Vafaie, F., and Badaruddin, S. (2014). Vertical leakage in sharp-interface seawater intrusion models of layered coastal aquifers. *Journal of Hydrology*, 519 (Part A), 1097-1107.

Mercer, J. W., Larson, S. P., Faust, C. R. (1980). Simulation of Salt-Water Interface Motion. *Ground Water*, 18(4), 374-385.

Michael, H. A., Mulligan, A. E., and Harvey, C. F. (2005). Seasonal oscillations in water exchange between aquifers and the coastal ocean. *Nature*, 436(7054), 1145-1148.

Miller, G. R., and Elmore, A. C. (2005). Modeling of a groundwater circulation well removal action alternative. *Pract. Period. Hazard. Toxic Radioact. Waste Manage.*, 9(2), 122-129.

Miller, P. G., and Roote, D. S. (1997). In-well Vapor Stripping. GWRTAC Technology, *Overview Report TO-97-01*.

Mohrlok, U., Weber, O., Jirka, G. H., and M. Scholz (2003). Grundwasser-zirkulations-brunnen (GZB) zur in-situ-grundwassersanierung. *J. of Grundwasser*, Springer, 8(1), 13-22.

Mohrlok, U., Weber, O., and Scholz, M. (2000). NAPL phase remediation of heterogeneous aquifers applying in situ flushing with a groundwater circulation well. *Proc., Int. Conf. on Groundwater Research*, D. Rosbjerg *et al*., eds., Balkema, Rotterdam, The Netherlands, 357-358.

Montemagno, C. D., and Gray, W. G. (1995). Photoluminescent volumetric imaging-a technique for the exploration of multiphase flow and transport in porous-media. *Geophys. Res. Lett.*, 22, 425-428.

Montgomery *et al.* (2002). Bacterial Production Stimulated Across the Zone of Influence of a Ground Water Circulation Well in a BTEX-Contaminated Aquifer. *Ground Water Monitoring & Remediation*, 22(3), 144-150.

Morgan, L. K., Stoeckl, L., Werner, A. D., and Post, V. E. A. (2013). An assessment of seawater intrusion overshoot using physical and numerical modeling. *Water Resources Research*, 49, 6522-6526.

Narayan, K. A., Schleeberger, C., Charlesworth, P. B. and Bristow, K. L. (2003). Modelling saltwater intrusion in the lower Burdekin Delta north Queensland, Australia. *Denver Annual Meeting, The Geological Society of America (GSA).*

Narayan, K. A., Schleeberger, C., Charlesworth, P. B., and Bristow, K. L. (2007). Effects of groundwater pumping on saltwater intrusion in the lower Burdekin Delta, north Queensland. *CSIRO Land and Water*, Davies Laboratory, Townsville, Australia.

Nawa, N., and Miyazaki, K. (2009). The analysis of saltwater intrusion through Komesu underground dam and water quality management for salinity. *Paddy and Water Environment*, 7(2): 71-82.

Nishikawa, T., Siade, A. J., Reichard, E. G., Ponti, D. J., Canales, A. G., and Johnson, T. A. (2009). Stratigraphic controls on seawater intrusion and implications for groundwater

management, Dominguez Gap area of Los Angeles, California, USA. *Hydrogeology Journal*, 17(7): 1699-1725.

Ofelia, T., Marcela P., and Monica D. (2004). Salt water vertical upward intrusion due to intensive exploitation, Santa Fe, Argentina. *Proceeding of the 18th Salt Water Intrusion Meeting*, Cartagena, Spain.

Oldenburg, C. M., and Pruess, P. (1995). Dispersive transport dynamics in a strongly coupled groundwater-brine flow sytem. Water Resour. Res., 31(2), 289-302.

Oostrom, M., Dane, J. H., Guven, O., Hayworth, J. S. (1992). Experimental investigation of dense solute plumes in an unconfined aquifer model. *Water Resour. Res.*, 28, 2315-2326.

Oude Essink, G. H. P. (2001). Salt Water Intrusion in a Three-dimensional Groundwater System in The Netherlands: A Numerical Study. *Transport in Porous Media, 43*(1), 137-158.

Oude Essink, G. H. P. (2001). Improving fresh groundwater supply-problems and solutions. *Ocean and Coastal Management*, 44, 429-449.

Oz, I., Shalev, E., Yechieli, Y., Gavrieli, I., and Gvirtzman, H. (2014). Flow dynamics and salt transport in a coastal aquifer driven by a stratified saltwater body: Lab experiment and numerical modeling. *Journal of Hydrology*, 511, 665-674.

Paniconi, C., Khalaifi, I., Lecca, G., Giacomelli, A., and Tarhouni, J. (2001). Modelling and analysis of seawater intrusion in the coastal aquifers of eastern Cap-Bon, Tunisia. *Proceeding of the 1st international conference and workshop on saltwater intrusion and coastal aquifers, monitoring, modelling, and management*, Morocco.

Papadopoulou, M., Karatzas, G., Koukadaki, M., and Trichakis, Y. (2005). Modeling the saltwater intrusion phenomenon in coastal aquifers-A case study in the industrial zone of Herakleio in Crete. *Global NEST J*, 7(2): 197-203.

Papini, M. P., Majone, M., Arjmand, F., Silvestri, D., Sagliaschi, M., Sucato, S., Alesi, E., Barstch, E., and Pierro, L. (2016). First pilot test on the integration of GCW (Groundwater Circulation Well) with ENA (Enhanced Natural Attenuation) for chlorinated solvents source remediation, *Chemical Engineering Transactions*, 49, 91-96.

Park, C. H., and Aral, M. M. (2004). Multi-objective optimization of pumping rates and well placement in coastal aquifers. *Journal of Hydrology*, 290, 80-99.

Park, S., Kim, J., Yum, B., and Yeh, G. (2011). Three-Dimensional Numerical Simulation of Saltwater Extraction Schemes to Mitigate Seawater Intrusion due to Groundwater Pumping in a Coastal Aquifer System. *Journal of Hydrologic Engineering*, 17(1): 10-22.

Parker, L., Yarwood, R., and Selker, J. (2006). Observations of gas flow in porous media using a light transmission technique. *Water Resources Research*, 42(5).

Pinto, M. J., Haim, G., and Steven, M. G. (1997). Laboratory-scale analysis of aquifer remediation by in-well vapor stripping 2, modeling results. *J. of Contam. Hydrol.*, 29, 41-58.

Pool, M., and Carrera, J. (2010). Dynamics of negative hydraulic barriers to prevent seawater intrusion. *Hydrogeology Journal*, 18(1): 95-105.

Pramada, S. K., Minnu, K. P., and Roshni, T. (2018). Insight into sea water intrusion due to pumping: a case study of Ernakulam coast, India. *ISH Journal of Hydraulic Engineering*, 2164-3040.

Rahman, A., Jose, S., Nowak, W., and Cirpka, O. (2005). Experiments on vertical transverse mixing in a large-scale heterogeneous model aquifer. *J. of Contam. Hydrol.*, 80, 130-148.

Ranjan, P., Kazama, S., and Sawamoto, M. (2006). Effects of climate change on coastal fresh groundwater resources. *Global Environmental Change*, *16*(4), 388-399.

Rastogi, A., Choi, G. W., and Ukarande, S. (2004). Diffused Interface Model to Prevent Ingress of Sea Water in Multi-Layer Coastal Aquifers. *Journal of Spatial Hydrology*, 4(2).

Rejani, R., Jha, M., Panda, S. N., and Mull, R. (2008). Simulation Modeling for Efficient Groundwater Management in Balasore Coastal Basin, India. *Water Resources Management*, 22(1): 23-50.

Robbins, G. A. (1989). Methods for determining transverse dispersion coefficients of porous-media in laboratory column experiments. *Water Resour. Res.*, 25: 1249-1258.

Robinson, C., Li, L., and Prommer, H. (2007). Tide-induced recirculation across the aquifer ocean interface, *Water Resour. Res.*, *43*(7), W07428.

Robinson, G., Hamill, G. A., and Ahmed, A. A. (2015). Automated image analysis for experimental investigations of salt water intrusion in coastal aquifers. *Journal of Hydrology*, 530, 350-360.

Robinson, G., Ahmed, A. A., and Hamill, G. A. (2016). Experimental saltwater intrusion in coastal aquifers using automated image analysis: Applications to homogeneous aquifers. *Journal of Hydrology*, 538, 304-313.

Rozell, D. J., and Wong, T.-F. (2010). Effects of climate change on groundwater resources at Shelter Island, New York State, USA. *Hydrogeology Journal*, *18*, 1657-1665.

Sanford, W. E., and Konikow, L. F. (1985). *A two-constituent solute transport model for ground water having variable density*. U.S. Geol. Surv. (USGS), Water Resour. Invest.

Schincariol, R. A., Herderick, E. E., and Schwartz, F. W. (1993). On the application of image analysis to determine concentration distributions in laboratory experiments. *Journal of Contaminant Hydrology*, 12:197-215.

Schincariol, R. A., and Schwartz, F. W. (1990). An experimental investigation of variable density flow and mixing in homogeneous and heterogeneous media. *Water Resources Research*, 26(10), 2317-2329.

Scholz, M., Mohrlok, U., and Stamm, J. (1998b). Detailed threedimensional field experiment with a groundwater circulation well for in situ flushing. *Groundwater quality: Remediation and protection*, IAHS Publication No. 250, M. Herbert and K. Kovar, eds., IAHS, Wallingford, U.K., 133-140.

Scholz, M., and Stamm, J. (1997). Detailed 3D field experiment with a groundwater circulation well for aquifer remediation. *Proc., XXVII World IAHR Congress, Groundwater: An Endangered Resource*, F. M. Holly et al., eds., ASCE, Reston, Va., 113-119.

Scholz, M., Stamm, J., and Eldho, T. I. (1998c). Limits of 3D numerical flow and transportation modeling for the simulation of a vertical circulation flow system in the remediation of a research field site. *Proc., XII Int. Conf. on Computational Methods in Water Resources*, CMP, Southampton.

Scholz, M., Weber, O., Mohrlok, U., and Eldho, T. I. (1998a). Large scale experiments for in situ flushing with groundwater circulation wells: Identification of processes and limiting parameters. *Groundwater quality: Remediation and protection*, IAHS Publication No.250, M. Herbert and K. Kovar, eds., IAHS, Wallingford, U.K., 185-189.

Scholz, M., Weber, O., Stamm, J., Eldho, T. I., and Jirka, G. H. (1997). Large-scale laboratory investigation of in situ groundwater remediation using vertical circulation flow systems, *Proc., XXVII World IAHR Congress, Groundwater: An Endangered Resource*, F. M. Holly et al., eds., ASCE, Reston, Va., 120-125.

Scholze, O., Hillmer, G., and Schneider, W. (2002). Protection of the groundwater resources of Metropolis CEBU (Philippines) in consideration of saltwater intrusion into the coastal aquifer. *Proceeding of the 17th Salt Water Intrusion Meeting*, Delft, the Netherlands.

Servan-Camas, B., and Tsai, F. T.-C. (2010). Two-relaxation-time lattice Boltzmann method for the anisotropic dispersive Henry problem. *Water Resources Research*, 46, W02515.

Sherif, M. M., and Al-Rashed, M. F. (2001). Vertical and horizontal simulation of seawater intrusion in the Nile Delta aquifer. *First International Conference on Saltwater Intrusion and Coastal Aquifers-Monitoring, Modeling, and Management*, Essaouira, Morocco.

Sherif, M., and Hamza, K. (2001). Mitigation of seawater intrusion by pumping brackish water. *Transport in Porous Media*, 43(1): 29-44.

Sherif, M., and Kacimov, A. (2008). Pumping of brackish and saline water in coastal aquifers: an effective tool for alleviation of seawater intrusion. *Proceeding of 20th Salt Water Intrusion Meeting (SWIM)*, Naples, Florida, USA.

Sherif, M. M., Singh, V. P., and Amer, A. M. (1990). A sensitivity analysis of '2D-FED', a model for seawater encroachment in leaky coastal aquifers. *Journal of Hydrology*, 118(1-4): 343-356.

Sherif, M., Sefelnasr, A., Ebraheem, A., and Javadi, A. (2013). Quantitative and qualitative assessment of seawater intrusion in Wadi Ham under different pumping scenarios. *Journal of Hydrologic Engineering*, 19(5): 855-866.

Shi, L., and Jiao, J. J. (2014). Seawater intrusion and coastal aquifer management in China: a review. *Environ. Earth Sci.*, 72, 2811-2819.

Simmons, C. T., Pierini, M. L., and Hutson, J. L. (2002). Laboratory investigation of variable-density flow and solute transport in unsaturated-saturated porous media. *Transport in Porous Media*, 47, 215-244.

Simpson, M.J., and Clement, T.P. (2004). Improving the worthiness of the Henry Problem as a benchmark for density-dependent groundwater flow models. *Water Resour. Res.*, 40, W01504.

Sorek, S., and Pinder, G. F. (1999). Survey of Computer Codes and Case Histories. In: Bear, J., Cheng, A. D., Sorek, S., Ouazar, D. & Herrera, I. (eds.) *Seawater Intrusion in Coastal Aquifers-Concepts, Methods and Practices.* Springer Netherlands.

Sreekanth, J., and Datta, B. (2010). Multi-objective management of saltwater intrusion in coastal aquifers using genetic programming and modular neural network based surrogate models. *Journal of Hydrology*, 393(3-4): 245-256.

Sreekanth, J., and Datta, B. (2011). Optimal combined operation of production and barrier wells for the control of saltwater intrusion in coastal groundwater well fields. *Desalination and Water Treatment*, 32(1-3): 72-78.

Stallard, W. M., Wu, K. C., Shi, N., and Corapcioglu, M. Y. (1996). Two-dimensional hydraulics of recirculating groundwater remediation wells in unconfined aquifers. *J. of Environ. Eng.*, 122(8), 692-699.

Stamm, J. (1998). Vertical circulation flow for in situ bioremediation in aquifers, *Book on bioremediation: Principles and practice*, S. K. Sikdar and R. L. Irwine, eds., Technomics, Lancaster, Pa.

Stamm, J., Eldho, T. I., and Scholz, M. (1998). Flow simulation of a system of groundwater circulation well and pumping well for NAPL site remediation. *Proc., 12th Int.*

Conference on Computational Methods in Water Resources, Crete, Greece, June 15-18, 99-106.

Stamm, J., Scholz, M., and Loseke, M. (1996). 3D vertical circulation flows around groundwater circulation wells (GZB) for aquifer remediation: Numerical calculations and field experiments. *Contaminated soil*, W. J. van den Brink, R. Bosman, and F. Arendt, eds., Kluwer Academic, Dordrecht, The Netherlands, 171-181.

Stoeckl, L., and Houben, G. (2012). Flow dynamics and age stratification of freshwater lenses: Experiments and modeling. *Journal of Hydrology*, 458-459, 9-15.

Strack, O. D. L. (1976). A single-potential solution for regional interface problems in coastal aquifers. *Water Resour. Res.*, 12(6), 1165-1174.

Sugio, S., Nakada, K., and Urish, D. (1987). Subsurface Seawater Intrusion Barrier Analysis. *Journal of Hydraulic Engineering*, 113(6): 767-779.

Sutton, D. J., Kabala, Z. J., Schaad, D. E., and Ruud, N. C. (2000). The dipole-flow test with a new single-borehole tracer test for aquifer characterization. *J. of Contam. Hydrol*., 44, 71-101.

Swartz, C. H., and Schwartz, F. W. (1998). An experimental study of mixing and instability development in variable-density systems. *J. of Contam. Hydrol.*, 34, 169-189.

Taniguchi, M., Ishitobi, T., and Shimada, J. (2006). Dynamics of submarine groundwater discharge and freshwater-seawater interface. *Journal of Geophys. Res.*, 111, C01008.

Tawabini, B., and Makkawi, M. (2018). Remediation of MTBE-contaminated groundwater by integrated circulation wells and advanced oxidation technologies. *Water Science & Technology: Water Supply*, 18(2), 399-407.

Taylor, J. R. (1997). An introduction to error analysis: The study of uncertainties in physical measurements. *2nd edition University Science Books*, Herndon, VA.

Thorenz, C., Kosakowski, G., Kolditz, O., and Berkowitz, B. (2002). An experimental and numerical investigation of saltwater movement in coupled saturated-partially saturated systems. *Water Resources Research*, 38(6), 1069.

Tidwell, V. C., and Glass, R., J. (1994). X-ray and visible-light transmission for laboratory measurement of 2-dimensional saturation fields in thin-slab systems. *Water Resources Research*, 30(11), 2873-2882.

Tidwell, V. C., and Glass, R., J. (1995). Laboratory investigation of matrix imbibition from a flow fracture. *Geophys. Res. Lett.*, 22, 1405-1408.

Todd, D.K. (1959). *Ground Water Hydrology*. John Wiley & Sons, New York.

Troisi, S., Coscarelli, R., and Straface, S. (1994). Sea water intrusion in the coastal aquifer of Reggio Calabria: guidelines for management. *Proceedings of the 13th Salt Water Intrusion Meeting (SWIM)*, Cagliari, Italy.

Tsanis, I. K., and Song, L.-F. (2001). Remediation of Sea Water Intrusion: A Case Study. *Ground Water Monitoring & Remediation*, 21 (3): 152-161.

U.S. Environmental Protection Agency (USEPA) (1995). Unterdruck-verdampfer-brunnen technology (UVB) vacuum vaporising well. *Rep. No. EPA/540/R-95/500a*, U.S. Environmental Protection Agency, Cincinnati.

U.S. Environmental Protection Agency (USEPA) (1998). Field application of in situ remediation technologies: Ground-water circulation wells, *EPA Rep. No. 542-R-98-009*, Washington, D.C.

USNECO-WWAP (2009). The United Nations World Water Development Report 3: Water in a Changing World, The United Nations Educational, Scientific and Cultural Organisation, Paris.

Vandenbohede, A., Lebbe L., and Houtte, E. V. (2008). Artificial Recharge of Fresh Water in the Belgian Coastal Dunes. *Proceeding of 20th SWIM*, Naples, Florida, USA.

Volker, R. E., Zhang, Q., and Lockington, D. A. (2002). Numerical modeling of contaminant transport in coastal aquifers. *Mathematics and Computers in Simulation*, 59, 35-44.

Voss, C. I. (1984). *A finite-element simulation model for saturated-unsaturated, fluid density-dependent ground-water flow with energy transport or chemicallyreactive single-species solute transport*. U.S. Geol. Surv. (USGS),Water Resour. Invest.

Voss, C. I., and Provost, A. M. (2010). *SUTRA-A model for saturated-unsaturated variabledensity ground-water flow with solute or energy transport*. U.S. Geol. Surv. (USGS),Water Resour. Invest.

Voss, C. I., and Souza, W. R. (1987). Variable density flow and solute transport simulation of regional aquifers containing a narrow freshwater-saltwater transition zone. *Water Resour. Res.*, *23*(10), 1851-1866.

Wildenschild, D., and Jensen, K .H. (1999). Laboratory investigations of effective flow behavior in unsaturated heterogeneous sands. *Water Resour. Res.*, 35, 17-27.

Webb, M. D., and Howard, K. W. F. (2011). Modeling the Transient Response of Saline Intrusion to Rising Sea-Levels. *Ground Water*, 49 (4), 560-569.

Werner, A. D., Bakker, M., Post, V. E. A., Vandenbohede, A., Lu, C., Ataie-Ashtiani, B., Simmons, C. T., and Barry, D. A. (2013). Seawater intrusion processes, investigation and

management: Recent advances and future challenges. *Advances in Water Resources*, 51(0): 3-26.

Werner, A. D., and Simmons, C. T. (2009). Impact of Sea-Level Rise on Sea Water Intrusion in Coastal Aquifers. *Ground Water*, 47(2), 197-204.

Werner, A. D., Jakovovic, D., and Simmons, C. T. (2009). Experimental observations of saltwater up-coning. *Journal of Hydrology*, 373(1-2), 230-241.

Xu, M., and Eckstein, Y. (1995). Use of weighted least-squares method in evaluation of the relationship between dispersivity and field scale. *Ground Water*, 33(6): 905-908.

Yeh, G. T. (1987). *3DFEMWATER: A three-dimensional finite element model of water flow through saturated-unsaturated media*. ORNL-6368, Oak Ridge National Laboratory, Oak Ridge, TN.

Yeh, G. T. (1990). *3DLEWASTE: A hybrid Lagrangian-Eulerian finite element model of waste transport through saturated-unsaturated media*. PSU Technical Report, Department of Civil Engineering, The Pennsylvania State University, University Park, PA.

Yu, W., Voss, C., Michael, H., Ahmed, K. M., Feinson, L., Khan, M. R., and Tuinhof, A. (2010). Implications of climate change for fresh groundwater resources in coastal aquifers in Bangladesh. *Rep.*, The world bank US Geological Survey.

Zhang, Q., Volker, R. E., and Lockington, D. A. (2002). Experimental investigation of contaminant transport in coastal groundwater, *Adv. Environ. Res*., 6 (3), 229-237.

Zhao, Y., Qu, D., Zhou, R., Yang, S., and Ren, H. (2016). Efficacy of forming biofilms by Pseudomonas migulae AN-1 toward in situ bioremediation of aniline-contaminated aquifer by groundwater circulation wells. *Environ. Sci. Pollut. Res.*, 23: 11568-11573.

Zhou, X., Chen, M., Ju, X., Ning, X., and Wang, J. (2000). Numerical simulation of seawater intrusion near Beihai, China. *Environmental Geology*, 40(1-2): 223-233.

Zhou, X., Chen, M., and Liang, C. (2003). Optimal schemes of groundwater exploitation for prevention of seawater intrusion in the Leizhou Peninsula in southern China. *Environmental geology*, 43: 978-985.

Zlotnik, V., and Ledder, G. (1994). Effect of boundary conditions on dipole flow. *In: Peters, A. et al. (Eds.). Computational Methods in Water Resources X*, 2. Kluwer Academic, Dordrecht, Netherlands, pp. 907-914.

Zlotnik, V., and Ledder, G. (1996). Theory of dipole flow in uniform anisotropic aquifers. *Water Resour. Res.*, 32, 1119-1128.

Zlotnik, V. A., and Zurbuchen, B. R. (1998). Dipole probe: design and field applications of a single-borehole device for measurements of vertical variations of hydraulic conductivity. *Ground Water*, 36, 884-893.

Zlotnik, V. A., and Zurbuchen, B. R. (2003). Field study of hydraulic conductivity in a heterogeneous aquifer: Comparison of single-borehole measurements using different instruments. *Water Resour. Res.*, 39, 1101.

Zlotnik, V. A., Zurbuchen, B. R., and Ptak, T. (2001). The steady-state dipole-flow test for characterization of hydraulic conductivity statistics in a highly permeable aquifer: Horkheimer Insel site, Germany. *Ground Water*, 39, 504-516.

List of Publications

Journal:

- Sharma, B., Rishi, D. S., Mudai, M. K., and Bhattacharjya, R. K. (2017). "Influence of clay lens on contaminant transport in unconfined coastal aquifers." *European Water*, 58: 359-364.
- Sharma, B., and Bhattacharjya, R. K. (2020). "Behavior of contaminant transport in unconfined coastal aquifers: An experimental evaluation." *Journal of Earth System Science*, 129, 140, https://doi.org/10.1007/s12040-020-01405-0.
- Vats, O. P., Sharma, B., Stamm, J., and Bhattacharjya, R. K. (2020). "Groundwater Circulation Well for Controlling Saltwater Intrusion in Coastal aquifers: Numerical study with Experimental Validation." *Water Resources Management*, 34: 3551-3563, https://doi.org/10.1007/s11269-020-02635-z.

Conference:

- Sharma, B., Mudai, M. K., Rishi, D. S., and Bhattacharjya, R. K. (2018). "Laboratory Scale Study of Saltwater Intrusion Dynamics in Costal Unconfined Aquifers." *HYDRO-2018 INTERNATIONAL (Hydraulics, Water Resources and Coastal Engineering)*, 19-21 December, 2018, NIT Patna, India.
- Sharma, B., Rishi, D. S., Mudai, M. K., and Bhattacharjya, R. K. (2017). "Laboratory scale investigation of contaminant transport in unconfined coastal aquifers." *7th International GROUND WATER CONFERENCE, IGWC-2017: GROUND WATER VISION 2030, Water Security, Challenges and Climate Change Adaptation*, December 11-13, 2017, New Delhi, India.
- Sharma, B., Rishi, D. S., Mudai, M. K., and Bhattacharjya, R. K. (2017). "Influence of clay lens on contaminant transport in unconfined coastal aquifers." *10th World Congress of EWRA on Water Resources and Environment*, EWRA-2017, 5-9 July, 2017, Athens, Greece.